

©2018

Timothy Russnak

ALL RIGHTS RESERVED

INVESTIGATING THE UBIQUITIN-PROTEASOME SYSTEM FOR TARGETED REVERSAL OF HIV-1

LATENCY

by

TIMOTHY RUSSNAK

A dissertation submitted to the

School of Graduate Studies

Rutgers, The State University of New Jersey

In partial fulfillment of the requirements

For the degree of

Doctor of Philosophy

Graduate Program in Microbiology and Molecular Genetics

Written under the direction of

Joseph Dougherty

And approved by

---

---

---

---

New Brunswick, New Jersey

January 2018

# **ABSTRACT OF THE DISSERTATION**

Investigating The Ubiquitin-Proteasome System For Targeted Reversal of HIV-1 Latency

By TIMOTHY RUSSNAK

Dissertation Director:

Joseph Dougherty

HIV is a worldwide epidemic, remaining the ever-present specter among all matters regarding blood or other bodily fluids, such as sexual intercourse, healthcare, blood transfusions, or even surgery, particularly in resource-poor areas. While antiretroviral drug therapy is highly successful in suppressing the virus and preventing transmission, it cannot cure the infection due to latency – the ability of HIV to go into a silent state within cells; once drug therapy is stopped, reactivating latent virus will cause a surge of the viral load within days or weeks. Current drug therapies do not act on this latent reservoir, necessitating lifelong adherence to medication, which is both extremely costly and comes with negative side effects. The mainstay of research into HIV latency deals with teasing apart the mechanisms involved in establishing and maintaining latency, in the hopes of finding drug compounds which can efficiently reverse latency and thus purge the body of hidden HIV.

In searching for cellular pathways involved in latency, our lab has employed a genome-wide negative-selection screen, which indicated that the ubiquitin-proteasome system plays a

role in maintaining latency. This led us to discover that proteasome inhibitors act as bifunctional antagonists of HIV, both reversing the latent state and reducing infectivity of virions. We went on to identify the specific ubiquitin-proteasome pathway that is involved in maintaining latency. We then investigated the activity of a small-molecule inhibitor of one component of the ubiquitin-proteasome system, showing its ability to reactivate latent HIV in both a primary cell model and in cells taken from aviremic HIV+ patients. These results are a proof-of-concept that inhibition of a specific ubiquitin-proteasome pathway can allow for specific reversal of HIV latency.

## **Acknowledgements**

First and foremost, I need to thank my advisor, Joseph Dougherty, for being my mentor throughout my graduate career. I'd like to also thank the rest of my committee: Céline Gélinas, Nancy Walworth, and Huizhou Fan. To the only other member of our lab, Yoshifumi Kobayashi, and the previous student to graduate before me, Leia Miller, I need to thank as much of our work has been a collaboration, and to previous members Rose Lee, Len Edelstein, and Brad Phelan. I need to acknowledge two of our collaborators and friends, Yacov Ron and Chiann-Chyi Chen, both of whom have passed. I must also thank Dr. Ronald Nahass of ID Care for providing crucial patient specimens, and I must likewise thank his patients for their donations. I also have to thank Janet Alder and Jim Millonig for assisting me in the final days of my degree and helping me finish up.

Obviously, I need to thank my mom, Ann Longendyck, for supporting me all these years, as well as my dad, Richard Russnak, who has passed, for doing the same. I guess I should mention my siblings, Matt and Lauren, and their endless "So, when are you graduating?" questions over the many, many years. I need to thank my closest friend, Erica Smith, for always being there for me, often with her own tales of graduate student woe. And last, but surely not least, I need to thank my partner, Anthony Di Tommaso, for really being my rock and always being there for me through the highs and many, many lows.

I must acknowledge that Chapter 2 is from a manuscript in preparation, with authors Leia K Miller, Yoshifumi Kobayashi, Timothy A Russnak, Chiann-Chyi Chen, Yacov Ron, Joseph P Dougherty, as is Chapter 4, with authors Yoshifumi Kobayashi, Timothy Russnak, Leia Miller, Ronald Nahass, Celine Gelinass, and Joseph P. Dougherty. Chapter 3 is derived from published work entitled "Proteasome inhibitors act as bifunctional antagonists of human

immunodeficiency virus type 1 latency and replication" Miller, L. K., Y. Kobayashi, C. C. Chen, T. A. Russnak, Y. Ron and J. P. Dougherty (2013). *Retrovirology* 10: 120.

## **List of Abbreviations**

<b>AIDS</b> – Acquired immunodeficiency syndrome	<b>AP1</b> – activator protein 1
<b>ART</b> – antiretroviral therapy	<b>BRD4</b> – bromodomain containing 4
<b>β-TRCP</b> – beta-transducin repeat containing E3 ubiquitin protein ligase	<b>CBF-1</b> – C-repeat/DRE binding factor 1
<b>CA</b> – capsid protein	<b>CBF-β</b> – core-binding factor beta
<b>CCR5Δ32</b> – allele of CCR5 containing a 32-base pair deletion that contains a premature stop codon	<b>cDNA</b> – complementary DNA
<b>CUL4A</b> – cullin-4A	<b>CUL5</b> – cullin-5
<b>DDB1</b> – damage specific DNA binding protein 1	<b>DNMT</b> – DNA methyltransferase
<b>eGFP</b> – enhanced green fluorescent protein	<b>EHMT2</b> – euchromatin histone lysine methyltransferase
<b>ELOBC</b> – elongin-BC	<b>GALT</b> – gut-associated lymphoid tissue
<b>GAPDH</b> – glyceraldehydes-3-phosphate dehydrogenase	<b>GFP</b> – green fluorescent protein
<b>HAART</b> – highly active antiretroviral therapy	<b>HDAC</b> – histone deacetylase
<b>HDACI</b> – histone deacetylase inhibitor	<b>HIV-1</b> – Human immunodeficiency virus-1
<b>HLA</b> – human leukocyte antigen	<b>HMT</b> – histone methyltransferase
<b>IFITM1</b> – interferon induced transmembrane protein 1	<b>Lag-3</b> – lymphocyte-activating gene 3
<b>LEF1</b> – lymphoid enhancer binding factor 1	<b>LRA</b> – latency reversal agent
<b>LSF</b> – late SV40 factor	<b>LTNP</b> – long-term nonprogressor
<b>LTR</b> – long terminal repeat	<b>MA</b> – matrix protein
<b>NFAT</b> – nuclear factor of activated T-cells	<b>NFκB</b> – nuclear factor kappa light chain enhancer of activated B-cells
<b>PCR</b> – polymerase chain reaction	<b>PD-1</b> – programmed cell death protein 1
<b>PI</b> – proteasome inhibitor	<b>PKC</b> – protein kinase C
<b>PRC2</b> – polycomb repressive complex 2	<b>PSMA7</b> – proteasome subunit alpha type 7
<b>qPCR</b> – quantitative PCR	<b>RBX2</b> – RING-box protein 2
<b>RLUC</b> – Renilla luciferase	<b>RNAi</b> – RNA interference
<b>RNAPII</b> – RNA polymerase II	<b>RT</b> – reverse transcriptase
<b>SAHA</b> – suberoylanilide hydroxamic acid	<b>SEAP</b> – secreted alkaline phosphatase
<b>shRNA</b> – short-hairpin RNA	<b>siRNA</b> – short-interfering RNA
<b>SMYD2</b> – SET and MYND domain containing 2	<b>Sp1</b> – specificity protein 1

<b>SUV39H1a</b> – suppressor of variegation 3-9 homolog 1a	<b>Tim-1</b> – T-cell immunoglobulin and mucin domain 1
<b>UPS</b> – ubiquitin-proteasome system	
<b>YY1</b> – yin yang 1	



## **Table of Contents**

<b>ABSTRACT OF THE DISSERTATION .....</b>	<b>ii</b>
<b>Acknowledgements.....</b>	<b>iv</b>
<b>List of Abbreviations .....</b>	<b>vi</b>
<b>Table of Contents .....</b>	<b>viii</b>
<b>List of Tables.....</b>	<b>x</b>
<b>List of Figures.....</b>	<b>xi</b>
<b>Chapter 1: Introduction.....</b>	<b>1</b>
Human Immunodeficiency Virus.....	1
Structure and life-cycle .....	2
Infection .....	4
Treatment .....	6
T-cell depletion .....	10
Microbial translocation.....	11
Immune dysregulation and inflammation .....	12
HAND.....	14
Disease progression and non-progression.....	15
Post-ART control .....	18
HIV Latency .....	19
Discovery.....	19
Latent reservoirs .....	20
Notable cases of HIV “cures” .....	24
Mechanisms of latency .....	25
Latency-reversing agents .....	27
HIV and the ubiquitin-proteasome system.....	31
<b>Chapter 2: Identification of Genes and Pathways Involved in Maintenance of HIV-1 Latency</b>	
<b>Utilizing an RNAi Screen.....</b>	<b>34</b>
Abstract.....	34
Introduction .....	35
Materials and Methods.....	37
Results.....	48

Discussion .....	56
Tables .....	62
Figures.....	72
<b>Chapter 3: Characterization of the Activity of Proteasome Inhibitors as HIV-1 Latency</b>	
<b>Antagonists.....</b>	<b>83</b>
Abstract.....	83
Introduction .....	85
Materials and Methods.....	87
Results.....	95
Discussion .....	99
Figures.....	107
<b>Chapter 4: Inhibition of a Specific Ubiquitin-Proteasome Pathway Activates Latent HIV .....</b>	<b>114</b>
Abstract.....	114
Introduction .....	115
Materials and Methods.....	117
Results.....	122
Discussion .....	127
Figures.....	130
<b>Concluding Remarks.....</b>	<b>140</b>
<b>Bibliography .....</b>	<b>143</b>

## **List of Tables**

Table 2.1. Highly significant (p-value <0.001) gene "hits" .....	62
Table 2.2: Highly enriched (p-value <0.01) canonical pathways .....	67
Table 2.3: Highly enriched (p-value <0.01) functional annotations.....	68
Table 2.4: Predicted upstream regulators of gene "hits" (p-value <0.05) and their predicted functionality in the context of the activation of latent HIV-1.....	69
Table 2.5: Significant (p-value <0.05) gene "hits" that can be categorized into the ubiquitin- proteasome system .....	70

## **List of Figures**

Figure 2.1. Reverse genetic screen protocol.....	72
Figure 2.2. Validation follow-up of significant gene “hits” identified in the screen.....	74
Figure 2.3. Proteasomal inhibition activates latent HIV-1 reporter gene transcription.....	76
Figure 2.4. PIs stabilize $\beta$ -catenin in primary, resting CD4+ T cells and OM-10.1 cells .....	78
Figure 2.5. $\beta$ -catenin becomes enriched on the HIV-1 5' LTR following proteasomal inhibition ..	80
Figure 2.6. $\beta$ -catenin knockdown reduces the magnitude of Velcade-induced activation of latent HIV-1 .....	81
Figure 2.7. Potential pathway through which PIs activate latent HIV-1 transcription .....	82
Figure 3.1. HIV-1 constructs.....	107
Figure 3.2. PIs activate latent HIV-1 gene expression in tissue culture model systems.....	108
Figure 3.3. PIs activate latent HIV-1 in primary human CD4+ T cell models .....	109
Figure 3.4. Expression of CD25 early activation marker in primary human resting CD4+ T Cells treated with MG-132 .....	110
Figure 3.5. PI-treatment of productively infected primary human CD4+ T Cells results in the production of HIV-1 virions with reduced infectivity .....	111
Figure 3.6. HIV-1 virions produced as a result of PI-mediated activation of latent viral gene expression exhibit reduced infectivity .....	112
Figure 4.1. Protocol for establishing latent virus infection in primary resting CD4+ T cells.....	130
Figure 4.2. Activation of latent virus in the primary cell model by GS143 .....	131
Figure 4.3. HIV-1 mRNA induction by GS143 and representative LRAs with the primary resting CD4+ T cell model .....	132
Figure 4.4. Toxicity profile of GS143 alone and in combination .....	133
Figure 4.5. Activation profile of GS143 alone and in combination .....	134
Figure 4.6. HIV-1 expression induced by GS143 in resting CD4+ T cells isolated from patients on suppressive ART .....	135
Figure 4.7. GS143 combinational drug assay on HIV-1 activation in resting T cell.....	136
Figure 4.8. Synergy of GS143 with JQ1 or chidamide .....	138
Figure 4.9. HIV-1 expression induced by representative LRAs, or those combinations with GS143, in resting CD4+ T cells isolated from patients on suppressive ART .....	139

## **Chapter 1: Introduction**

### **Human Immunodeficiency Virus**

Over three decades ago, a retrovirus termed human immunodeficiency virus (HIV) was discovered to be the causative agent of acquired immunodeficiency syndrome (AIDS) [1, 2], a new and fatal disease which resulted in death from rare cancers or otherwise easy to treat infections. Since that time, the virus has achieved pandemic levels, spreading to every corner of the world; as of 2015, there were almost 37 million people infected, only 17 million of whom are on medication [3]. As there is no cure for the virus, these numbers will only continue to increase.

Since the discovery of HIV, treatments have been developed which allow patients to live relatively normal lives. However, cost of care for HIV+ patients is high, despite advances in drug development. According to a study analyzing US data from 2006, the average yearly cost of antiretroviral therapy alone is \$13, 024, with that cost increasing substantially for patients whose CD4 counts drop, indicative of disease progression [4]. When considering the cost of all healthcare associated with HIV, lifetime estimates for taking care of one infected person exceed \$560,000, almost 70% of which represents the cost of antiretroviral therapy (ART) [5]. This is largely due to the unique nature of HIV which creates a lasting incurable infection, necessitating daily life-long drug therapy and routine monitoring of viral load, resistance development, and comorbidities.

### **Structure and life-cycle**

HIV-1 is a retrovirus – it has an RNA genome which is reverse transcribed into DNA to complete its infection of a cell. The virion is covered by a lipid bilayer containing viral Envelope (Env) and various cellular proteins and is constructed of many copies of matrix (MA, or p17). Within this shell is contained the viral core, comprised of capsid (CA, or p24); the core itself contains two copies of the viral RNA genome bound to nucleocapsid (NC, or p7) as well as the viral enzymes reverse transcriptase (RT), integrase (IN), and protease (PR) and the accessory proteins Vif, Vpr, and Nef [6]. Infection of a cell begins with attachment of the virion to cell-surface receptors and entry of the viral core into the cell, ending with integration of the viral genome into the host cell DNA; if the integrated provirus is expressed, virions will then be produced and bud off the cell surface.

The first step of infection is viral entry, with Env – a trimer of gp120 and gp41 heterodimers – binding to the cellular receptor CD4 via gp120, which causes rearrangements leading to binding of the co-receptor, either CCR5 or CXCR4. Virus strains can be classified based on co-receptor usage: R5 binds CCR5, X4 binds CXCR4, and those that can bind either are called R5X4; it is mainly R5 or R5X4 viruses that are transmitted between individuals. Co-receptor binding leads to gp41 inserting into the cell membrane, causing fusion and entry of the virion into the cell [7]. Upon entering the cell, the virion releases its contents into the cytoplasm, and it is here that reverse transcription takes place, wherein the plus-strand viral genomic RNA is used as a template, and a cellular tRNA as a primer; RT from the virion creates a double-stranded DNA product. RT has no proofreading ability, thus large numbers of mutations can arise directly from reverse transcription, while recombination also occurs when the RT switches between RNA templates during the process [8].

The completion of reverse transcription marks the formation of the pre-integration complex (PIC), containing the viral dsDNA genome, RT, MA, Vpr, IN, CA, and various cellular proteins. Nuclear localization signals within MA and IN are recognized by cellular karyopherin alpha with Vpr enhancing this recognition; the PIC is then actively transported along microtubules and imported into the nucleus [9, 10]. IN then inserts the linear dsDNA into the cellular DNA, favoring active genes [11]. Once integrated, the viral genome is dependent upon cellular machinery to transcribe RNA. At both the 5' and 3' ends lay the long terminal repeats (LTR), identical regions comprised of regulatory sequences. However, in its basal state the LTR can only provoke short, abortive transcription: cellular transcription factors must bind enhancer elements in the LTR or the viral protein Tat must be expressed for efficient transcription to occur. Tat is a small viral protein which binds the trans-activation response (TAR) element, a stem-loop that exists on the 5' end of all HIV transcripts, and in doing so recruits P-TEFb which phosphorylates the C-terminal domain (CTD) of RNA Pol II (RNAPII), allowing for elongation of the viral transcript [12, 13].

Viral RNA undergoes inefficient splicing via cellular machinery, giving rise to singly-spliced and multiply-spliced transcripts – only the latter of which can leave the nucleus of their own accord, and this is how Nef, Tat, and Rev get translated first; their production marks the early-phase of cellular infection. Tat can go on to stimulate more transcription, while Rev enters the nucleus and binds to the rev response element (RRE) on unspliced and singly-spliced RNA, allowing export from the nucleus; this defines the late-phase. Singly-spliced RNAs produce Vpr, Vif, Vpu, and Env, while unspliced RNAs produce Gag and Gag-Pol fusion protein as well as serve as the genomic RNA for virion production [14]. Viral proteins are then trafficked to the plasma membrane, where assembly begins with two copies of the RNA genome being incorporated into the immature virion. The cellular ESCRT pathway is used to finish assembly and catalyze budding

of the virion from the cell. Once released, viral protease within the virion activates and cleaves Gag/Gag-Pol at several sites, producing: CA, MA, NC, p6, PR, RT, and IN; these proteins rearrange to form the finalized, mature virion [15].

The four accessory proteins of HIV – Vif, Vpr, Vpu, and Nef – serve to enhance various aspects of infection and to counter antiviral defenses. Vif tags the cytidine deaminase APOBEC3G with ubiquitin, leading to its degradation; APOBEC3G would otherwise get packaged within the virion and mutate the viral genome once reverse transcription takes place in a newly infected cell [16]. Vpr is packaged into the virion. It improves infection of the cell, particularly in non-dividing cells, by increasing RT fidelity and assisting in transport of the PIC through the nuclear envelope. It can also cause G2 arrest and apoptosis [17]. Vpu counters BST-2, which tethers the virion to the cell membrane, preventing release. It also tags CD4 within the ER for degradation, preventing it from getting stuck to viral Env, and induces apoptosis through indirect inhibition of NF $\kappa$ B [18]. One of the main functions of Nef is to remove both CD4 and MHC class I from the cell surface. It can also activate T-cells [19].

### **Infection**

HIV enters the body primarily at mucosal surfaces through sexual contact, via mother-to-child transmission during birth or breastfeeding, or directly through the use of contaminated blood products or sharps [20]. In the case of mucosal exposure, the virus can enter through tears in the mucosa or be transported by epithelial cells which selectively capture R5-virus. Once across the epithelia, virions infect CD4-expressing dendritic cells (DCs), T-cells, or macrophages; DCs can also internalize virions without becoming infected, then pass them on to other target cells such as T-cells [21].



After transmission, HIV infection follows three phases: 1) acute, where the viral load peaks before dropping due to the immune response, 2) chronic asymptomatic, where the viral load steadily increases while CD4+ T-cell numbers decrease – this phase can last many years, 3) symptomatic (AIDS), where the CD4+ T-cell count is too low to sustain healthy immune function. During the acute phase, HIV replicates heavily in gut-associated lymphoid tissue (GALT), primarily in CCR5+ CD4+ memory T-cells; this tissue contains 60% of the body's CD4+ T-cells, and the widespread infection and destruction during the acute phase has lasting effects. The high viral load during the acute phase causes the early infection to account for nearly half of all HIV transmission events [22], as patients are 26 times more infectious than during the later asymptomatic, chronic phase [23]. As CD4+ cell numbers drop, CD8+ T-cells – including those HIV-1 specific – increase as the antiviral immune response is initiated, causing a shift to the chronic phase. During this phase, the GALT remains heavily depleted, and systemic inflammation and chronic immune activation cause both continuous T-cell proliferation and T-cell death [24]. Even after years of ART, in the majority of patients the GALT does not undergo complete immune reconstitution, despite peripheral immune recovery – CCR5+ cells were found to be depleted and the memory cell population displayed increased activation levels [25, 26].

Late-stage HIV infection, or AIDS, is characterized by a profound loss of CD4+ T-cells (below 200/ $\mu$ L) and increase in viral load. Often, the virus switches coreceptor use from CCR5 to CXCR4, and this X4 tropism is associated with higher viral load, lower CD4+ T-cell counts, and worsening of the disease [27]. At this point, the immune system cannot function properly and the patient is susceptible to opportunistic infections such as fungal infections (pneumocystosis, cryptococcosis, histoplasmosis, talaromycosis) [28] and meningitis, rare cancers like Kaposi's sarcoma, and symptoms of normally controlled chronic infections like cytomegalovirus, herpes

zoster, and toxoplasmosis [29-31]. Death from HIV comes from these opportunistic diseases, rather than directly from the virus itself.

Within the first few months of infection a 'set-point' is reached wherein the plasma RNA levels are stable over long periods of time, indicative of an equilibrium reached between viral replication and the anti-HIV immune response [32, 33]. This point constitutes the asymptomatic, chronic phase, and its value can have profound implications for the patient: a higher set-point is associated with a faster decline in CD4+ counts [34] and progression to AIDS [35]. Since plasma viral load is directly correlated with risk of sexual transmission [36, 37], it's been suggested that the set-point is an evolutionary trade-off which maximizes transmissibility, as the average viral load set-points found are also correlated with effective transmission [38].

Exactly what determines the set-point is still not completely known, however many associations have been found. The biggest factor seems to be the viral genome, as about one-third to one-half of variation in set-point values is due to the virus itself [39, 40]; this was determined by tracking transmission and treating the set-point as a heritable factor. The speed and magnitude of the CD8+ T-cell response during acute infection also determines the size of the set-point [41], with CD8+ T-cell responses towards Gag and Nef associated with low set-point [42]. Overall T-cell activation, however, may not be beneficial, as genital tract inflammation in women is associated with a higher set-point [43].

### **Treatment**

ART is highly successful when proper adherence is taken – treatment can reduce plasma viral load level by over 99% within two weeks [44], bringing it below 50 copies/mL, which is defined as “undetectable,” being below the limit of detection of commercially used assays. There are four major classes of drugs which target viral enzymes – nucleoside reverse

transcriptase inhibitors (NRTI), non-nucleoside reverse transcriptase inhibitors (NNRTI), protease inhibitors, and integrase strand transfer inhibitors (InSTI); a fifth class, entry inhibitors, can target viral or cellular proteins. Due to the high mutation rate of HIV and the sheer number of virions produced daily in an untreated person –  $10^{10}$  –  $10^{12}$  – it's possible that every possible single point mutation can occur multiple times each day [45]. This results in the viral population within an individual to be a quasispecies of many different genotypes, and thus a patient can carry virus that is resistant to one or many different drugs, even before started treatment. Thus treatment with a single agent can and will cause resistance to emerge within weeks [46]. Multiple drug treatment prevents this by requiring several mutations to occur simultaneously in two or more viral proteins, which is unlikely to happen when viral replication is effectively suppressed. Thus, treatment adherence is of the utmost importance.

NRTIs are deoxyribonucleoside analogs which lack a 3'-hydroxyl and thus, when phosphorylated within a cell, can become incorporated by RT and act as chain terminators, ending synthesis of the viral DNA strand. Requiring phosphorylation to become active, they serve as a pro-drug, and this requirement improves their clinical profile as phosphorylation traps them within cells and extends their half-life in the body. ART often includes two drugs from this class [47]. NNRTIs directly inhibit RT by binding near the active site, leading to conformational changes which obstruct catalytic activity. These drugs are often used as first-line therapy for HIV [48], and it was 3'-azidothymidine (AZT), an NRTI, which was the very first drug approved for use in treating HIV in 1987; it would prolong a patient's life by less than two years, due to resistance development.

Protease inhibitors are analogs of HIV protease substrate. Inhibition of PR serves to interfere with multiple steps of the viral life cycle, including entry, reverse transcription, and

post-reverse-transcription steps [49]. Protease inhibitor monotherapy has shown efficacy in treating HIV without major risk of resistance development; however, it is still inferior to combined ART [50, 51]. INSTIs block the strand-transfer reaction in viral integration, preventing the insertion of the HIV genome into the host cell. These drugs show a favorable efficacy and tolerability profile, and are thus used in first-line regimens, as well as in modified regimens following treatment failure with other drugs [52].

By targeting HIV's use of the CCR5 co-receptor, maraviroc was developed as an entry inhibitor. It acts as a CCR5 antagonist, binding to the cellular protein and preventing HIV from binding and entering the cell; in this regard, it is unique among ART drugs in that it binds a cellular target, thus making resistance development less likely, though it can occur – mainly through tropism switch to CXCR4 [53-55]. Another class of drugs which block entry is the fusion inhibitors – namely enfuvirtide, which binds to viral gp41 and disrupts fusion between viral envelope and the cell membrane. While this drug shows efficacy in ART, it has a low genetic barrier to resistance development [55, 56].

Current recommendations for ART advise that all HIV+ patients receive treatment immediately, a marked and important change from past policy which delayed treatment until CD4 counts drop below a certain threshold. Part of the reason for this change is due to ART preventing transmission – the PARTNER (Partners of People on ART—A New Evaluation of the Risks) study followed over 1,000 serodifferent couples (where the HIV+ partner had a viral load was <200 copies/mL) for 4 years and found not a single transmission event [57]. This was in line with other studies that found a direct correlation between low viral load and low transmissibility [36, 58]. Early treatment is also associated with better health outcomes, both AIDS-related and non-AIDS related [59], better immune function [60, 61], and overall increased quality of life [62].

Initial ART regimens are comprised of two NRTIs and one drug from another class, optimally an InSTI, but protease inhibitors or NNRTIs are also used [63].

Since patients must remain on ART for their entire lives, long-term side effects of these medications are becoming increasingly more visible and clinically important. NRTIs can cause lipodystrophy, myopathy, neuropathy, and hepatic toxicity; the main mechanism of these toxicities is the effect of NRTIs on mitochondrial DNA polymerase, leading to mitochondrial dysfunction. NNRTIs are better tolerated, though they alone cannot be a mainstay of treatment. Protease inhibitors are likewise well tolerated, although they are linked to dyslipidemia [64]. Drug interactions are also a major concern with life-long ART. Many of these drugs can inhibit or induce members of the cytochrome P450 enzyme family; likewise they can have effects on drug transporter proteins, such as the ATP-binding cassette superfamily [65]. Drug-drug interactions also need to be monitored, as it's been shown that between 27-44% of patients have interactions between ART and other medications [66, 67].

Over half of patients on successful ART experience viral blips – transient spikes of viremia above the standard 50 copies/mL detection limit [68]; these are not necessarily associated with treatment failure [69, 70], but rather thought to be stochastic fluctuations [71, 72] or laboratory artifacts [73-75], and thus may hold no clinical significance. However, large blips can be cause for concern, as blips >400-500 copies/mL are associated with virological rebound [76-78]. The frequency of blips may be related to the CD4+ count when therapy is initiated, and the mean size of blips in one study was found to be 158 copies/mL [79]; the frequency of blips is two-fold higher in those treated during chronic rather than primary infection, and in those treated during primary infection the viral set-point is related to the frequency [80].

Models have been made to explain blips by antigen-driven T-cell expansion from vaccinations [81] and infections [82], which create new susceptible targets for the virus to infect. Activation of latently-infected cells by antigen [83] can activate the latent provirus and thus cause a sudden spike in the viral load [84]. Similarly, latently-infected cells activated by antigen can undergo asymmetric division, wherein one cell remains in an active state while the other goes into a resting state [85], which can explain both blips and low-level viremia, as well as serve as a process that maintains the latent reservoir. Using this hypothesis that low-level viremia seen while on ART is due to random activation of latency-infected cells and that blips are statistical fluctuations, mathematical models have been proposed which match with clinical observations [86].

### **T-cell depletion**

HIV infection causes T-cell death in ways other than simply successful viral infection and virion production. Both CD4+ and CD8+ uninfected T-cells die from apoptosis [87], and in the lymph nodes uninfected cells account for the majority of cell death [88]. Experiments *ex vivo* with lymphoid tissues show that bystander apoptosis is caused mainly by CXCR4-trophic virus and requires interaction between CXCR4 and gp120 [89]. Using human lymphoid aggregate cultures made from tonsillar tissue which replicates an *in vivo* lymphoid environment, it was shown that CD4+ T-cells are selectively killed by X4-trophic HIV, however over 95% of these are not productively infected – reverse transcription is incomplete, leading to an accumulation of shortened viral DNA which ultimately triggers an antiviral, apoptotic response; similar results were seen with spleen tissue, suggesting that this process occurs in various lymphoid tissues [90]. The apoptotic response is primarily driven by caspase-1, leading to pyroptosis and a release of proinflammatory cytokines which can attract more susceptible cells to the sites of viral production [91]. Interestingly, peripheral CD4+ T-cells resist this pyroptosis, but coculturing

with lymphoid cells makes them susceptible [92]. Other causes of bystander cell death are extracellular Vpr being taken up by T-cells [93], extracellular Tat which can cause monocytes to express the apoptosis-inducing TRAIL [94], and both surface-bound and soluble Env [95].

Using RNA fluorescence in situ hybridization-flow cytometry (FISH-flow) to detect HIV RNA in single cells of unfractionated PBMCs, it was found that effector memory T-cells are the main subset of HIV RNA-expressing cells in both *ex vivo* infection of PBMCs and samples from untreated HIV patients and those on ART [96]. HIV-specific memory CD4+ T-cells are preferentially infected [97], a phenomenon also seen in macaques during simian immunodeficiency virus (SIV) infection, a virus closely related to HIV [98, 99].

CD4+ T-cell depletion occurs within the GALT at all stages of infection, primarily in CCR5+ cells [100]. However, during early infection there is massive cell loss which can only be restored by ART – the extent of the restoration depends on if ART was initiated during primary or chronic infection; it is likely that restoration is driven by cell trafficking rather than proliferation within the GALT [101]. Reconstitution can be slow and in the majority of patients is incomplete, despite recovery in the periphery [25, 26, 102]; this incomplete recovery is not due to ineffective ART penetrance nor residual HIV replication [103].

### **Microbial translocation**

Due to the massive infection of and damage to the GALT during HIV infection, the epithelial barrier is disrupted. Chronically infected patients have increased plasma lipopolysaccharride (LPS) levels which originate from the gastrointestinal tract through translocation of microbes or microbial products as a result of damage to the GALT; this circulating LPS is associated with an increase in immune activation markers. Successful ART decreases but does not eliminate LPS levels [104]. *In vitro* studies with epithelial monolayers

show a release of proinflammatory cytokines as a result of exposure to both intact HIV virions or simply Env gp120, leading to barrier disruption and translocation of virus and bacteria [105]. As plasma LPS levels are indicative of poor GALT barrier integrity and increased immune activation, it is not surprising that higher levels are associated with poorer clinical outcomes. Patients who maintain undetectable HIV RNA levels on ART but don't recover immunologically – with CD4 counts <200 cell/ $\mu$ L – have higher plasma LPS and enterobacterial DNA levels than those whose CD4 counts recover past 200 cell/ $\mu$ L [106]. There may also be a correlation with viral load and LPS, as patients on ART who were partially suppressed with 2.5-50 copies/mL had higher LPS levels than those fully suppressed with <2.5 copies/mL [107]. One retrospective study showed that circulating LPS levels during the first years of infection are a predictor of HIV disease progression independent of CD4+ T-cell count or viral load [108], suggesting that plasma LPS may be a useful biomarker to track and predict clinical outcomes. Similarly, in patients on ART but with a previous diagnosis of AIDS, gut epithelial dysfunction and inflammation are predictors of mortality [109].

### **Immune dysregulation and inflammation**

Early studies of telomere length showed that CD4+ T-cell depletion in HIV+ patients was not caused by high turnover leading to proliferative exhaustion [110] and the *in vitro* capacity of CD4+ T-cells remains the same for HIV+ and HIV- individuals [111]. However, T-cell exhaustion is seen in patients. One reason could be cytotoxic T-lymphocyte antigen 4 (CTLA-4), a molecule expressed on activated CD4+ T-cells and regulatory T-cells which can suppress T-cell activation and proliferation; it is specifically upregulated in HIV-specific CD4+ T-cells and is correlated with reduced proliferative capacity and disease progression [112]. Similarly, programmed death 1 (PD-1) expression inhibits proliferation and function of CD8+ T-cells, and it's been found to be upregulated in HIV-specific CD8+ T-cells [113]. In both cases, the upregulation of CTLA-4 and PD-



1 and dysfunction were absent in CMV-specific T-cells, and function could be restored by blocking the appropriate receptors, suggesting that this response is HIV-specific and not simply a characteristic of chronic infection with a virus.

As seen with incomplete GALT recovery, despite the success of ART in suppressing HIV and reducing viral load, the immune system does not necessarily completely recover; dysregulation and chronic inflammation can persist. In a study of HIV+ patients on ART able to maintain undetectable viral loads for at least 4 years, 69% of those who initiated ART with CD4 counts of 200 cells/ $\mu$ L did not achieve counts over 500 cell/ $\mu$ L during a 10 year period of therapy; this is opposed to 95% of those who initiated with counts of 300 cells/ $\mu$ L achieving counts of over 500 cells/ $\mu$ L [114]. This can be seen as a sort of immune 'set-point,' similar to that seen for viral load during chronic infection. 30-40% of patients who initiate ART with low CD4+ T-cell counts present with symptoms of mycobacterial, CMV, and hepatitis B and C infections and display markers of increased or persistent immune activation [115]. These infections could be a direct result of low CD4 count, or they could be a cause through an overactive immune system coupled with HIV infection.

Again, we see a link between overall health and plasma viral load: HIV-DNA and inflammation markers are lower in patients with persistently undetectable viremia than in those with repeated blips or with persistent viral load between 37-200 copies/mL [116]. This suggests that even small amounts of circulating virus are enough to trigger increased systemic inflammation. However, a recent study investigating immune activation markers in HIV+ patients lacking co-morbidities suggests that HIV does not cause chronic inflammation after 1 year of ART [117].

HIV+ patients on successful ART are at increased risk of various morbidities, such as cardiovascular disease, hypertension, type II diabetes, renal failure, and bone fractures. The risk of two or more of these comorbidities occurring simultaneously is also elevated, with a chance equivalent to people in the general population 10-15 years older. Low nadir CD4+ counts and duration of ART were both independent risk factors [118]. This echoes the fact that the frequency of non-AIDS events are also decreased with ART and is in line with a recent study of over 80,000 patients, comparing three-year survival and life expectancy upon starting ART between 1996-2013 which found all-cause mortality during all three years decreased as time went on, with a life expectancy increase of 10 years [119].

### **HAND**

HIV-associated neurocognitive disorders (HAND) are a group of neurocognitive impairments in memory, attention, psychomotor function, mental acuity, and behavior seen specifically in HIV patients. These impairments can range from mild to very debilitating, such as quick-onset HIV-dementia; before the discovery of ART, this dementia could be seen in up to 20% of patients [120]. Similarly, in one early study AIDS victims only 10% of brains were found to be normal – the others had various abnormalities and damage [121, 122]. Some common risk factors for HAND are age, incomplete viral suppression, and low nadir CD4+ counts.

These disorders continue to be extremely prevalent in the face of successful ART – half of patients have some form of neurological impairment, and this number hasn't changed from the pre-ART era, although the rate of severe impairment has decreased [123]. Cognitive impairments seen in ART-treated patients are associated with brain volume reduction and linked to previous immunosuppression [124], suggesting a lasting effect of untreated acute infection. However, immunosuppression alone cannot explain these disorders, as the cognitive

performance of infected individuals with normal CD4+ was found to be lower than uninfected, and improved with ART [125], while paradoxically one report showed that neurocognitive function can improve upon ART cessation in patients who maintain normal CD4+ counts [126], suggesting that ART toxicity may play a role.

### **Disease progression and non-progression**

While HIV is incurable and the vast majority of patients will eventually progress to end-stage AIDS without medical intervention, the time it takes varies between individuals. Plasma viral load is a significant predictor of progression to AIDS: within a 6 year time period, the chance to progress to AIDS climbs from 5.4% at 500 copies/mL to 80% at >30,000 copies/mL; with low CD4+ counts and high viral loads this chance reaches almost 98% [127]. This is in line with a high viral set-point being predictive of AIDS development [128], while viral load in the years preceding development of AIDS having no correlation [129] – the initial viral load and set-point set the pace of the infection. Similarly, low initial CD4+ counts lead to poor prognosis [130]. Not surprisingly, HIV-DNA levels are also associated with disease progression [130-134].

Development of HIV-specific CD8+ T-cells correlates with control of viremia and the end of the acute phase of infection; lack of an adequate CD8+ response can cause prolonged acute infection [135, 136]. However, the nature of the response is important, as a CD8+ response specific for Gag is associated with lowering viremia [137] more than that towards other viral proteins. Moreover, in patients with better viral control we see CD8+ cells that have increased proliferative capacity, antigen sensitivity, and cytokine production [138].

Not all those who become infected and remain untreated will develop symptoms and progress to AIDS: long-term non-progressors (LTNP) are those confirmed HIV+ but with CD4+ T-cell counts that remain above 200-400/ $\mu$ L [139]. This group, composed of ~8% of those infected,

stood out because they remained relatively healthy even without treatment. However, one early study tracking HIV+ patients over 78 months showed that LTNP experience a loss of CD4+ T-cells during the early stages of HIV infection which never recovers but remains their new baseline. This group theorized that LTNPs are not a distinct subpopulation of patients, but rather the extreme end of a distribution of CD4+ T-cell decay rates, and that they are still undergoing disease progression, albeit at a much reduced speed [140]. Many LTNPs have viremia and, like with the majority of HIV patients, their decline in CD4+ count is associated with the degree of viral load [141].

CD8+ T-cell function plays an important role in control of HIV infection, and many associations are seen with non-progression. CD8+ levels are higher in LTNPs as compared to progressors [139] or those uninfected [142]. When tested *ex vivo*, CD8+ T-cells from LTNPs have a greater proliferative capacity and higher perforin expression [143]. Similarly LTNPs have HIV-specific CD8+ T-cells with a higher quality HIV-specific response [144]. LTNP have increased NK cell activity compared to progressors [145], which can be explained at least in part by low CD8+ T-cell-mediated NK cell inhibition [146].

There are many noted genetic factors in non-progression, both in the virus as well as the host. The accessory genes of HIV in LTNP often carry mutations, while those of progressors are usually intact [147]. Nef is commonly mutated [148-152], and it's been shown that mutations in Nef can reduce replication potential of HIV [153]. Mutations in Vpr are seen in LTNPs [141], specifically R77Q which is associated with decreased T-cell apoptosis [154]. However it is seen in both slow-progressors and normal progressors [155], while one study found that R77Q had no impact on Vpr apoptotic activities. Vpr Q65R was inactive in degradation function and failed to

induce cell cycle arrest [156] and F77L was associated with decreased incorporation into virions [157]; both of these mutations have been seen in LTNP.

People homozygous for a 32 bp deletion in the CCR5 gene (CCR5 $\Delta$ 32) are naturally resistant to HIV infection [158], while heterozygosity is associated with slower disease progression [158-161]. Promoter variants of CCR5 which cause a higher amount of CCR5 expression are associated with disease progression, and are not often found in LTNP [162-164]. Similarly, CCR5 molecule density on the cell surface of non-activated CD4<sup>+</sup> T-cells is lower in slow-progressors [165]. However, since the deletion mutant has no effect on the disease in progressors and thus a potential protective role is not absolute, it's been suggested that there may be other factors coexisting in non-progressors [166].

Other cellular proteins have associations with disease progression. Higher expression or activity of the antiviral APOBEC3G is associated with higher CD4<sup>+</sup> counts and lower viral load [167, 168]. LEDGF/p75 polymorphisms may be associated with non-progression [169-171]. Several HLA variants are associated with non-progression: HLA-Bw4 [172, 173], HLA-B5701 [174, 175], and HLA-B57 [173, 175, 176]. These are associated with stronger CD8<sup>+</sup> T-cell responses to HIV through enhanced recognition of viral peptide presentation.

While LTNP are generally characterized by normal CD4<sup>+</sup> counts, there's a subset within that group that concurrently maintains a viral load of <50 copies/mL: elite controllers (and viremic controllers, who maintain a load of 50-2000 copies/mL). LTNP are estimated to be 5%-15% of the HIV<sup>+</sup> population, while elite controllers comprise <1%. [177]. However, these controllers can still experience CD4<sup>+</sup> T-cell loss [178, 179], and this may be in part due to higher levels of T-cell activation [180]. In one study, controllers who experienced viral blips <200 copies/mL had a significantly increased rate of pathological events such as drops in CD4<sup>+</sup> counts

and development of cancers [181]. As such, it is important to note that all types of non-progressors can eventually begin to lose CD4+ cells.

The mechanisms of elite control remain a focal point of much study. Unlike with some LTNPs, elite control is not associated with any viral genetic defects – controllers are infected with intact, fully competent virus [182]. While it's been shown that the CD4+ T-cells from elite controllers are just as susceptible to HIV infection [184], it's also been shown that they can resist infection through upregulation of p21, an inhibitor of cyclin-dependent kinases, which contributes to less effective reverse transcription and proviral DNA transcription [183]. A less contentious point is that, as seen in LTNPs, CD8+ T-cells play a large role in control. Elite controllers have high frequencies of HIV-specific CD8+ T-cells which can efficiently kill infected CD4+ T-cells [184], which is related to their ability to quickly express perforin [185]. Antibodies are important in elite control, however, they seem to exist mainly to assist CD8+ T-cell function, as elite controllers had levels of neutralizing antibodies lower than viremic patients, and comparable to patients on ART [186-188], while they displayed higher levels of antibody-dependent cell cytotoxicity (ADCC) than viremic patients [187, 189]. This ADCC-inducing antibody response that can also produce antibodies that can induce phagocytosis, complement activation, and NK cell activation; these effects are also induced by a lower antibody titer [190].

### **Post-ART control**

Upon cessation of ART, the vast majority of patients quickly experience viral load rebound within as fast as nine days as does the level of HIV-DNA in plasma [191, 192]. However some patients can maintain complete or partial control for longer periods of time. In one study of patients who started ART within three months of seroconversion the median time to viral rebound was 1.7 months, with 4.2% of patients maintaining a viral load of <50 copies/mL for 24

months [193]. Several studies have seen similar results, where starting ART early in infection leads to better control upon cessation of treatment [193-195]. Some patients can maintain post-treatment control for several years, the reasons for which are still not entirely known. They tend to lack the protective HLA-B alleles and even have alleles associated with disease progression, while their HIV-specific CD8+ T-cell response and overall immune activation status are both low [196, 197]. Viral rebound is associated with higher plasma HIV RNA [194] and DNA levels [131], shorter ART duration [198] and expression of T-cell exhaustion markers, such as PD-1, Tim-1, Lag-3 [199].

## **HIV Latency**

### **Discovery**

Initial evidence of HIV latency – a silent stage of HIV infection within a cell marked by a lack of viral protein production – came before 1991 in studies that showed a large disparity in the frequency of cells that express HIV RNA and those that harbor proviral DNA, especially evident in asymptomatic patients [200-203]. In 1995, inverse PCR used on resting CD4+ T-cells from infected patients showed fully integrated HIV, detecting higher frequencies in those with lower CD4+ counts, with some patients being undetectable [204]. In 1997, a culture assay was developed wherein resting CD4+ cells from patients are activated, thus activating latent provirus, and then cultured in activated CD8-depleted PBMCs from uninfected donors, allowing the virus to expand; p24 is then measured, and frequencies of latent cells can be detected by serial dilutions. This assay detected replication-competent virus in all patients studied and found latent provirus mainly in resting memory CD4+ cells [205].

These latent cells persist in the face of treatment, as replication-competent virus can be recovered from resting CD4+ T-cells from patients on successful ART for several years, at a

frequency of 0.2-16 /10<sup>6</sup> cells; the recovered virus shows no sign of evolution, and the frequency does not significantly decrease with time on therapy [206, 207]. The decay rate of the latent reservoir is very slow, with an estimated half-life of ~44 months; assuming a reservoir total size of 10<sup>6</sup>, this translates to over 70 years for eradication [208], which just reinforces HIV as a life-long disease. Ultrasensitive assays can detect HIV RNA in all patients tested, with levels as low as 1 copy/mL [209]. This shows that simply expressing HIV RNA does not mean virions will be produced.

### **Latent reservoirs**

Latently infected resting CD4+ T-cells are generated early in infection, before symptoms of primary infection even appear [210]. Starting ART early in infection cannot prevent the development of the latent reservoirs. Resting T-cells can be directly infected but integration is not completed – the viral DNA exists in an extrachromosomal form which can become integrated upon T-cell activation [211-213]; it is labile with a short half-life [214]. Transcription can still occur from these unintegrated forms [212, 215]; early viral proteins like Nef and Tat can induce T-cell activation [216], which could allow for integration to complete. However, fully integrated latent provirus in resting CD4+ cells is still transcribed, but inefficiently – short, abortive transcripts can be found, and fully processed spliced and unspliced forms can only be detected at a very low level [217]. Latency is thus defined by the lack of viral protein production, not simply lack of proviral transcription.

While resting cells can be directly infected *in vivo*, the majority of the reservoir lies in the memory subset – through direct infection of memory T-cells [218, 219] or formed after activated, infected cells revert to a resting memory phenotype; HIV provirus follows suit and enters a resting, latent state [220, 221]; there's also evidence of latent infection within T-



memory stem cells, which could be a self-renewing arm of the reservoir [222] and in T-regulatory cells [223]. The frequency of latently infected cells ranges from 1 in  $10^5$ - $10^8$ , largely influenced by when ART was initiated and the viral set point. Measurements also vary based on type of test used – DNA-based PCR assays will give higher values than those based on infectious virions produced or viral RNA expressed, as defective provirus will be counted [224, 225]. There's much debate in the field regarding the importance of such defective provirus – by its nature it'll be much harder to eliminate to achieve a sterilizing cure, wherein all HIV provirus is cleared from the body, as the lack of protein expression could make immune clearance impossible. However, since it cannot produce virions to spread the infection, it may not even be important to clear.

A major obstacle in identifying the latent reservoir stems from the very nature of latency – with little or no expression from the provirus, these cells are indistinguishable from uninfected cells without first stimulating them. On this front, some progress has been made. Using an *in vitro* model of HIV-1 infection of resting T-cells, one group found that CD32a is upregulated in latently infected cells; productively infected cells show no expression. They also found a subpopulation of CD32a+ cells from HIV+ patients which contains HIV-1 DNA and is enriched in inducible proviruses [226]. Grau-Exposito et al. also found an upregulation of CD32a in *ex vivo* infection of PBMCs, though they saw higher levels in cells expressing both viral RNA and protein [96]. IFITM1, a transmembrane protein induced by interferon which shows antiviral activity against HIV infection, was found to be upregulated in a cell model of latency and downregulated upon cellular activation. Upregulation was enough to induce killing by NK cells after labeling with an anti-IFITM1 antibody. The frequency of IFITM1+ CD4+ T-cells is increased in patients, including within the memory T-cell subset; sorted CD4+ cells from patients could

also be selectively labeled with anti-IFITM1 antibody and killed by autologous effector cells [227].

Since memory cells are quiescent and long-lived, the latent reservoir is very stable, making clearance by simple decay largely impossible during a lifetime. However, it's become apparent that there exists another complication – homeostatic proliferation. Latently-infected resting CD4+ T-cells can undergo mitogen-stimulated proliferation without reactivation of HIV. Sequencing studies have identified identical provirus from different cell populations within the same patients, indicating clonal expansion [228]; this can even be seen in samples taken up to five years apart [229]. The same results can be seen using single cell analysis, where identical HIV RNA sequences are seen in different cells taken from the same population at different time points [230].

It's been coming to light that the vast majority of provirus within an infected individual is defective. By analyzing samples from HIV-infected adults treated at different stages of infection, it's been shown that defective proviruses accumulate within 2-3 weeks after infection. This isn't surprising given the fact that up to 40% of provirus produced in a single-round *in vitro* infection can be defective; also, by its very nature defective provirus is more likely to avoid detection by the immune system. In an individual, over 90% of provirus is defective, and while early ART initiation can limit the size of the reservoir, it does not change the proportion of defects [231]. Expanding on this, it's been shown that during the course of the infection the proportion of provirus with hypermutations decreases, while that of provirus with large internal deletions increases. A striking finding is that defective proviruses can still produce RNA and that those containing hypermutations, multiple splice defects, or packaging signal defects can also produce protein and prime the cell for CTL-mediated killing [232, 233]. Interestingly, a study of

11 long-term suppressed children and adolescents who began ART before 6 months of age showed that their reservoirs were largely non-inducible and dominated by replication-defective genomes, mostly due to hypermutation or large deletions [234]. This stresses the importance of early treatment and poses an explanation for the post-ART control seen in such cases.

Studies have found that 1% or even less of the latent reservoir, as measured by HIV DNA levels, can be induced to express HIV RNA upon complete cellular activation – a state which should give maximal latent reactivation [235, 236]. One study found that while 88.3% of these non-induced proviruses are defective, 11.7% are fully replication-competent, integrated into active genes, and had hypomethylated LTRs. Furthermore, some provirus that was non-induced could be induced after repeated stimulation [237]. This was seen again in a recent study where multiple rounds of cellular stimulation can induce proviral activation in cells that were non-induced in previous rounds [238]. These results suggest that viral reactivation is a stochastic process.

One prominent question has been whether HIV persists solely through latent reservoirs or if there exists a ‘smoldering infection,’ perhaps in tissues where ART penetrance is low. The main reason for this debate is the presence of low level viremia – HIV RNA can be found in most patients who have reached undetectable status, at levels below 50 copies/mL. However, if this was due to active infection rather than simply reactivating latent cells, then viral evolution would be observed due to the high mutation rate; this is not seen [239-243]. Furthermore, virus that emerges during treatment interruptions is homogenous and similar to specific sequences obtained pretreatment, and varies between interruptions – implying that distinct latent reservoirs get reactivated once ART is ceased [244].

### **Notable cases of HIV “cures”**

A serendipitous confluence of circumstance led to excitement throughout the world with the first ever recorded case of an HIV cure with the “Berlin patient,” an HIV+ male with acute myeloid leukemia who received a CD34+ peripheral-blood stem cell transplant from a *CCR5Δ32* homozygous donor subsequently and tested negative for HIV despite lack of ART [245]; years of follow-up have confirmed that he remains free of any detectable HIV [246]. The *CCR5Δ32* mutation conferred resistance to R5-tropic virus and cured the patient of HIV infection. While such a procedure is by no means an effective cure on a wide scale – due to the rarity of *CCR5Δ32* homozygotes and the cost and risk of a stem cell transplant – it did demonstrate that a cure is possible. It is also not an absolute cure, as when a similar transplant was done in another patient, the virus rebound with an X4-tropism [247].

Several studies have followed HIV+ patients undergoing cancer treatment, without a *CCR5Δ32* donor, to see what effect ablation and reconstitution of the immune systems would have on the HIV reservoir. Two HIV+ patients who underwent hematopoietic stem cell transfer for lymphomas were initially free of detectable HIV DNA or viral outgrowth in coculture assays. However, several months after ART interruption, they each tested positive for HIV and concurrently had symptoms of acute infection; interestingly, it was shown that only one or a few provirus contributed to the rebound [248]. The treatment did, however, reduce the size of the latent reservoir [249]. Similar reductions have been seen in other studies of patients undergoing stem cell transplant [250-254].

There have been several other notable cases which have given hope for a cure, all involving infants born to HIV+ mothers. The so-called “Mississippi baby” began ART 30 hours post birth; samples taken around the same time confirmed presence HIV DNA and RNA. At 18

months, ART was discontinued, and both HIV and DNA were undetectable at 30 months [255]. However, a clinical follow-up at 46.4 months showed a viral rebound [256]. In another case, a child born to a HIV+ mother received treatment within 30 minutes of birth, however upon cessation at 48 months HIV RNA was readily detected within 7 days [257]. In a more positive light is the “French teenager,” an infant born to HIV+ mother who received zidovudine for six weeks, and then was switched to ART at 3 months when HIV RNA spiked. She was taken off treatment between 5-8 years of age and, as of 18 years of age, has maintained undetectable levels of HIV RNA with low levels of HIV DNA [258]. While the ‘Berlin patient’ is an example of a sterilizing cure whereupon HIV was eradicated from his body, this patient exhibits a ‘functional cure’ where virus is maintained at low levels without ART, copying the elite controller phenotype.

### **Mechanisms of latency**

Where and how HIV integrates into the genome has an expectedly large effect on its expression. As mentioned above, integration is nonrandom and favors actively transcribed genes – sites chosen tend to be dense with non-inhibitory histone modifications [259]; however, integration sites can influence basal transcription positively or negatively, independently of methylation or acetylation status [260]. Orientation also matters, as transcriptional interference can occur where the RNA Pol II transcribing the host gene displaces that at the HIV-LTR, preventing proviral transcription; the transcribed provirus will be part of an intron and subsequently degraded [261]; evidence of this can be found in primary cells through the detection of host-viral chimeric transcripts [262]. If the interference is strong enough, it can prevent transcription of the provirus, leading to a latent state.

While integration site alone can influence HIV transcription, the chromatin environment has a very large effect as well. Repressive epigenetic modifications have been associated with latency, such as histone methylation [263-267], histone deacetylation [263, 268], and DNA methylation [269], although a recent study found little HIV DNA methylation within primary resting CD4+ T-cells from aviremic patients [270]. In many cases the methyltransferases and deacetylases themselves are also associated with the chromatin around the LTR.

HIV 5'-LTR is bound by two nucleosomes, nuc-0 and nuc-1 [271]. These are the nucleosomes largely implicated in latency, being targeted by various repressive proteins – particularly nuc-1 as it is situated around the transcription start site and can thus influence RNA Pol II (RNAPII), which is bound to the LTR-promoter, in a paused state [272]; this accounts for the short abortive transcripts found in latently infected cells – RNAPII cannot complete transcription without the help of Tat or activating transcription factors. Along with stabilizing transcription through PTEF-b, tat also recruits chromatin remodeling proteins [273, 274].

Transcription factors can act both positively and negatively on HIV expression, and the LTR contains binding sites for many factors [275], most notably NFkB, Sp1, AP-1, and NFAT. NFkB and NFAT activity are both upregulated by engagement of the T-cell receptor (TCR) and are involved in T-cell activation [276, 277]; thus, it is no surprise that they also serve to activate HIV directly through binding to the promoter. NFkB p50/p65 heterodimers bind with Sp1 and other factors like Lef-1 to activate transcription [278]; these heterodimers also cause PTEF-b activation and recruitment [279]. This is in contrast to the latent state, where NFkB p50 homodimers and Sp1 recruit HDAC1 to the LTR [280]; LSF, YY1, and CBF-1 can also bind the LTR with HDACs [281-283].

HIV infection of resting CD4+ T-cells sees the same biases in integration site selection as seen in other cells: within the introns of actively transcribed genes with no preference for orientation [284, 285]. PTEF-b activity in resting cells is low due to low expression of one of its components – Cyclin T1 – and low levels of phosphorylation of another component – CDK9; this activity increases upon cellular activation [286] and drops again if the cell reverts to a memory phenotype [287]. Furthermore, there's evidence that mRNA for Tat and Rev get retained in the nucleus; overexpression of polypyrimidine tract binding protein (PTB), an HIV RNA-binding protein upregulated in activated T-cells, allowed for mRNA export and subsequent virus production [288].

### **Latency-reversing agents**

The major goal of HIV persistence research lies in a cure, be it a sterilizing cure like the 'Berlin patient' where HIV is eradicated from the body or a functional cure like the 'French teenager' where HIV is controlled without drug therapy and maintained below detectable levels. One prevailing idea for a cure is a 'shock and kill' method wherein patients are treated with latency-reversing agents (LRAs) to reactivate the latent reservoir, leading to the death of these cells by viral cytopathic effects or immune system detection; cotreatment with ART will prevent new infections while the reservoirs are activated and eliminated. To this end, our lab and others work to investigate the different pathways involved in forming and maintaining latency in order to find, ideally, small-molecule drugs which work as LRAs without widespread side effects or immune system activation.

Given the strength of HIV reactivation seen with NFkB signaling, it has been a popular target in persistence research. One major class of LRAs are the protein kinase C (PKC) agonists which activate various isoforms of PKC, culminating in activation of NFkB [289]. PKC agonists

such as prostratin [290], bryostatin [291], and ingenol-3-angelate [292] have all been shown to reactivate latent HIV while also inhibiting infection via CD4 and CXCR4 downregulation [293-295]. However, activating through NFkB raises the concern of T-cell activation, which is unfavorable in an LRA as systemic immune activation is harmful [296]. Two important markers of T-cell activation, CD25 and CD69, are upregulated by prostratin and bryostatin [297, 298], though one study found bryostatin lacking in this ability [295]. In our own experience, our lab found PKC agonists to upregulate these markers, which caused us to shy away from investigating them further.

As epigenetics play a large part in maintaining HIV latency, it comes as no surprise that compounds which modify chromatin and DNA can also activate HIV. Since as early as 1996 it's been known that HDAC inhibitors (HDACI) have the ability to reactivate latent HIV [299]. Similar to the PKC agonists, they've also been shown to downregulate CXCR4 [300]. HDACIs have an advantage over many other LRAs in that they're already used clinically, such as phenylbutyrate for sickle-cell anemia [301], valproic acid for epilepsy and bipolar disorder [302], and for cancer, such as vorinostat (or SAHA) [303] and romidepsin [304] for T-cell lymphoma and panobinostat for multiple myeloma [305]. These and various other HDACIs have been shown to reactivate HIV in resting CD4+ T-cells from aviremic HIV+ patients [306-309]. Indeed, HDACIs are among those drugs being investigated in clinical trials for purging the latent reservoir. While an early trial of valproic acid found a reduction in the HIV reservoir [310], several trials since found no change [311-313]. Trials of SAHA likewise found an increase in plasma HIV levels but no change in the reservoir size [314, 315]. Romidepsin can raise plasma RNA levels from undetectable to above 50 copies/mL when administered to patients [316]; other trials are underway investigating romidepsin by itself (NCT01933594) or in combination with a broadly-neutralizing antibody (NCT02850016) or therapeutic HIV vaccine (NCT02092116).



Histone and DNA methylation can also be inhibited to allow for HIV transcription.

Histone methyltransferases such as PRC2, EHMT2 [317], and SMYD2 [318] have been found to associate with the 5'-LTR and become displaced upon latency reversal, and that small-molecule inhibitors can reverse latency in resting CD4+ T-cells from patients. Chaetocin and BIX-01294, which inhibit SUV39H1a and G9a respectively, can also activate HIV in patient samples, and have been shown to work synergistically with SAHA or prostratin [319]. While the DNA methyltransferase inhibitor decitabine has been shown to be an LRA in cell lines [269, 320], the role of DNA methylation is somewhat controversial as one study found large amounts of 5'-LTR hypermethylation [321] in patient samples while another found little [270]; however the Van Lint group found decitabine to be an active LRA in patient samples and synergistic with HDACIs [322].

Stimulating HIV transcription through enhancement of elongation is another latency reversal strategy; targeting this pathway takes advantage of the fact that RNAPII is paused at the promoter, ever ready to elongate. Bromodomain containing 4 (BRD4) blocks Tat-mediated recruitment of the elongation complex to the 5'-LTR; the BET bromodomain inhibitor JQ1 can block this interaction and dissociate BRD4 from the LTR, activating latent HIV [323]. JQ1 can also increase PTEF-b levels by dissociating it from the inhibitory 7SK snRNP complex [324], thus serving to stimulate elongation on two fronts. However, in resting cells from aviremic patients JQ1 is not very active on its own, through it synergizes with PKC agonists and T-cell activation [325, 326]. Similarly, HMBA – which causes release of PTEF-b and activation of HIV [327] – was recently found to also inhibit BET bromodomain proteins, displacing them from chromatin [328].

The LRA repertoire is constantly growing, often times with new compounds in known classes, but sometimes unique activation pathways are found. Benzotriazoles work by inhibiting

STAT5 SUMOylation, thus increasing binding of STAT5 directly to the HIV-1 LTR [329]. One study identified benzazole compounds which activate latent HIV in cell models and don't act through T-cell activation, NFkB, nor HDAC inhibition, and which don't work upon other latent viruses [330]. Smac mimetics – small molecules which mimic a tetrapeptide sequence able to bind to inhibitor of apoptosis proteins (IAPs) – can inhibit BIRC2, allowing for non-canonical NFkB activation. They've been shown to activate HIV-1 in resting T-cells from infected individuals, and to act synergistically with HDACs [331]. Our group recently implicated the ubiquitin-proteasome system (UPS) in latency, showing that inhibiting the 26S proteasome results in both viral activation and reduced infectivity [332].

Given that, as seen above, only a small amount of the latent reservoir can be reactivated even with cellular activation, it should be no surprise that no current LRA can achieve consistently high levels of latency activation. In fact, one study compared LRAs using several different primary cell models, cell line models, and patient samples, and found that only PKC agonists consistently showed activity [333]; this was echoed in another study in which only bryostatin induced viral outgrowth from patient cells [334]. It's becoming increasingly obvious that a multi-pronged approach is necessary, targeting different latency mechanisms in order to achieve a synergistic reactivation effect. Using resting CD4+ cells from aviremic patients, one group found that single drug treatments with JQ1, HDACIs or PKC agonists resulted in only little to mild activation, while combination of JQ1 or HDACIs with either bryostatin or prostratin led to synergistic activity [335]. Similar results have been seen using PKC agonists with JQ1 [292, 336], HDACs with PKC agonists [337, 338], and HDACIs with a DNA demethylating agent [322].

### **HIV and the ubiquitin-proteasome system**

Another issue with current known LRAs is the lack of specificity. HDACs, HMTs, and DNMTs are enzymes which affect and are physically associated with many genes, not just the 5'-LTR of HIV. Likewise, NFκB is a major transcription factor and, in T-cells, controls cellular activation, a process that must be avoided in HIV purging strategies, while PTEF-b is central to transcriptional elongation. Inhibitors or modulators of these proteins have effects on many different pathways within the cell. In looking for more specificity, our lab was drawn to the UPS from the results of an RNAi screen looking at cellular factors involved in maintaining HIV latency, in which various proteins from the UPS were highly represented. Briefly, this protein degradation pathway starts with activation of ubiquitin by E1 enzymes, then the transfer of the thioesterified ubiquitin to E2. E3 then recognizes and binds the protein substrate and E2, after which ubiquitin is transferred to the substrate; a poly-ubiquitin chain of four or more is required to direct the substrate to the 26S proteasome, where it is degraded. Mammalian genomes code for two E1 enzymes, ~40 E2, and over 600 E3, and it is the combinations of different E2s and E3s which give this system its ability to specifically degrade numerous different targets [339]. By identifying specific UPS pathways and E3 ligases which maintain HIV latency, we posit that we can then identify small molecule inhibitors of said E3 ligases, allowing for the development of LRAs which act to more specifically reverse latency and thus have fewer off-target effects.

HIV and the UPS have already been shown to be intimately linked. Several viral proteins hijack this system to enhance infection: Vpr and Vif can both target interferon regulatory factor 3 (IRF-3), an early antiviral protein, for proteasomal degradation [340], while Vpr also uses DDB1-CUL4A E3 ligase to ubiquitinate unknown cellular proteins, ultimately leading to G2 arrest [341] and Vif targets the antiviral protein APOBEC3G for ubiquitylation by forming a complex with the E3 ligase components CUL5/RBX2, ELOB, and the transcription factor CBF-β [342]. Vpu

exerts its effect by using the E3 ligase  $\beta$ -TRCP to ubiquitinate both CD4 and the antiviral protein tetherin [343, 344]. Ubiquitylation also directly controls at least two transcription factors which can activate HIV transcription –  $\beta$ -catenin which is constantly degraded by  $\beta$ -TRCP until an activating signal prevents its ubiquitylation and NF $\kappa$ B which is bound by an inhibitory I $\kappa$ B complex until an activating signal causes ubiquitylation of I $\kappa$ B [345]; both of these transcription factors can directly bind the HIV 5'-LTR and stimulate transcription.

The UPS is already being investigated as a major drug target. Velcade (or bortezomib) is a proteasome inhibitor currently FDA-approved for the treatment of multiple myeloma and mantle cell myeloma [346], while carfilzomib is a second-generation proteasome inhibitor, FDA-approved for relapsed and refractory multiple myeloma, including use in patients for whom bortezomib treatment failed [347]. Specific E3 ligase inhibitors have also been developed, such as the nutlins, a class of compounds that can disrupt the interaction between the E3 ligase MDM2 and the tumor suppressor p53, preventing its ubiquitylation [348], and PRT4165 which inhibits both RNF2 and RING 1A [349] or inhibitors of Skp2 [350, 351]. A clever drug development strategy has emerged which utilizes bifunctional molecules that can bind E3 ligases to specifically target a protein – proteolysis-targeting chimeras (PROTACS). These molecules contain two functional groups – one which binds the protein of interest while the other binds an E3 ligase – and can direct said protein to become ubiquitylated and, ultimately, degraded. This can allow for the inhibition of so-called 'undruggable' targets – proteins which lack enzymatic activity and are thus much harder to target chemically. Peptide PROTACS have utilized large molecules, such as a long sequence from I $\kappa$ B which is recognized by the E3  $\beta$ -TRCP. Small molecule PROTACS have also been developed, such as ARV-825 which binds both the oncoprotein BRD4 and the E3 cereblon, causing proteasomal degradation of BRD4 [352].



## **Chapter 2: Identification of Genes and Pathways Involved in Maintenance of HIV-1 Latency Utilizing an RNAi Screen**

### **Abstract**

Latent human immunodeficiency virus type I (HIV-1) infection represents a barrier to virus eradication as latent HIV-1 is impervious to the effects of antiretroviral drugs and can avoid detection by the host immune system. Strategies to clear latent HIV-1 infection in patients have so far failed in clinical trials, underscoring the need for continued study of HIV-1 latency. To uncover cellular genes and pathways involved in the maintenance of HIV-1 latency, we employed a genome-wide RNA interference screen. One of the validated gene “hits” from the screen was proteasome subunit, alpha type, 7 (PSMA7). We were able to show that the knockdown of PSMA7 activated latent HIV-1 in the context of decreased proteasome function. These results, in conjunction with the finding that additional genes belonging to the ubiquitin-proteasome system (UPS) were also identified as “hits” in the screen, led to the hypothesis that the UPS is important in the maintenance of HIV-1 latency. This hypothesis was supported by experiments indicating that proteasome inhibitors (PIs) can activate latent HIV-1 transcription. Further analysis of the screen results suggested that Wnt/ $\beta$ -catenin signaling pathway might be involved in the activation of latent HIV-1. Since  $\beta$ -catenin is subjected to proteasomal degradation in the absence of Wnt signaling, experiments were performed to determine if  $\beta$ -catenin mediated the latency antagonist effects of PIs. It was found that PIs stabilize  $\beta$ -catenin protein levels and result in the association of  $\beta$ -catenin with the HIV-1 5' promoter region. Moreover, downregulation of  $\beta$ -catenin resulted in a significant reduction in the magnitude of PI-mediated activation of latent HIV-1. Therefore, this study suggests that the UPS is involved in maintaining HIV-1 latency, at least in part, through the regulation of  $\beta$ -catenin.

## **Introduction**

It is estimated that 34 million people worldwide are infected with human immunodeficiency virus type 1 (HIV-1) [353]. Despite effective antiretroviral therapy (ART), a cure for the infection is still out of reach. An important reason for this is the fact that HIV-1 establishes latency early in the course of the infection [354] and to-date, there are no FDA-approved drugs capable of effectively targeting latent virus. Therefore, infected individuals must remain adherent to lifelong ART to avoid significant viral rebound and the development of drug resistance; thus it is necessary to continue to study virus-host interactions that regulate HIV-1 latency to support the development of strategies to eliminate persistent HIV-1 infection.

Post-transcriptional gene silencing via RNA interference (RNAi) is a valuable experimental tool for performing functional gene studies. The RNAi pathway is found in a wide range of eukaryotic cells, including mammalian cells, and appears to have evolved as a biological defense mechanism against RNA viruses (reviewed in [355]). It is triggered by double-stranded RNA, which is processed into small interfering RNAs (siRNAs) that can subsequently bind complementary cellular mRNAs, resulting in their downregulation [356, 357]. Genome-wide libraries have been designed for large-scale RNAi-based screening [358, 359] and employ either short hairpin RNAs (shRNA), typically expressed from retroviral vectors, or siRNAs. Four whole-genome RNAi screens have been performed to uncover cellular factors involved in HIV-1 replication (reviewed in [360]). Despite almost no overlap in terms of the specific cellular factors identified in each screen, they each elucidated similar biological pathways and gene function clusters, as well as previously unidentified factors and pathways that are important for HIV-1 replication [360]. Therefore, these studies demonstrate the potential utility of RNAi technology to explore cellular regulators of HIV-1 latency.

In this study, a genome-wide RNAi screen was performed to probe cellular factors involved in maintaining HIV-1 latency. Results from the screen indicated a novel role for the ubiquitin-proteasome system (UPS) in the regulation of HIV-1 latency. It was demonstrated that proteasome inhibitors (PIs) potentially activate latent HIV-1 transcription in an *in vitro* model system. Although the UPS is best known for its highly regulated proteolytic function, it has become clear that the UPS plays an important role in gene expression utilizing both its proteolytic and nonproteolytic activities [361]. Mechanistically, experiments indicate that PIs activate latent HIV-1, at least in part, through the stabilization of the transcription factor  $\beta$ -catenin. More specifically, PIs stabilize  $\beta$ -catenin protein levels and enrich  $\beta$ -catenin association with the HIV-1 5' LTR. Of note,  $\beta$ -catenin can form a transcriptionally active heterodimer with lymphoid enhancer binding factor 1 (LEF1) in the nucleus, which has been shown to bind sites within the HIV-1 promoter and result in the upregulation of HIV-1 transcription [362-365]. Finally, we show that the shRNA-mediated downregulation of  $\beta$ -catenin reduces the activation of latent HIV-1 induced by PI treatment. Taken together, the results presented here demonstrate a role for the UPS in the regulation of HIV-1 latency.



## **Materials and Methods**

### **Cells and culture media**

HeLa#14 cells were cultured in MEM GlutaMAX medium (Life Technologies, Grand Island, NY) supplemented with 10% FetalClone III Serum (Thermo Scientific Hyclone, Logan, UT), 2X MEM Non-essential amino acids solution (Life Technologies, Grand Island, NY), and 100U/mL penicillin-100µg/mL streptomycin solution (Life Technologies, Grand Island, NY). The construct present in HeLa#14 cells (RLUC/RFP) is an HIV-1<sub>NL4-3</sub>-based construct harboring *Renilla luciferase* (RLUC) in the *env* position and *red fluorescence protein* (RFP) in the *nef* position. The RLUC/RFP construct has a 2.5 kbp deletion in *pol* and a 1.0 kbp deletion in *env* to render the vector replication-incompetent. Additionally, the *vpu* start codon is mutated for robust marker gene expression [366]. OM-10.1 (from Dr. Salvatore Butera, NIH) and human primary resting CD4<sup>+</sup> T cells were cultured in RPMI 1640 GlutaMAX, HEPES medium (Life Technologies, Grand Island, NY) supplemented with 10% fetal bovine serum (Thermo Scientific Hyclone, Logan, UT), 2X MEM Non-essential amino acids solution, and 100U/mL penicillin-100µg/mL streptomycin solution. Human primary resting CD4<sup>+</sup> T cells were isolated from leukocyte enriched blood samples from healthy adult donors purchased from the New York Blood Center. To obtain a purified population of peripheral blood mononuclear cells, buffy coats were isolated from the blood by a Ficoll gradient using Histopaque 1077 (Sigma Aldrich, St. Louis, MO). Red blood cells were lysed using ACK lysing buffer (Lonza, Inc., Allendale, NJ). Resting CD4<sup>+</sup> T cells were then isolated using the Dynabeads Untouched™ Human CD4<sup>+</sup> T Cells kit (Life Technologies, Grand Island, NY) according to the manufacturer's instructions with the addition of mouse IgG anti-human CD25 antibody (BD Biosciences, Franklin Lakes, NJ) to remove activated T cells.

### **Reverse genetic screen**

A generic summary is shown in Fig. 2.1. HeLa#14 cells and HeLa cells were each seeded in ten 100 cm tissue culture plates at  $2.5 \times 10^6$  cells per plate. The number of plates needed was calculated as follows:  $200,000 \text{ shRNA constructs} \times 25\text{-fold coverage (the desired titer)}/0.2$  (the desired multiplicity-of-infection [MOI]) =  $2.5 \times 10^7$  total cells to infect/ $2.5 \times 10^6$  cells per plate = 10 plates. In parallel, an extra 100 mm plate ( $2.5 \times 10^6$  cells) and a 6-well plate ( $5 \times 10^5$  cells per well) were seeded with HeLa cells to facilitate MOI analysis following transduction. Twenty-four hours later, the GeneNet Genome-wide Human 50K Lentiviral shRNA library (System Biosciences, Mountain View, CA) was diluted 8,000-fold in serum-free culture media containing  $8 \mu\text{g/mL}$  polybrene (Sigma-Aldrich, St. Louis, MO). Culture media was removed and 5 mL of diluted virus was added to the cells in the 100 mm plates. Five, 10-fold serial dilutions were made from the initial 8,000-fold diluted virus and were added to the cells in the 6-well plate at 1 mL per well. Cells were incubated with virus for 6 hours and were then washed twice with 1X phosphate buffered saline and then cultured in standard culture media.

Two days post-transduction, puromycin (Sigma-Aldrich, St. Louis, MO) was added to the culture media ( $0.75 \mu\text{g/mL}$ ) to select transduced cells. Four days post-transduction, genomic DNA was isolated from the extra 100 mm plate of infected HeLa cells for copy number quantitative polymerase chain reaction (qPCR) to analyze the actual multiplicity of infection (MOI). Genomic DNA was isolated from  $1.5 \times 10^7$  infected HeLa cells using the GenElute Mammalian Genomic DNA Miniprep Kit (Sigma-Aldrich, St. Louis, MO) according to the manufacturer's instructions. A standard curve was set up using linearized Positive Control DNA (System Biosciences), which represented a range from  $1 \times 10^6$  copies to 10 copies. The qPCR reactions contained 300 ng genomic DNA (corresponding to  $\sim 8.57 \times 10^4$  genome equivalents assuming 3.5 pg of DNA per cell [75]), Maxima Sybergreen qPCR Master Mix (Thermo Scientific Fermentas, Waltham, MA), and the puromycin resistance gene primer set (Forward 5'-GGTCACCGAGCTGCAAGAACT-3' and

Reverse 5'-ACCCACACCTTGCCGATGT-3'). qPCR was performed using the BioRad CFX 96 Real-Time System C1000 Thermal Cycler with the following program settings: 95°C for 10 minutes, followed by 40 cycles of 95°C for 15 seconds, 60°C for 30 seconds, 72°C for 30 seconds, 75°C for 5 seconds, followed by a melt curve. The puromycin resistance gene copy number was extrapolated from the standard curve and the MOI was calculated as follows:  $3.391 \times 10^4$  puromycin resistance gene copies /  $8.57 \times 10^4$  genome equivalents = MOI of  $\sim 0.395$ .

Five days post-transduction, puromycin selection media was refreshed on all cells. Seven days post-transduction, all cells were expanded into 150 mm tissue culture plates and puromycin selection media was refreshed. Nine days post-transduction, puromycin selected colonies were counted in the 6-well plate to obtain a second measure of the actual MOI. Two hundred and one colonies were counted in the 1,000-fold dilution well. The titer was calculated as follows:  $(201 \text{ colonies} \times 1,000 \text{ dilution factor}) / 1 \text{ mL of virus added to the well} = 2.01 \times 10^5$  infectious units (IFUs)/mL. The MOI was then calculated as follows:  $(2.01 \times 10^5 \text{ IFUs/mL} \times 5 \text{ mL virus added to the plates}) / 2.5 \times 10^6 \text{ cells (number of cells seeded in the plates)} = \sim 0.402$ . Ten days post-transduction, 25% of the cells were moved into new 150 mm plates (as per System Biosciences technical staff instruction in order to maintain proper genomic coverage of the transduced library) and puromycin selection media was refreshed. At 14 days post-transduction, 33% of the cells were moved to new 150 mm plates (as per System Biosciences technical staff instruction) and puromycin selection media was refreshed. Finally, at 17 days post-transduction, cells were flash frozen in liquid nitrogen (a total of  $3.8 \times 10^8$  HeLa cells and a total of  $4.1 \times 10^8$  HeLa#14 cells) and shipped overnight to System Biosciences. System Biosciences performed the cell lysis, isolated the total RNA, reverse transcribed and amplified cDNAs, and hybridized the cDNAs to an Affymetrix GeneChip Array (HG-U133+ 2.0) for shRNA identification according to GeneChip Expression Analysis Technical Manual (P/N 702232 Rev. 3) protocols. Microarrays were scanned

using GeneChip Scanner 3000 7G and hybridization signals were normalized and summarized as gene expression values using Affymetrix GeneChip Operating Software (v1.4), at which time the data was sent back to our laboratory. shRNA probe IDs were assigned gene names using System Biosciences GeneNet software. The microarray data have been deposited in NCBI's Gene Expression Omnibus (GEO) [76] and are accessible through GEO series accession number GSE59758 (<http://www.ncbi.nlm.nih.gov/geo/query/acc.cgi?acc=GSE59758>). Redundant siRNA activity (RSA) analysis software (Release 1.2) was downloaded from <http://carrier.gnf.org/publications/RSA/> and the analysis was performed according to their instructions [24]. Interactive Pathway Analysis of complex 'omics data (IPA) software (Ingenuity Systems, Redwood City, CA) version 1.0 was used for functional annotation clustering analysis according to their instructions.

### **Screen “hit” validations**

HeLa#14 cells were transiently transfected with either GIPZ lentiviral shRNA constructs targeting the genes listed in Fig 2.2 or with a scrambled duplex (SD) non-silencing lentiviral shRNA construct (Thermo Fisher Scientific, Waltham, MA). The pGIPZ construct expresses eGFP from a cytomegalovirus promoter and a puromycin resistance gene/shRNAmir construct fusion from an internal ribosome entry site. Twenty-four hours prior to transfection, HeLa#14 cells were seeded in 6-well plates at  $2 \times 10^5$  –  $5 \times 10^5$  cells per well. A pool of three to four GIPZ shRNAs, each targeting a different sequence within a specific gene, were transfected into duplicate wells at concentrations of approximately 1.0  $\mu$ g - 1.3  $\mu$ g DNA per construct (for pools of four or three shRNAs, respectively) for a total of approximately 4  $\mu$ g DNA per well. SD was transfected into duplicate wells at a concentration of 4  $\mu$ g DNA per well. The transfections were performed using

Lipofectamine 2000 (Life Technologies, Grand Island, NY) according to the manufacturer's instructions.

Ninety-six hours post-transfection, the number of transfected (GFP+) and total live HeLa#14 cells were determined via standard trypan blue exclusion test and quantification using fluorescence microscopy and cell counting with a hemocytometer. Then, cells were lysed and protein concentrations were measured via standard Bradford assay (Bio-Rad Laboratories, Hercules, CA), and RLUC activity was measured using the Renilla luciferase Assay System (Promega, Madison, WI) according to the manufacturer's instructions. Luminescence was measured on the Turner Biosystems 20/20n Luminometer with a 10 second integration setting.

#### **Confirmation of PSMA7 mRNA knockdown and subsequent proteasomal inhibition**

To confirm the knockdown of PSMA7 mRNA, HeLa#14 cells were transiently transfected with either GIPZ lentiviral shRNA constructs targeting PSMA7 or with a scrambled duplex non-silencing lentiviral shRNA construct. Twenty-four hours prior to transfection, HeLa#14 cells were seeded in 6-well plates at  $2.5 \times 10^5$  cells per well. A pool of 3 GIPZ shRNAs, each targeting a different sequence within PSMA7, was transfected into triplicate wells at a concentration of approximately 1.3  $\mu$ g DNA per construct for a total of approximately 4  $\mu$ g DNA per well. SD was transfected into triplicate wells at a concentration of 4  $\mu$ g DNA per well. The transfections were performed using Lipofectamine 2000 (Life Technologies, Grand Island, NY) according to the manufacturer's instructions.

Forty-eight hours post-transfection, the number of transfected (GFP+) and total live HeLa#14 cells were determined via standard trypan blue exclusion test and quantification using fluorescence microscopy and a hemocytometer. Cells were then lysed and total RNA was isolated using TRIzol Reagent (Life Technologies, Grand Island, NY) according to the

manufacturer's instructions. RNA samples were then treated with RQ1 DNase (Promega, Madison, WI) according to the manufacturer's instructions. Reverse transcription PCR was performed to convert RNA to cDNA using the High-Capacity cDNA Reverse Transcription Kit employing random primers (Applied Biosystems (ABI), Foster City, CA) according to the manufacturer's instructions. The cDNA was then used as a template for qPCR to determine PSMA7 mRNA expression levels. The qPCR reactions contained Power Sybergreen Green PCR Master Mix (ABI, Foster City, CA) and one of the following primer sets: the PSMA7 primer set (Forward 5'-GTTTCGACTTTGATGGCACTC-3' and Reverse 5'-CATCTGTTTCAATGGCTTCGTC-3') or the GAPDH (glyceraldehyde 3-phosphate dehydrogenase; reference gene) primer set (Forward 5'-AATCCCATCACCATCTCCAG-3' and Reverse 5'-CTTCTCCATGGTGGTGAAGAC-3'). qPCR was performed using the BioRad CFX 96 Real-Time System C1000 Thermal Cycler with the following program settings: 95°C for 10 minutes, followed by 40 cycles of 95°C for 15 seconds, 60°C for 30 seconds, followed by a melt curve.

To analyze proteasomal activity following PSMA7 knockdown, HeLa#14 cells were seeded in 6-well plates at  $4 \times 10^5$  cells per well. Twenty-four hours later, HeLa#14 cells were transfected in duplicate with either a pool of three GIPZ shRNAs targeting PSMA7 or with SD shRNA as described above. Forty-eight hours post-transfection, the number of transfected (GFP+) and total live HeLa#14 cells were determined via standard trypan blue exclusion test and quantification using fluorescence microscopy and a hemocytometer. Then,  $1 \times 10^4$  cells from each well were collected and proteasome function was measured using the Proteasome-Glo Chymotrypsin-Like Cell-Based Assay (Promega, Madison, WI) according to the manufacturer's instructions. Luminescence was measured on the Turner Biosystems 20/20n Luminometer using default settings.

### **PI treatment to analyze activation of latent HIV-1 transcription**

To confirm that PIs inhibit proteasomal activity, HeLa#14 cells were plated in 6-well plates at  $4 \times 10^5$  cells per well. Twenty-four hours later, cells were treated in duplicate with 15 nM Velcade (Selleckchem, Houston, TX) or were left untreated (negative control). Two hours post-treatment,  $1 \times 10^4$  cells from each treatment were collected and proteasome function was measured as described above.

To analyze PI-mediated activation of HIV-1 transcription, HeLa#14 cells were plated in 6-well plates at  $4 \times 10^5$  cells per well. Twenty-four hours later, cells were treated in duplicate with 15 nM Velcade or were left untreated. At the indicated time points, total RNA was isolated, treated with DNase, and reverse transcribed as described above using the High-Capacity cDNA Reverse Transcription Kit (Applied Biosystems, Foster City, CA). The cDNA was then used as a template for qPCR to determine RLUC RNA expression levels. qPCR was performed as described above with the following primer sets: the RLUC primer set (Forward 5'-CAAAGAGAAAGGTGAAGTTCGTC-3' and Reverse 5'-TGTACAACGTCAGGTTTACCAC-3'), or the GAPDH (reference gene) primer set (described above).

### **Western Blots**

OM-10.1 cells were plated in 6-well plates at  $2 \times 10^6$  cells per well. Human primary resting CD4<sup>+</sup> T cells were plated in 12-well plates at  $5 \times 10^6$  cells per well. Immediately, cells were treated with 10 nM Velcade or were left untreated (negative control) for 4h, 12h, and 24h (time course). Protein lysates were isolated using the PARIS kit (Life Technologies, Grand Island, NY) according to the manufacturer's instructions. Proteins (25  $\mu$ g) were separated on a 7.5% SDS-PAGE gel. Membrane transferred proteins were detected with rabbit IgG anti-human  $\beta$ -catenin, clone D10A8 antibody (Cell Signaling, Danvers, MA) or with rabbit IgG anti-human  $\beta$ -actin, clone D6A8

antibody (Cell Signaling, Danvers, MA) as a loading control. Band signals were detected using the Supersignal Femto Fast Western Blot Kit (Thermo Scientific Pierce, Rockford, IL) according to the manufacturer's instructions. Kodak Image Station 4000R (Kodak, Rochester, NY) and Carestream Molecular Imaging Software (Carestream Health inc., Rochester, NY) were used to quantify the signal. Signal intensity of  $\beta$ -catenin bands was normalized to those of  $\beta$ -actin bands for each sample.

### **Chromatin Immunoprecipitation**

OM-10.1 cells were plated in 100 mm tissue culture dishes at  $1 \times 10^7$  cells per dish. Immediately, cells were treated with 15 nM Velcade or were left untreated. Six hours post-treatment, cells were collected and incubated in a 1% formaldehyde solution on a rocking platform for 30 minutes at room temperature to crosslink. To quench the crosslinking reaction, glycine was added to a final concentration of 0.125 M and cells were incubated on a rocking platform for an additional five minutes at room temperature. Cells were then pelleted, washed twice in cold 1X phosphate buffered saline, and resuspended in 1 mL SDS lysis buffer (1% SDS, 50 mM Tris-HCl [pH 8.0], 10 mM EDTA, and 1X Protease Inhibitor Cocktail [Cell Signaling Technology, Danvers, MA]). Cells were sonicated on ice for 10 cycles of 10 seconds each, with 60 seconds of rest in between each cycle, using a Branson Sonifier equipped with a microtip probe set to an output of 5 and a duty cycle of 90%. Samples were spun at 12,000 x g and chromatin lysates were diluted in ChIP Dilution Buffer (0.01% SDS, 1.1% Triton X-100, 1.2 mM EDTA, 16.7 mM Tris-HCl [pH 8.0], 16.7 mM NaCl, and 1X Protease Inhibitor Cocktail) and then pre-cleared with ChIP-Grade Protein G Agarose Beads (Cell Signaling Technology, Danvers, MA) on a rocking platform for one hour at 4°C.



Agarose beads were pelleted, 1% of the supernatants were collected to serve as 'input' samples, and the remaining supernatants were incubated with either 1  $\mu$ g Normal Goat IgG Control antibody (R&D Systems, Minneapolis, MN), 2  $\mu$ g goat IgG anti-human  $\beta$ -catenin polyclonal antibody (R&D Systems, Minneapolis, MN), or with 1  $\mu$ g mouse IgG anti-human RNA Polymerase II, clone CTD4H8 antibody (EMD Millipore, Billerica, MA). Antibody incubations were carried out on a rocking platform overnight at 4°C. Chromatin/antibody complexes were immunoprecipitated by adding ChIP-Grade Protein G Agarose Beads to the samples and incubating them on a rocking platform for one hour at 4°C. Beads were then washed twice with Low Salt Immune Complex Wash Buffer (0.1% SDS, 1% Triton X-100, 2 mM EDTA, 20 mM Tris-HCl [pH 8.0], and 150 mM NaCl), once with High Salt Immune Complex Wash Buffer (0.1% SDS, 1% Triton X-100, 2 mM EDTA, 20 mM Tris-HCl [pH 8.0], and 500 mM NaCl), once with Lithium Chloride Immune Complex Wash Buffer (0.25 M LiCl, 1% NP40, 1% Sodium Deoxycholate, 1 mM EDTA, and 10 mM Tris-HCl [pH 8.0]), and twice with TE Buffer (10 mM Tris-HCl [pH 8.0] and 1 mM EDTA) for 10 minutes per wash. Elution buffer (1% SDS and 0.1 M Sodium Bicarbonate) was added and samples were incubated for 30 minutes at room temperature. Eluted chromatin was incubated overnight at 65°C to reverse the crosslinks. Samples were incubated with 20  $\mu$ g RNase A (Sigma-Aldrich, St. Louis, MO) for 30 minutes at 37°C and with 20  $\mu$ g Proteinase K (Sigma-Aldrich, St. Louis, MO) for two hours at 42°C and then DNA was purified using the GenElute PCR Clean Up Kit (Sigma-Aldrich, St. Louis, MO) according to the manufacturer's instructions.

Immunoprecipitated DNA was quantified using qPCR. The qPCR reactions contained Power Sybergreen PCR Master Mix and one of the following primer sets: the Nuc-1 primer set (Forward 5'-TCTCTGGCTAACTAGGGAACC-3' and Reverse 5'-AAAGGGTCTGAGGGATCTCTAG-3') corresponding to HIV-1LAV sequence numbers 37-155 spanning the R and U5 regions of the 5' LTR, or the GAPDH promoter primer set (Forward 5'-TACTAGCGGTTTTACGGGCG-3' and Reverse

5'-TCGAACAGGAGGAGCAGAGAGCGA-3'). qPCR was performed using the BioRad CFX 96 Real-Time System C1000 Thermal Cycler with the following program settings: 95°C for 10 minutes, followed by 50 cycles of 95°C for 15 seconds, 60°C for 60 seconds, followed by a melt curve. DNA quantifications were calculated using the  $\Delta C(t)$  method comparing  $C(t)$  values of immunoprecipitated samples to  $C(t)$  values of 'input' samples.

### **$\beta$ -catenin knockdown to analyze effects on PI-mediated activation of latent HIV-1**

HeLa#14 cells were plated in 6-well plates at  $4 \times 10^5$  cells per well. Twenty-four hours later, duplicate wells were transiently transfected with either a pool of 3 GIPZ shRNAs, each targeting a different sequence within  $\beta$ -catenin, or with the non-silencing SD shRNA as described above. Forty-eight hours post-transfection, half of the transfected cells were harvested for  $\beta$ -catenin RNA analysis. For this analysis, the number of transfected (GFP+) and total live HeLa#14 cells were determined via standard trypan blue exclusion test and quantification using fluorescence microscopy and cell counting with a hemocytometer. Total RNA was isolated, treated with DNase, and reverse transcribed as described above using the High-Capacity cDNA Reverse Transcription Kit (Applied Biosystems, Foster City, CA). The cDNA was then used as a template for qPCR to determine  $\beta$ -catenin RNA expression levels. qPCR was performed as described above with the following primer sets: the  $\beta$ -catenin primer set (Forward 5'-GTTTCAGTTGCTTGTTCTGTC-3' and Reverse 5'-GTTGTGAACATCCCGAGCTAG-3'), or the GAPDH (reference gene) primer set (described above).

The remaining transfected cells were either treated with 15 nM Velcade or were left untreated. Forty-eight hours post-treatment, the number of transfected (GFP+) and total live HeLa#14 cells were determined as described above. Then, half of the cells were harvested for RLUC RNA analysis and the other half were harvested for RLUC activity analysis. For the RNA experiment,

total RNA was isolated, treated with DNase, and reverse transcribed as described above using the High-Capacity cDNA Reverse Transcription Kit (Applied Biosystems, Foster City, CA). The cDNA was then used as a template for qPCR to determine RLUC RNA expression levels. qPCR was performed as described above with the RLUC and GAPDH (reference gene) primer sets described above. For the RLUC activity analysis, cells were lysed, protein concentration was measured via standard Bradford assay (Bio-Rad Laboratories, Hercules, CA), and RLUC activity was measured as described above.

## **Results**

### **Reverse genetic screen identifies genes and pathways that potentially regulate HIV-1 latency**

The GeneNet Genome-wide Human 50K Lentiviral shRNA Library (System Biosciences (SBI), Mountain View, CA) was used to perform a reverse genetic screen to query cellular factors and pathways that modulate the maintenance of HIV-1 latency. The library consists of approximately 200,000 shRNA constructs targeting about 38,000 human transcripts. It includes 3-5 shRNA constructs per gene, each targeting a different sequence within that gene. The lentiviral vectors are self-inactivating vectors consisting of a CMV promoter driving the expression of a selectable marker gene conferring resistance to puromycin and an H1 Polymerase III promoter driving the expression of the 27 nucleotide shRNA construct. Each lentiviral shRNA construct included in the library is packaged into virions that are pseudotyped with the vesicular stomatitis virus Envelope.

The shRNA library was previously optimized by SBI for use with HeLa and HEK293 human cell lines. Although neither cell line is of T cell or myeloid cell origin, we previously found that one could establish a latent HIV-1 infection in HeLa cells. This closely resembled latency in T cells in that the virus was transcriptionally quiescent but could be activated in similar fashion to latent virus in T cells. Therefore, for this screen a HeLa-based model of viral latency (HeLa#14 cell line) was established and employed [366]. The HeLa#14 cell line harbors a latent HIV-1<sub>NL4-3-</sub> derived reporter construct that is rendered replication-incompetent via deletions in *pol* and *env* and upon viral reactivation expresses red fluorescence protein (RFP) from the *nef* position and *Renilla* luciferase from the *env* position [366].

A negative selection protocol was used to identify shRNAs that activated latent virus by taking advantage of the cytotoxic effects of the HIV-1 viral protein Vpr [367-372] (Fig. 2.1).

Briefly, latently infected HeLa#14 cells (referred to as the experimental sample) and uninfected, parental HeLa cells (referred to as the reference control sample) were transduced with the library. Transduced cells were selected with puromycin and cultured for a total of 17 days, which was experimentally determined to provide ample time for shRNA expression and knockdown of the target gene, as well as viral reactivation and viral protein-mediated cell death in the experimental sample [367-376]. Following the culture period, cells were lysed and total RNA was isolated, reverse transcribed, amplified, and hybridized to an Affymetrix GeneChip Array (HG-U133+ 2.0) for identification (Fig. 2.1). As the functional assay employed in this screen involved viral protein-mediated cell death upon the re-activation of latent HIV-1, signals from the reference control sample microarray that were at least three times greater than the corresponding signals from the experimental sample microarray were scored as “hits” and statistically analyzed further. Absent or extremely low-level signals on the reference control sample microarray represent lost library coverage and/or shRNAs that targeted essential genes. It should be noted that shRNAs targeting approximately 70% of the total number of genes were detected on the reference control sample microarray indicating a relatively robust genomic coverage.

The gene “hits” were statistically analyzed using redundant siRNA activity (RSA) analysis [377]. RSA calculates the probability of a real “hit” based on the reasoning that biologically significant “hits” will be identified several times, whereas non-significant “hits” might appear once likely representing false positives. RSA analysis was possible with this data set because the SBI library contains 3-5 shRNA constructs per gene. RSA analysis assigned a p-value to all genes in the data set that indicated the statistical significance of a gene “hit” based on the scores of each shRNA that targeted that gene, calculated via an iterative hypergeometric distribution formula. A positive signal on the reference control sample microarray that was at least three

times higher than the corresponding signal on the experimental sample microarray was considered the minimum acceptable shRNA score. In this analysis, a gene with several moderately scoring shRNAs was weighed more heavily than a gene with fewer higher scoring shRNAs to potentially avert off-target, false positive “hits”. Table 2.1 lists the top 198 gene “hits” from the screen as determined by RSA analysis using an accumulative hypergeometric p-value cutoff of  $<0.001$ .

All gene “hits” that were assigned p-values of  $<0.05$  by RSA analysis (~2500 genes), were entered into the Ingenuity Systems Interactive Pathway Analysis (IPA) software program as a data set for functional annotation clustering analysis. IPA calculated a p-value (right-tailed Fisher exact test) for the enrichment of a particular function and/or pathway by taking into account both the number of genes in the data set that share that function or participate in that pathway and the total number of genes in the IPA Knowledge Base that are known to participate in that pathway or function overall. The pathways listed in Table 2.2 are the significantly enriched canonical pathways (p-value cutoff  $<0.01$ ) in the data set. The functions listed in Table 2.3 are the significantly enriched functional annotations (p-value cutoff  $<0.01$ ) in the data set. The factors listed in Table 2.4 are enriched upstream regulators of genes in the data set. Here, IPA calculated a p-value for the enrichment of a particular upstream regulator by taking into account both the number of genes in the data set that are known to be regulated by the factor and the overall number of genes in the IPA Knowledge Base that are known to be regulated by that factor overall. Additionally, IPA calculated a prediction for the status of the upstream regulators in the context of the activation of latent HIV-1. The software made predictions for the status of upstream regulators using the regulation z-score algorithm, which takes into account both the expression patterns of the regulated genes in the data set that were “observed” (i.e. downregulated as this screen was performed using shRNA technology) and the expression

patterns of the regulated genes in the data set that would be expected if the upstream regulator was either activated or inhibited (according to the literature in the IPA Knowledge Base). A z-score of less than or equal to -2 represents a significant prediction that the upstream regulator is inhibited during latency activation, whereas a z-score of greater than or equal to 2 represents a significant prediction that the upstream regulator is activated during latency activation (Table 2.4).

### Select gene “hits” validation

Next, we sought to validate some of the significant gene “hits” identified in the screen. Genes were selected from the highly significant gene “hit” list (Table 2.1) based on p-value, availability of shRNA constructs, known interactions with HIV-1 proteins or known involvement in HIV-1 replication, and/or whether they were unexpected yet interesting. For these reasons, we chose the following genes for the first round of validation: *adipogenin* (ADIG; 149685), *akirin 2* (AKIRIN2; 55122), *arginine vasopressin receptor 2* (AVPR2; 554), *long intergenic non-protein coding RNA 467* (LINC00467; 84791), *coiled-coil domain containing 40* (CCDC40; 55036), *fibroblast growth factor receptor 1* (FGFR1; 2260), *FK506 binding protein 15, 133kDa* (FKBP15; 23307), *GLI family zinc finger 4* (GLI4; 2738), *MACRO domain containing 1* (MACROD1; 28992), *peroxiredoxin 5* (PRDX5; 25824), *proteasome (prosome, macropain) subunit, alpha type, 7* (PSMA7; 5688), *SHQ1, H/ACA ribonucleoprotein assembly factor* (SHQ1; 55164), and *sialophorin* (SPN; 6693). HeLa#14 cells were transiently transfected with a pool of three or four GIPZ lentiviral shRNAs (Thermo Fisher Scientific, Waltham, MA), each targeting a different sequence within their respective gene, or were transfected with the scrambled duplex non-silencing lentiviral shRNA construct as a negative control; it should be noted that GIPZ lentiviral shRNAs were used in this validation strategy (instead of shRNAs from SBI) to bolster confidence in the

validation results, as they likely target alternative sequences within their target genes than those that were targeted in the original screen. Seventy-two to ninety-six hours post transfection (time course experiments were performed to determine optimal time points for analysis following the transfection of each shRNA pool; data not shown), *Renilla* luciferase (RLUC) activity was measured. Figure 2.2 indicates that the downregulation of AKIRIN2, AVPR2, LINC00467, CCDC40, and PSMA7 in these cells resulted in a significant induction of RLUC activity, compared to cells transfected with the scrambled duplex construct, potentially validating a role for these genes in the maintenance of HIV-1 latency.

### **The proteasome is involved in maintaining HIV-1 latency**

A more thorough follow-up of one of the validated gene “hits”, PSMA7, was carried out for three reasons. First, it was previously reported that PSMA7 interacts with the HIV-1 protein Tat [378]. Second, the PSMA7 “hit” suggested that the UPS might be involved in maintaining the latent state, which is unexpected since proteasomal activity is required for the activation of NF $\kappa$ B, a potent HIV-1 transcription factor [379]. Third, proteasome inhibitors have been developed and are being used clinically as chemotherapeutic drugs [380-384]. To confirm shRNA-mediated knockdown of PSMA7 mRNA, HeLa#14 cells were transiently transfected with a pool of three GIPZ lentiviral shRNAs, each targeting a different sequence within PSMA7. Then, PSMA7 mRNA levels were analyzed 48 hours later. Figure 2.3A confirms that PSMA7 mRNA was downregulated approximately 80% following shRNA transfection. As a subunit of the 20S catalytic core particle of the 26S proteasome [385], PSMA7 was hypothesized to maintain HIV-1 latency through a proteasome activity-mediated mechanism. Indeed, as shown in figure 2.3B, the knockdown of PSMA7 reduced proteasome activity by approximately 40%. Equally as interesting, 43 genes involved in the ubiquitin-proteasome system were identified as significant



gene “hits” ( $p < 0.05$ ) by RSA analysis (Table 2.4), which corroborated our broadened hypothesis that proteasome function is important in the maintenance of HIV-1 latency.

To confirm our hypothesis, latently infected cells were treated with a proteasome inhibitor to analyze the activation of proviral transcription. HeLa#14 cells were treated with the PI Velcade, which is an inhibitor of the chymotrypsin-like activity of the 20S proteasome core particle [381, 386] that is also FDA approved for the treatment of multiple myelomas, leukemias, and lymphomas [380-384]. Figures 2.3C and D indicate that Velcade inhibited the proteasome in HeLa#14 cells within two hours (Fig. 2.3C) and activated latent HIV-1 transcription, as evidenced by a significant increase in the level of RLUC RNA within 24 hours post-treatment (Fig. 2.3D). Of note, we have confirmed and detailed the robust activation of latent HIV-1 transcription, gene expression, and virion production induced by PIs in multiple model systems in a recent publication [332].

### **Velcade stabilizes $\beta$ -catenin and enhances its association with the HIV-1 5' LTR**

The finding that PIs abrogate HIV-1 latency prompted an exploration into the mechanism underpinning this observation. It is possible that inhibiting the proteasome modulates numerous pathways within the cell and therefore, it should be noted that multiple pathways might influence PI-mediated activation of latent HIV-1. Nevertheless, results obtained in the screen point to a particular pathway that might be involved. Table 2.2 indicates that genes involved in the Wnt/ $\beta$ -catenin signaling pathway were the most highly enriched in the screen.  $\beta$ -catenin is the end-point signal transduction molecule of the Wnt pathway and is constantly degraded by the proteasome in the absence of a Wnt signal (reviewed in [387]). However, upon stabilization,  $\beta$ -catenin can bind its co-transcription factor LEF1 (lymphoid enhancer-binding factor 1) that has a binding site in the HIV-1 5' LTR and can modulate chromatin assembly

around the HIV-1 promoter [363, 364] and augment the activity of the enhancer region of the HIV-1 promoter [365]. Therefore, we analyzed  $\beta$ -catenin protein levels via Western blot following proteasome inhibition in both human primary resting CD4<sup>+</sup> T cells and OM-10.1 cells (Fig. 2.4). OM-10.1 cells are a clonal population of HL-60 promyelocytes that are latently infected with the replication-competent HIV-1<sub>LAV</sub> strain [388-392]. Velcade treatment resulted in the stabilization of  $\beta$ -catenin in human primary resting CD4<sup>+</sup> T cells (Fig. 2.4A and B) and OM-10.1 cells (Fig. 2.4C and D) within four hours. It is noteworthy that the  $\beta$ -catenin laddering observed is commonly seen owing to ubiquitylation while the bands detected below  $\beta$ -catenin at later time points are likely degradation products (Fig. 2.4A and C). Overall the results indicate that Velcade exerts its effects on latent HIV-1, at least in part, through  $\beta$ -catenin.

To explore this hypothesis further,  $\beta$ -catenin association with the HIV-1 5' LTR promoter region was assessed following Velcade treatment. OM-10.1 cells were treated with 15 nM Velcade for six hours and then subjected to chromatin immunoprecipitation using anti- $\beta$ -catenin, as well as anti-RNA Polymerase II (RNAPII) antibodies. As shown in Fig. 2.5,  $\beta$ -catenin was enriched (approximately 3.5-fold) on the HIV-1 5' LTR promoter region (Nuc-1) following Velcade treatment. Additionally, RNAPII was found to be associated with the HIV-1 5' LTR following Velcade treatment but interestingly, it was also associated with the silenced viral promoter in untreated cells. This indicates that RNAPII is "preloaded" on the latent HIV-1 promoter in OM-10.1 cells, essentially paused but poised for transcription. Although worthy of note, this is not surprising as this has been shown to occur on gene promoters throughout the human [393-399], yeast [400], and drosophila genomes [401]. The GAPDH promoter region served as a positive control for RNAPII binding and also as a negative control for  $\beta$ -catenin binding. Of note, RNAPII became considerably more enriched on the GAPDH promoter region

following Velcade treatment, approximately 4 fold, compared to untreated cells. This is most likely indicative of the induction of cellular stress as a result of Velcade treatment [402].

### **Downregulation of $\beta$ -catenin reduces the degree of Velcade-induced activation**

To mechanistically confirm  $\beta$ -catenin involvement in Velcade-induced activation of latent HIV-1, shRNAs were used to downregulate  *$\beta$ -catenin* in HeLa#14 cells prior to Velcade treatment. Figure 2.6A confirms that  *$\beta$ -catenin* mRNA was downregulated approximately 60% following shRNA transfection. Forty-eight hours post-transfection, cells were treated with 15 nM Velcade for an additional forty-eight hours, at which time *RLUC* mRNA levels as well as RLUC activity were measured to assess latent virus reactivation. Velcade-induced activation of latent HIV-1 was markedly reduced in cells in which  $\beta$ -catenin had been downregulated, compared to cells that had been transfected with non-specific shRNA (Fig. 2.6B and C). Although the reduction in the magnitude of Velcade-induced activation was considerable in  $\beta$ -catenin-specific shRNA transfected cells, activation was not completely abolished. This might be due to the fact that  *$\beta$ -catenin* expression was not entirely knocked out, but it might also indicate that additional pathways are involved in PI-mediated activation of latent HIV-1, as discussed earlier.

## Discussion

Here, we report the results from a genome-wide RNAi screen that was carried out to identify previously unknown cellular regulators of HIV-1 latency. One of the highly significant and validated gene “hits” from the screen was PSMA7, a proteasome subunit gene important for proteasome assembly and hence important for proteasome function. Through the use of proteasome inhibitors, we show that the proteasome plays an important role in the maintenance of HIV-1 latency. Moreover, evidence is presented that PIs activate latent HIV-1, at least partially, through the stabilization of the transcription factor  $\beta$ -catenin.

It was not anticipated that the RNAi screen would identify every cellular factor involved in HIV-1 latency, nor was it expected to be able to avoid the identification of some false positive “hits” based on previously reported RNAi screen data [360]. However, those reports do indicate that RNAi screens can produce interesting and biologically significant findings. In line with this, we believe the results obtained from this RNAi screen should be reported not only because it was possible to validate five of the genes identified, including one in thorough detail, but also because at least some genes and functional pathways that have been reported to play a role in HIV-1 pathogenesis were identified. Indeed, the following gene “hits” listed in Table 2.1 have been shown to either bind HIV-1 proteins and/or to positively or negatively influence HIV-1 replication, gene expression, latency, and/or immune escape: *ATP-binding cassette, sub-family A (ABC1), member 1* (19); *adenylate cyclase 1 (brain)* (107); *ADP-ribosylation factor guanine nucleotide-exchange factor 2 (brefeldin A-inhibited)* (10564); *Rho guanine nucleotide exchange factor (GEF) 12* (23365); *Rho guanine nucleotide exchange factor (GEF) 7* (8874); *BCL2-associated X protein* (581); *DEAD (Asp-Glu-Ala-Asp) box helicase 3, X-linked* (1654); *exocyst complex component 6* (54536); *golgi-associated, gamma adaptin ear containing, ARF binding protein 2* (23062); *interferon (alpha, beta, and omega) receptor 2* (3455); *mannosidase, alpha,*

*class 1A, member 2* (10905); *minichromosome maintenance complex component 4* (4173); *prohibitin* (5245); *phosphatidylinositol 3-kinase, catalytic subunit type 3* (5289); *polymerase (RNA) II (DNA directed) polypeptide L, 7.6kDa* (5441); *protein phosphatase 2, regulatory subunit B, gamma* (PPP2R2C; 5522); *PSMA7*; *paraspeckle component 1* (55269); *RAB6A, member RAS oncogene family* (5870); *Sep (O-phosphoserine) tRNA:Sec (selenocysteine) tRNA synthase* (51091); *SET nuclear proto-oncogene* (SET; 6418); *SPN*; *transmembrane protein 192* (201931); *trichorhinophalangeal syndrome I* (7227); *UL16 binding protein 2* (80328); and *VAMP (vesicle-associated membrane protein)-associated protein A, 33kDa* (9218). For example, PPP2R2C has been shown to negatively impact HIV-1 gene expression. In fact, the inhibition of PPP2R2C preserves the phosphorylation status of the transcription factor Sp1 and has been shown to enhance HIV-1 transcription and gene expression [403, 404]. Also, aside from its interaction with the HIV-1 protein Rev [405], SET has the potential to negatively impact HIV-1 gene expression through its function as an inhibitor of histone acetyltransferase activity. Likewise, the functional annotation classification ‘phospholipid synthesis and concentration’ (Table 2.3) might include genes involved in the regulation of the protein kinase C pathway, whose activation has been shown to activate latent HIV-1 (reviewed in [289]). Additionally, based on specific gene “hits” identified in the screen, the Ingenuity software program predicted that the inhibition of the upstream regulators TGF $\beta$  (transforming growth factor beta) and p73 (tumor protein p73) would activate latent HIV-1 (Table 2.4). Indeed, it has been shown that the activation of latently infected U1 cells via the phorbol ester PMA is drastically reduced when cells are treated simultaneously with TGF $\beta$  [406]. In addition, p73 is known to inhibit Tat-mediated transactivation of HIV-1 transcription by binding Tat and preventing its acetylation [407]. Genes were also identified that have no known function in HIV-1 pathogenesis, including genes with no known function at all, and therefore this screen has potentially revealed novel functions for at

least some genes. In summary, this screen has uncovered a wealth of leads to validate and explore in future studies.

In the current study, we validated five genes identified in the screen: AKIRIN2, AVPR2, LINC00467, CCDC40, and PSMA7. AKIRIN2 is a highly conserved nuclear protein that is required for NF $\kappa$ B-dependent gene expression in drosophila and mice [408] and has been shown to act as a transcriptional repressor in complex with 14-3-3  $\beta$  proteins [409]. AVPR2 is a seven-transmembrane-domain G protein-coupled receptor that can stimulate adenylate cyclase to increase intracellular levels of cyclic AMP. Cyclic AMP is known to activate protein kinase A, which has been shown to inhibit PMA-induced activation of latent HIV-1 gene expression as well as to inhibit HIV-1 replication in cells of myeloid origin [410]. LINC00467 is an intergenic non-protein coding RNA with no known function to date. CCDC40 is necessary for cilia function in humans [411] but its homolog in drosophila is a heterochromatin protein responsible for proper chromosome condensation [412]. Although we have only pursued further studies into PSMA7 so far, future plans include extensive investigations into the remaining four validated genes as well as pursuits to validate additional gene “hits” from the screen.

PSMA7 was shown to be important for proteasome function in this report (Fig. 2.3B), and it was subsequently demonstrated that proteasomal inhibition results in the activation of latent reporter virus transcription in HeLa#14 cells (Fig. 2.3D). In support of this, we have previously shown that PIs are potent activators of latent HIV-1 in several latency model systems, including primary CD4<sup>+</sup> T cell models [332]. Moreover, additional genes associated with the ubiquitin-proteasome system were identified as “hits” in the screen (Table 2.5). These results strongly suggest that the UPS plays a role in the regulation of HIV-1 latency. As a side note, the

proteasome has also been linked to the regulation of Epstein-Barr virus latency [413], which is an unrelated viral species.

As previously mentioned, several pathways within the cell might be modulated following proteasomal inhibition and therefore, the alteration of a single pathway may not account for the full extent of PI-mediated activation of latent HIV-1. As indicated in Figure 2.6, the downregulation of *β-catenin* markedly reduced but did not abolish Velcade-mediated activation of latent HIV-1 transcription and protein expression. However, complete knockout of *β-catenin* expression was not achieved, so it cannot be concluded that *β-catenin* is the only regulator of PI-mediated latency activation. This question could be explored further by developing a gene-knockout cell model, such as with CRISPR technology, ensuring a complete silencing of *β-catenin* expression.

Figure 2.7 summarizes a potential explanation for PI-mediated activation of latent HIV-1 transcription through the stabilization of *β-catenin*. In the absence of a Wnt signal (normal conditions), *β-catenin* is phosphorylated by CK1 (casein kinase 1α) and GSK3β (glycogen synthase kinase 3β) of the APC/Axin1 destruction complex. Phosphorylated *β-catenin* is then recognized by E3 ubiquitin ligase(s), which ubiquitinates *β-catenin* resulting in its degradation via the proteasome (reviewed in [414]). However, during proteasomal inhibition, is it logical to assume that phosphorylated *β-catenin* is not degraded and would be available for nuclear translocation and gene expression modulation. Indeed, it has been reported that proteasomal inhibition induces the nuclear accumulation of *β-catenin* [415-417], and it has been shown that *β-catenin* can be dephosphorylated in the presence of PIs [416] negating the requirement for the nuclear translocation of phosphorylated *β-catenin*. It is not clear whether or not ubiquitinated *β-catenin* can translocate to the nucleus but evidence indicates that proteasomal

inhibition decreases the availability of free ubiquitin in the cell [418, 419]. Therefore, it is likely that PIs induce the accumulation of a pool of non-ubiquitinated  $\beta$ -catenin that could translocate to the nucleus. Indeed, we found that Velcade induced the stabilization of both ubiquitinated and non-ubiquitinated  $\beta$ -catenin (Figs. 2.4A and C). A more definitive answer could be found by isolating nuclear fractions from cells treated with PIs and performing Western blots for  $\beta$ -catenin, looking for the same banding patterns indicating ubiquitylation.

Once in the nucleus,  $\beta$ -catenin can bind one of its co-transcription factors LEF1, TCF1 (T cell factor-1), TCF3 (T cell factor-3), or TCF4 (T cell factor-4). It has been shown that LEF1 has a binding site in the enhancer region of the HIV-1 5' LTR [362]. Additionally, evidence indicates that LEF1 can modulate chromatin assembly around the HIV-1 promoter [363, 364] and induce HIV-1 transcription in Jurkat T cells [365]. Therefore, we propose that upon proteasomal inhibition,  $\beta$ -catenin is stabilized, translocates to the nucleus, and binds LEF1 to contribute to the activation of latent HIV-1 transcription (Fig. 2.7). Of note, previous reports have indicated that  $\beta$ -catenin can act as a transcriptional repressor on the HIV-1 promoter [420, 421] and can suppress viral replication [422-424] when complexed with TCF4. However, another study found that the stabilization of  $\beta$ -catenin (through the downregulation of Axin1) resulted in  $\beta$ -catenin/TCF4 complex formation and the upregulation of HIV-1 reporter gene expression [425]. Therefore, the effects of the  $\beta$ -catenin/TCF4 complex on HIV-1 transcription are unclear. It will be of interest to explore additional pathway(s) and/or transcription factors that are modulated by proteasomal inhibition and result in the activation of latent HIV-1 in future studies.

In summary, we present results from a genome-wide shRNA screen performed to identify cellular regulators of the maintenance of HIV-1 latency. The screen not only identified genes and pathways that had already been implicated in the regulation of HIV-1 latency and/or



pathogenesis, but it also identified genes with no known association with HIV-1 infection and some genes with no known function at all. Therefore, it has potentially uncovered novel functions for some human genes and has provided numerous leads for future investigations. One of the five gene “hits” that was validated (PSMA7) indicated a role for the proteasome in the regulation of HIV-1 latency. Follow-up experiments using PIs denoted that the inhibition of proteasome function induced the transcription of latent HIV-1, partially through the stabilization of  $\beta$ -catenin. It will be important to determine the contribution of additional pathway(s), that are modulated via proteasomal inhibition, on the activation of latent HIV-1, as well as to follow up on additional results obtained from the screen in future studies.

## Tables

**Table 2.1. Highly significant (p-value <0.001) gene "hits"**

<b>Gene Name or GenBank Accession Number</b>	<b>Gene Abbr.</b>	<b>p-value</b>
Family with sequence similarity 83, member C	FAM83C	1.084E-10
Acyl-CoA synthetase long-chain family member 4	ACSL4	2.267E-10
Arginine vasopressin receptor 2	AVPR2	2.812E-09
MACRO domain containing 1	MACROD1	1.742E-08
Adipogenin	ADIG	2.152E-08
Sialophorin*	SPN	2.318E-08
SHQ1 homolog (S. cerevisiae)	SHQ1	3.394E-08
Coiled-coil domain containing 40	CCDC40	1.465E-07
GLI family zinc finger 4	GLI4	1.555E-07
Neuroblastoma breakpoint family, member 3	NBPF3	1.855E-07
Akirin2	AKIRIN2	2.088E-07
Chromosome 1 open reading frame 97	C1orf97	2.247E-07
Peroxiredoxin 5	PRDX5	2.252E-07
Kallikrein-related peptidase 4	KLK4	3.505E-07
Discoidin, CUB and LCCL domain containing 1	DCBLD1	4.674E-07
Dual adaptor of phosphotyrosine and 3-phosphoinositides	DAPP1	8.720E-07
BQ007743	-----	9.460E-07
AT rich interactive domain 5A (MRF1-like)	ARID5A	2.749E-06
SET nuclear oncogene*	SET	4.265E-06
Pleckstrin and Sec7 domain containing	PSD	4.279E-06
Sorting and assembly machinery component 50 homolog (S. cerevisiae)	SAMM50	5.354E-06
Frizzled family receptor 8	FZD8	5.767E-06
NOP16 nucleolar protein homolog (yeast)	NOP16	8.172E-06
Proteasome (prosome, macropain) subunit, alpha type, 7*	PSMA7	1.564E-05
Leucyl-tRNA synthetase 2, mitochondrial	LARS2	1.583E-05
AI733144	-----	1.849E-05
Two pore segment channel 1	TPCN1	2.020E-05
U61087	-----	2.174E-05
Fibroblast growth factor receptor 1	FGFR1	2.214E-05
MCF.2 cell line derived transforming sequence	MCF2	2.320E-05
N-acetylglucosaminidase, alpha	NAGLU	2.358E-05
AA744622	-----	2.585E-05
BC035247	-----	2.589E-05
BC020820	-----	2.591E-05
Long intergenic non-protein coding RNA 441	LINC00441	2.763E-05
BC037818	-----	2.859E-05
FK506 binding protein 15, 133kDa	FKBP15	2.971E-05
Zinc finger, CCHC domain containing 2	ZCCHC2	3.019E-05
SplA/ryanodine receptor domain and SOCS box containing 2	SPSB2	3.214E-05
BQ024490	-----	3.316E-05
Chromosome 9 open reading frame 117	C9orf117	3.579E-05

BC043513	-----	3.698E-05
AA632049	-----	4.014E-05
Golgi SNAP receptor complex member 2	GOSR2	4.314E-05
Chromosome 3 open reading frame 15	C3orf15	4.616E-05
BC042880	-----	5.108E-05
BC033970	-----	5.469E-05
NADH dehydrogenase (ubiquinone) 1 beta subcomplex, 3, 12kDa	NDUFB3	5.486E-05
FXD domain containing ion transport regulator 5	FXD5	5.546E-05
Pyrophosphatase (inorganic) 2	PPA2	5.705E-05
ZFX4 antisense RNA 1	ZFX4-AS1	6.174E-05
U38460	-----	6.502E-05
BM091363	-----	6.700E-05
PR domain containing 16	PRDM16	6.959E-05
TNF receptor-associated protein 1	TRAP1	6.978E-05
GTP binding protein 5 (putative)	GTPBP5	7.395E-05
Armadillo repeat containing 4	ARMC4	7.476E-05
AI953278	-----	8.649E-05
Ras association (RalGDS/AF-6) domain family member 6	RASSF6	9.202E-05
VAMP (vesicle-associated membrane protein)-associated protein A, 33kDa*	VAPA	9.244E-05
BE139685	-----	9.311E-05
Lipase, family member J	LIPJ	1.006E-04
ADP-ribosylation factor guanine nucleotide-exchange factor 2 (brefeldin A-inhibited)*	ARFGEF2	1.043E-04
Integrin, beta 8	ITGB8	1.082E-04
Rho guanine nucleotide exchange factor (GEF) 7*	ARHGEF7	1.109E-04
Pygopus homolog 2 (Drosophila)	PYGO2	1.193E-04
RAB6A, member RAS oncogene family*	RAB6A	1.270E-04
BF512491	-----	1.294E-04
Golgi-associated, gamma adaptin ear containing, ARF binding protein 2*	GGA2	1.301E-04
DiGeorge syndrome critical region gene 2	DGCR2	1.316E-04
RAS, dexamethasone-induced 1	RASD1	1.454E-04
Leukemia NUP98 fusion partner 1	LNP1	1.479E-04
BC038210	-----	1.525E-04
Polymerase (RNA) II (DNA directed) polypeptide L, 7.6kDa*	POLR2L	1.600E-04
Ribosomal RNA processing 8, methyltransferase, homolog (yeast)	RRP8	1.618E-04
BC030259	-----	1.664E-04
Tripartite motif containing 11	TRIM11	1.849E-04
BF805425	-----	1.855E-04
Aminopeptidase-like 1	NPEPL1	1.989E-04
Slingshot homolog 2 (Drosophila)	SSH2	2.034E-04
Small nucleolar RNA host gene 12 (non-protein coding)	SNHG12	2.105E-04
B9 protein domain 1	B9D1	2.139E-04

Exosome component 8	EXOSC8	2.218E-04
Methyl-CpG binding domain protein 3	MBD3	2.387E-04
AK022031	-----	2.433E-04
Trio Rho guanine nucleotide exchange factor	TRIO	2.494E-04
Rabaptin, RAB GTPase binding effector protein 2	RABEP2	2.534E-04
BU177699	-----	2.542E-04
Paraspeckle component 1*	PSPC1	2.553E-04
BC041833	-----	2.588E-04
TEX26 antisense RNA 1	TEX26-AS1	2.678E-04
AF143888	-----	2.736E-04
HECT domain containing E3 ubiquitin protein ligase 2	HECTD2	2.743E-04
DOCK9 antisense RNA 2	DOCK9-AS2	2.773E-04
Mitochondrial translational initiation factor 3	MTIF3	2.807E-04
SIX homeobox 5	SIX5	2.825E-04
AW009385	-----	2.958E-04
AK057554	-----	2.959E-04
Radial spoke head 4 homolog A (Chlamydomonas)	RSPH4A	3.143E-04
AK098715	-----	3.227E-04
Phosphoglucomutase 2	PGM2	3.259E-04
Phosphatidylinositol 3-kinase, catalytic subunit type 3*	PIK3C3	3.308E-04
Vacuolar protein sorting 26 homolog B (S. pombe)	VPS26B	3.328E-04
Solute carrier family 7 (glycoprotein-associated amino acid transporter), member 9	SLC7A9	3.349E-04
Discs, large (Drosophila) homolog-associated protein 1	DLGAP1	3.427E-04
Sep (O-phosphoserine) tRNA:Sec (selenocysteine) tRNA synthase*	SEPSECS	3.512E-04
Ribosomal protein L21	RPL21	3.562E-04
DnaJ (Hsp40) homolog, subfamily C, member 12	DNAJC12	3.570E-04
L23852	-----	3.700E-04
G10732645	-----	3.724E-04
BC042816	-----	3.833E-04
Plexin D1	PLXND1	3.873E-04
Protein phosphatase 2, regulatory subunit B, gamma*	PPP2R2C	4.033E-04
Protein O-fucosyltransferase 2	POFUT2	4.067E-04
UL16 binding protein 2*	ULBP2	4.078E-04
AI339536	-----	4.173E-04
AW451624	-----	4.261E-04
ATPase, H <sup>+</sup> transporting, lysosomal 9kDa, V0 subunit e1	ATP6V0E1	4.437E-04
Transmembrane protein 192*	TMEM192	4.514E-04
Rho guanine nucleotide exchange factor (GEF) 12*	ARHGEF12	4.519E-04
BQ024890	-----	4.609E-04
Torsin A interacting protein 2	TOR1AIP2	4.621E-04
Adenylate cyclase 1 (brain)*	ADCY1	4.648E-04
Neuropeptide FF receptor 2	NPFFR2	4.691E-04
Olfactory receptor, family 7, subfamily D, member 2	OR7D2	4.804E-04
Family with sequence similarity 160, member A2	FAM160A2	4.806E-04

Muscleblind-like splicing regulator 3	MBNL3	4.962E-04
Primase, DNA, polypeptide 2 (58kDa)	PRIM2	4.982E-04
AK056249	-----	4.987E-04
Cysteine-rich hydrophobic domain 1	CHIC1	4.991E-04
T-complex 1	TCP1	5.027E-04
N74507	-----	5.032E-04
Immunoglobulin heavy constant alpha 1	IGHA1	5.107E-04
SRY (sex determining region Y)-box 15	SOX15	5.141E-04
Zinc finger CCCH-type containing 18	ZC3H18	5.176E-04
H29626	-----	5.361E-04
Leukocyte immunoglobulin-like receptor, subfamily A (with TM domain), member 5	LILRA5	5.410E-04
AL137513	-----	5.545E-04
Pitrilysin metalloproteinase 1	PITRM1	5.567E-04
Pleckstrin homology-like domain, family B, member 3	PHLDB3	5.577E-04
Trichorhinophalangeal syndrome I*	TRPS1	5.730E-04
Solute carrier family 41, member 2	SLC41A2	5.915E-04
Mitochondrial ribosomal protein S21	MRPS21	6.008E-04
U64494	-----	6.013E-04
AK024860	-----	6.074E-04
Atonal homolog 7 (Drosophila)	ATOH7	6.100E-04
Coiled-coil domain containing 171	CCDC171	6.101E-04
WW domain containing E3 ubiquitin protein ligase 2	WWP2	6.257E-04
Chromosome 17 open reading frame 28	C17orf28	6.285E-04
Carcinoembryonic antigen-related cell adhesion molecule 3	CEACAM3	6.391E-04
Phosphatase and tensin homolog pseudogene 1	PTENP1	6.465E-04
Myosin IIIB	MYO3B	6.469E-04
Lysine (K)-specific demethylase 4C	KDM4C	6.585E-04
Interferon (alpha, beta and omega) receptor 2*	IFNAR2	6.682E-04
Family with sequence similarity 153, member B	FAM153B	6.752E-04
GTP binding protein 3 (mitochondrial)	GTPBP3	6.787E-04
Methionine sulfoxide reductase B2	MSRB2	6.845E-04
BSD domain containing 1	BSDC1	6.898E-04
Centrosomal protein 89kDa	CEP89	6.915E-04
AF075038	-----	6.932E-04
Zinc finger protein 10	ZNF10	7.024E-04
ybeY metalloproteinase (putative)	YBEY	7.027E-04
Mannosidase, alpha, class 1A, member 2*	MAN1A2	7.170E-04
AK001007	-----	7.206E-04
AA007276	-----	7.209E-04
Polymerase (DNA directed) nu	POLN	7.236E-04
AK055091	-----	7.248E-04
ATP synthase, H <sup>+</sup> transporting, mitochondrial F1 complex, epsilon subunit	ATP5E	7.393E-04
SOCS2 antisense RNA 1	SOCS2-AS1	7.411E-04
Family with sequence similarity 66, member D	FAM66D	7.417E-04

AF086147	-----	7.459E-04
Exocyst complex component 6*	EXOC6	7.557E-04
Chromosome 15 open reading frame 48	C15orf48	7.578E-04
BC036418	-----	7.763E-04
BF516607	-----	7.854E-04
BCL2-associated X protein*	BAX	7.879E-04
Solute carrier family 30 (zinc transporter), member 5	SLC30A5	7.898E-04
Zinc finger protein 45	ZNF45	7.948E-04
Protein phosphatase, Mg <sup>2+</sup> /Mn <sup>2+</sup> dependent, 1K	PPM1K	8.176E-04
AI912566	-----	8.227E-04
PRKR interacting protein 1 (IL11 inducible)	PRKRIP1	8.502E-04
G4506444	-----	8.543E-04
KDEL (Lys-Asp-Glu-Leu) endoplasmic reticulum protein retention receptor 3	KDEL3	8.635E-04
AV650867	-----	8.687E-04
U61087	-----	8.740E-04
3'-phosphoadenosine 5'-phosphosulfate synthase 2	PAPSS2	8.793E-04
Prohibitin*	PHB	9.000E-04
TIA1 cytotoxic granule-associated RNA binding protein	TIA1	9.056E-04
ATP-binding cassette, sub-family A (ABC1), member 1*	ABCA1	9.092E-04
Fibroblast growth factor 9 (glia-activating factor)	FGF9	9.207E-04
Zinc finger, HIT-type containing 2	ZNHIT2	9.603E-04
DEAD (Asp-Glu-Ala-Asp) box polypeptide 3, X-linked*	DDX3X	9.611E-04
U-box domain containing 5	UBOX5	9.630E-04
Peroxisome proliferator-activated receptor delta	PPARD	9.679E-04
Distal-less homeobox 6	DLX6	9.757E-04
Zinc finger protein 668	ZNF668	9.795E-04
SET and MYND domain containing 3	SMYD3	9.958E-04
Minichromosome maintenance complex component 4*	MCM4	9.980E-04

Microarray signal data was statistically analyzed employing RSA (redundant siRNA activity) analysis. A software parameter was set in which a signal (or shRNA score) from the reference control sample microarray had to be at least three times greater than the corresponding signal from the experimental sample microarray to be considered a positive signal. RSA analysis assigned p-values to every gene for which a positive signal was identified. The p-values indicate the statistical significance of a gene "hit" based on the scores of each shRNA that targeted that gene. A total of approximately 2500 genes were assigned p-values <0.05 and were therefore considered significant "hits". This table lists those "hits" that were assigned p-values <0.001 in descending order from the most significant. \*Indicates a gene "hit" with a known interaction with HIV-1 proteins and/or a known function associated with HIV-1 infection.

**Table 2.2: Highly enriched (p-value <0.01) canonical pathways**

<b>Enriched Canonical Pathway</b>	<b>p-value</b>
Wnt/ $\beta$ -catenin Signaling	3.26E-03
Breast Cancer Regulation by Stathmin1	3.74E-03
TR/RXR Activation	4.05E-03
Molecular Mechanisms of Cancer	5.21E-03
EGF Signaling	6.12E-03
CREB Signaling in Neurons	8.91E-03
B Cell Receptor Signaling	9.33E-03
IL-2 Signaling	9.99E-02

All gene “hits” that were assigned p-values of <0.05 by RSA analysis (~2500 genes) were entered into the IPA software program for functional annotation clustering analysis. This table lists significantly enriched canonical pathways (p-value <0.01) in descending order from the most significant. Abbreviations: RSA (redundant siRNA activity); IPA (interactive Pathway Analysis of complex ‘omics).

**Table 2.3: Highly enriched (p-value <0.01) functional annotations**

<b>Functional Annotation</b>	<b>p-value</b>
Synthesis of Phosphatidylinositol Phosphate	4.77E-04
Outgrowth of Neurites	5.31E-04
Modification of NADPH	7.70E-04
Viral Infection	1.19E-03
Transmigration of Macrophages	1.66E-03
Myeloproliferative Disorder	2.09E-03
Mineralization of Tooth	4.68E-03
Morphology of Chromosomes	4.84E-03
Transport of Protein	5.02E-03
Proliferation of Tumor Cell Lines	5.36E-03
Apoptosis of Tumor Cell Lines	5.65E-03
Abnormal Morphology of Interdigital Web	5.86E-03
Concentration of Phospholipid	6.25E-03
Organization of Cytoplasm	6.38E-03
Development of Blood	6.39E-03
Transmigration of Cells	6.64E-03
Alternative Splicing of mRNA	8.43E-03
Abnormal Quantity of Leukocytes	9.29E-03

All gene “hits” that were assigned p-values of <0.05 by RSA analysis (~2500 genes) were entered into the IPA software program for functional annotation clustering analysis. This table lists significantly enriched functional annotations (p-value <0.01) in descending order from the most significant. Abbreviations: RSA (redundant siRNA activity); IPA (interactive Pathway Analysis of complex ‘omics).



**Table 2.4: Predicted upstream regulators of gene "hits" (p-value <0.05) and their predicted functionality in the context of the activation of latent HIV-1**

Gene Name	Gene Abbr.	Prediction	z-score	p-value
Transforming growth factor, beta 1	TGFB1	Inhibited	-4.661	3.66E-02
Tumor protein p73	TP73	Inhibited	-4.542	4.05E-02
Catenin (cadherin-associated protein), alpha 1, 102kDa	CTNNA1	Activated	4.162	2.06E-02
E1A binding protein p300	EP300	Inhibited	-3.624	1.19E-02
Nuclear receptor subfamily 1, group I, member 3	NR1I3	Inhibited	-3.524	6.51E-03
GATA binding protein 1 (globin transcription factor 1)	GATA1	Inhibited	-3.204	1.43E-03
SMAD family member 3	SMAD3	Inhibited	-2.983	2.74E-02
miR-21-5p (seed AGCUUAAU)	----	Activated	2.947	4.69E-02
miR-17-5p (seed AAAGUGC)	----	Activated	2.687	2.51E-02
RuvB-like 1 (E. coli)	RUVBL1	Inhibited	-2.621	4.04E-02
miR-204-5p (seed UCCCUUU)	----	Activated	2.412	2.25E-02
miR-141-3p (seed AACACUG)	----	Activated	2.391	2.78E-02
Wingless-type MMTV integration site family, member 3A	WNT3A	Inhibited	-2.328	2.52E-02
CAR ligand-CAR-Retinoic acid-RXR $\alpha$ Complex	----	Inhibited	-2.216	2.05E-02
v-maf avian musculoaponeurotic fibrosarcoma oncogene homolog F	MAFF	Inhibited	-2.00	9.84E-03

All gene "hits" that were assigned p-values of <0.05 by RSA analysis (~2500 genes) were entered into the IPA software program for functional annotation clustering analysis. This table lists upstream regulators of the gene "hits" (assigned p-values of <0.05) for which statistically sound predictions were made (z-score <-2 for inhibited prediction; >2 for activated prediction) for the activity of those upstream regulators in the context of the activation of latent HIV-1. The upstream regulators exhibiting a predicted inhibited or activated functionality are listed in descending order from the most significant prediction according to z-score. Abbreviations: RSA (redundant siRNA activity); IPA (interactive Pathway Analysis of complex 'omics).

**Table 2.5: Significant (p-value <0.05) gene "hits" that can be categorized into the ubiquitin-proteasome system**

<b>Gene Name</b>	<b>Gene Abbr.</b>	<b>p-value</b>
HECT domain containing E3 ubiquitin protein ligase 2	HECTD2	2.7E-04
Ubiquitin associated and SH3 domain containing B	UBASH3B	1.7E-03
Ubiquitin specific peptidase 45	USP45	2.25E-03
Ubiquitin specific peptidase 25	USP25	2.33E-03
F-box and leucine-rich repeat protein 17	FBXL17	2.7E-03
F-box protein 42	FBXO42	3.7E-03
Pellino E3 ubiquitin protein ligase 1	PELI1	6.7E-03
F-box protein 38	FBXO38	1.31E-02
Makorin ring finger protein 2	MKRN2	1.34E-02
F-box and WD repeat domain containing 10	FBXW10	1.51E-02
Ring finger protein 126	RNF126	1.61E-02
Zinc and ring finger 2	ZNRF2	1.75E-02
SMAD specific E3 ubiquitin protein ligase 1	SMURF1	1.93E-02
Mindbomb E3 ubiquitin protein ligase 1	MIB1	2.11E-02
HECT domain containing E3 ubiquitin protein ligase 1	HECTD1	2.13E-02
F-box protein 34	FBXO34	2.15E-02
Itchy E3 ubiquitin protein ligase	ITCH	2.54E-02
Ubiquitin-conjugating enzyme E2G 2	UBE2G2	2.70E-02
Ligand of numb-protein X 1, E3 ubiquitin protein ligase	LNX1	2.92E-02
F-box protein 4	FBXO4	2.93E-02
F-box and WD repeat domain containing 9	FBXW9	3.02E-02
Ubiquitin-conjugating enzyme E2B	UBE2B	3.11E-02
Ring finger protein 31	RNF31	3.12E-02
F-box and WD repeat domain containing 2	FBXW2	3.28E-02
F-box protein 9	FBXO9	3.3E-02
Proteasome activator subunit 3	PSME3	3.44E-02
Cullin 7	CUL7	3.54E-02
Ubiquitin specific peptidase 9, X-linked	USP9X	3.61E-02
Ubiquitin specific peptidase 48	USP48	3.76E-02
Membrane-associated ring finger (C3HC4) 1, E3 ubiquitin protein ligase	MARCH1	3.81E-02
Ring finger protein 135	RNF135	3.92E-02
Ring finger protein 41	RNF41	3.94E-02
Membrane-associated ring finger (C3HC4) 9	MARCH9	4.00E-02
Ubiquitin-conjugating enzyme E2H	UBE2H	4.06E-02
Ariadne homolog, ubiquitin-conjugating enzyme E2 binding protein, 1(Drosophila)	ARIH1	4.24E-02
F-box and leucine-rich repeat protein 5	FBXL5	4.5E-02

Ubiquitin-like 5	UBL5	4.61E-02
Ring finger protein 25	RNF25	4.67E-02
WW domain containing E3 ubiquitin protein ligase 2	WWP2	4.68E-02
G2/M-phase specific E3 ubiquitin protein ligase	G2E3	4.74E-02
Proteasome activator subunit 1	PSME1	4.86E-02
Ring finger protein 34, E3 ubiquitin protein ligase	RNF34	4.89E-02
Proteasome 26S subunit, non-ATPase, 6	PSMD6	4.95E-02

All gene “hits” that were assigned p-values of <0.05 by RSA analysis (~2500 genes) were queried for keywords including UBE1, UBE2, UBE3, E1, E2 ubiquitin-conjugating enzyme, E3 ubiquitin ligase, cullin, F-box, ring finger, ubiquitin, and proteasome. The genes in this table show the query results and are listed in descending order from the most significant based on the original RSA analysis. Abbreviations: RSA (redundant siRNA activity)

## Figures

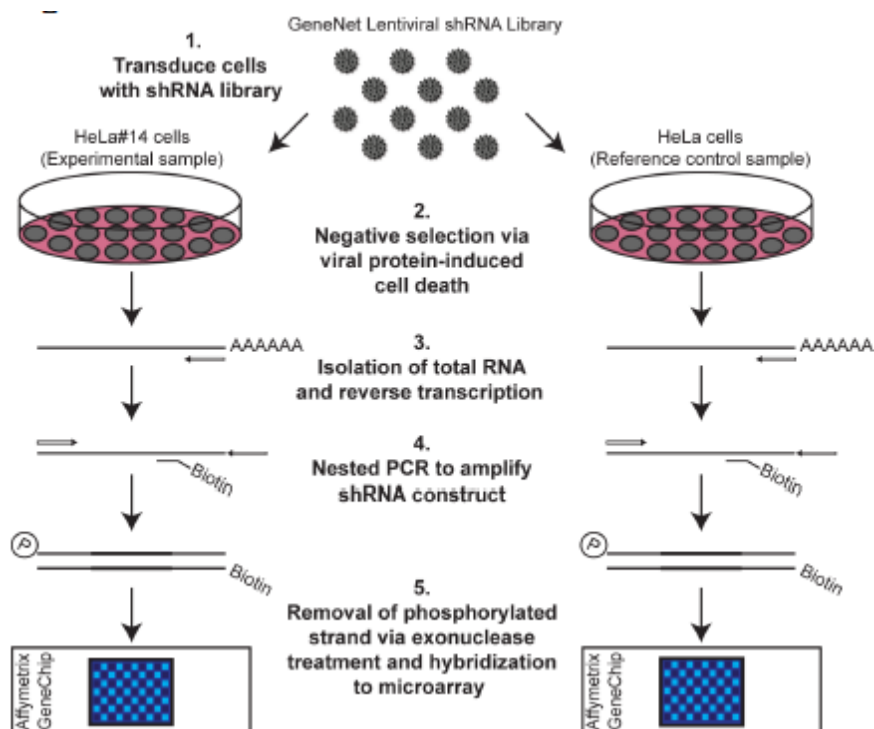


**Figure 2.1. Reverse genetic screen protocol.** Latently infected HeLa# 14 cells (referred to as the experimental sample) and parental, uninfected HeLa cells (referred to as the reference control sample) were transduced with the GeneNet Lentiviral shRNA Library at an MOI of approximately 0.4. The infected cells were selected with puromycin and cultured for a total of 17 days to allow for expression of the shRNA and knockdown of the target gene, as well as viral reactivation and virus protein-mediated cell death in the experimental sample. Following the culture period, total RNA was isolated, reverse transcribed, and amplified using 5' phosphorylated sense strand primers and 5' biotinylated antisense strand primers. The phosphorylated sense strands were degraded via lambda exonuclease treatment and the biotinylated antisense strands were hybridized to the Affymetrix GeneChip Array (HG-U133 + 2.0). Signals were detected following the addition of phycoerythrin-conjugated streptavidin. Signals from the reference control

sample array that were at least three times greater than the corresponding signal from the experimental sample array were considered “hits” and were statistically analyzed further.

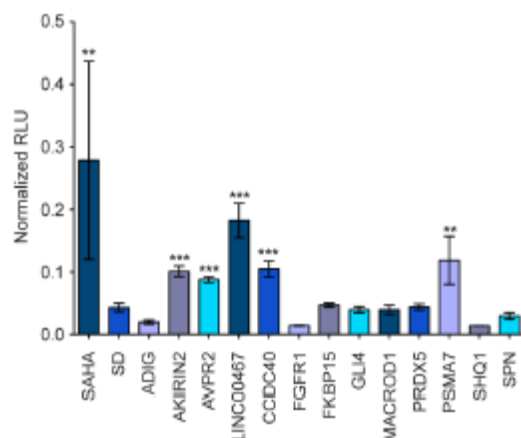


**Figure 2.2. Validation follow-up of significant gene “hits” identified in the screen.** HeLa#14 cells were transiently transfected in duplicate with pools of three or four gene-specific GIPZ lentiviral shRNAs (please refer to table S1 to define gene name abbreviations) or with the SD shRNA control. Transfection efficiencies were, on average, 75.5% (data not shown) as determined by the number of transfected cells expressing GFP, which is present in the shRNA expression constructs. Transfected cells were incubated for 72- to 96-hours (time course experiments were performed to determine optimal time points for analysis following the transfection of each shRNA pool; data not shown) after which RLUC activity was analyzed. RLUs from transfected samples were normalized to protein concentration and then to the number of transfected cells (# of GFP<sup>+</sup> cells). RLUs from cells treated with 2  $\mu$ M SAHA (positive control) were normalized to protein concentration and then to the number of live cells. Asterisks indicate a significant difference (\*\*  $p < 0.01$ ; \*\*\*  $p < 0.001$ ) in normalized RLU values between shRNA transfected cells or SAHA-treated cells and SD (negative control) transfected cells. P-values calculated using one-tailed Student’s t test. Error bars indicate standard error of the mean. The large error bar for SAHA is due to toxicity of the compound in HeLa cells. The figure represents average values from at least three independent experiments. Abbreviations: GFP

(green fluorescence protein); SD (scrambled duplex); RLUC (*Renilla* luciferase); RLU (relative light unit); SAHA (suberoylanilide hydroxamic acid).

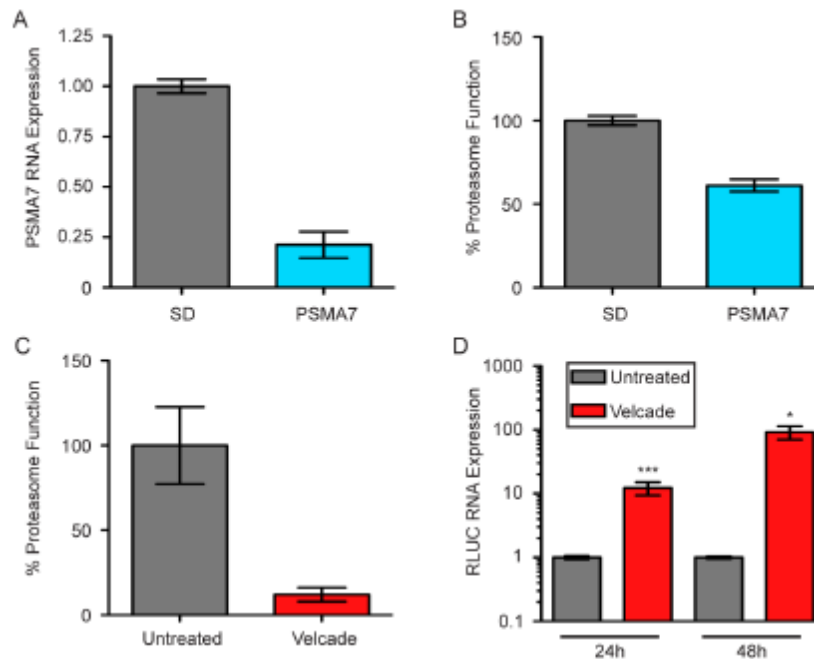


**Figure 2.3. Proteasomal inhibition activates latent HIV-1 reporter gene transcription.** HeLa#14 cells were transiently transfected in triplicate with a pool of three PSMA7 specific GIPZ lentiviral shRNAs or with the SD shRNA control. Transfection efficiencies were, on average, 84% (data not shown) as determined by the number of transfected cells expressing green fluorescence protein, which is present in the shRNA expression constructs. **A.** Forty-eight hours post-transfection, mRNA levels were analyzed via reverse transcription-quantitative PCR. PSMA7 expression values were calculated via  $\Delta\Delta C(t)$  method with the values normalized to the expression level of GAPDH in each transfected sample. PSMA7 expression level was arbitrarily set to 1 in the SD sample (negative control). **B.** Forty-eight hours post-transfection, proteasome activity was assessed. RLUs were normalized to the number of transfected cells and the values shown specify the percent proteasome function compared to SD transfected cells, whose function was set to 100%. **C.** HeLa#14 cells were treated with 15 nM Velcade or left untreated and proteasome activity was assessed two hours post-treatment. The values shown specify the percent proteasome function compared to untreated cells, whose function was set to 100%. **D.** HeLa#14



cells were treated with 15 nM Velcade or were left untreated for 24 h and 48 h. At each time point, *RLUC* RNA levels were analyzed via reverse transcription-quantitative PCR. RNA expression values were calculated via  $\Delta\Delta C(t)$  method with the values normalized to the expression level of GAPDH in each sample. Asterisks indicate a significant difference (\*  $p < 0.05$ ; \*\*\*  $p < 0.001$ ) in RNA expression levels between Velcade-treated cells and untreated (negative control) cells. P-values calculated using one-tailed Student's t test. Error bars indicate standard error of the mean. The figure represents average values from three independent experiments. Abbreviations: PSMA7 (proteasome subunit, alpha type, 7); SD (scrambled duplex); GAPDH (glyceraldehyde 3-phosphate dehydrogenase); RLU (relative light unit); RLUC (*Renilla* luciferase).

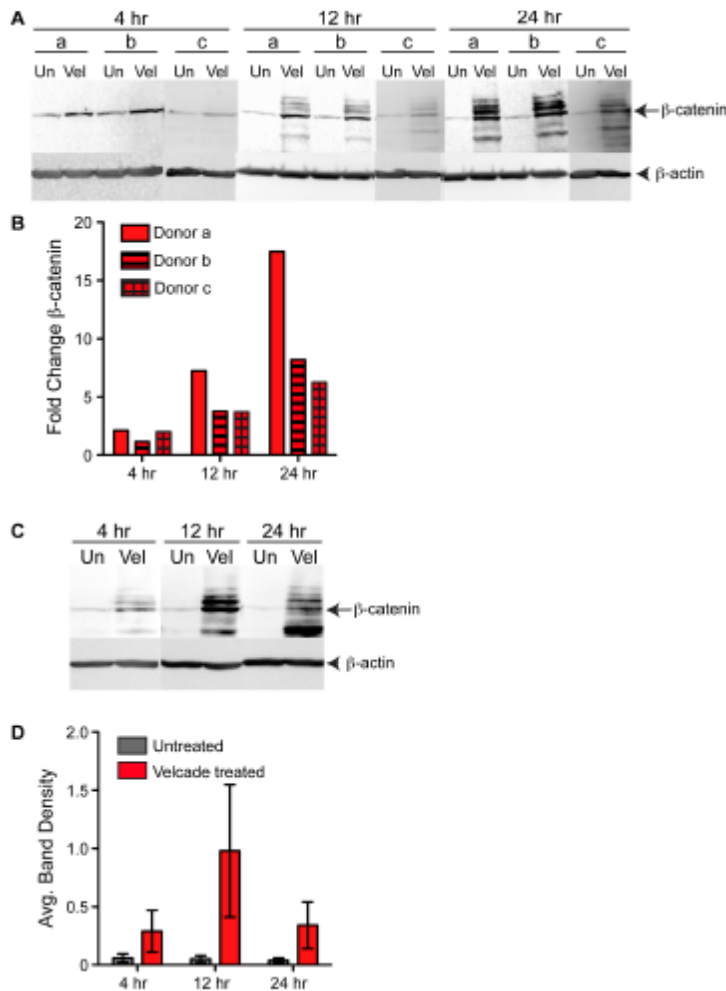


**Figure 2.4. PIs stabilize β-catenin in primary, resting CD4<sup>+</sup> T cells and OM-10.1 cells. (A)**

Western blot illustrates β-catenin protein levels in human primary, resting CD4<sup>+</sup> T cells isolated from healthy donors (a, b, and c) following either no treatment (Un, negative control) or treatment with 10 nM Velcade (Vel) for the indicated time course. Bands above full-length β-catenin represent the typical band pattern of ubiquitinated β-catenin. β-actin served as a loading control. **(B)** Densitometry analysis of Western blot depicted in (A) measuring only the β-catenin band indicated by the arrow. Values normalized to β-actin protein levels and bars represent the fold change in β-catenin protein levels in Velcade-treated samples over untreated samples. **(C)** Western blot illustrates β-catenin protein levels in OM-10.1 cells following

treatment as stated above. Bands above full-length  $\beta$ -catenin represent the typical band pattern of ubiquitinated  $\beta$ -catenin. Bands below are likely non-specific degradation from proteases owing to Velcade's pro-apoptotic cytotoxicity.  $\beta$ -actin served as a loading control. **(D)**

Densitometry analysis of Western blot depicted in (C) measuring only the  $\beta$ -catenin band indicated by the arrow. Values normalized to  $\beta$ -actin protein levels and bars represent average band density measurements in untreated and Velcade-treated samples per time point from three independent experiments. Error bars indicate standard error of the mean.

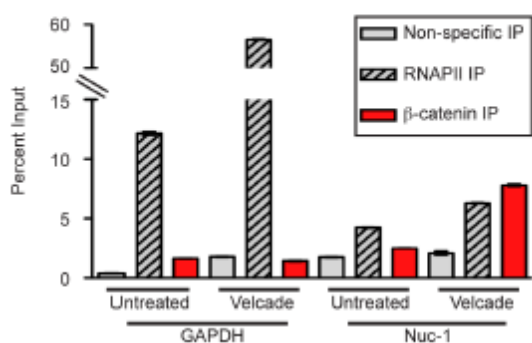


**Figure 2.5. β-catenin becomes enriched on the HIV-1 5' LTR following proteasomal inhibition.**

OM-10.1 cells were treated with 15 nM Velcade or were left untreated for approximately six hours. Samples were then crosslinked, sonicated, and immunoprecipitated overnight using either non-specific normal goat IgG antibody (negative control), mouse IgG anti-human RNAP II antibody, or goat IgG anti-human β-catenin antibody. Chromatin/antibody complexes were isolated using protein G agarose beads, samples were uncrosslinked overnight, and DNA was purified. The GAPDH promoter region and the Nuc-1 region of the HIV-1 5' LTR were detected using quantitative PCR and quantitations were calculated using the  $\Delta C(t)$  method. Values shown indicate the quantity of immunoprecipitated chromatin as a percentage of 'input' chromatin. Error bars represent standard error of the mean and the figure represents average values from three independent experiments. Abbreviations: RNAP II (RNA polymerase II); GAPDH (glyceraldehydes 3-phosphate dehydrogenase).

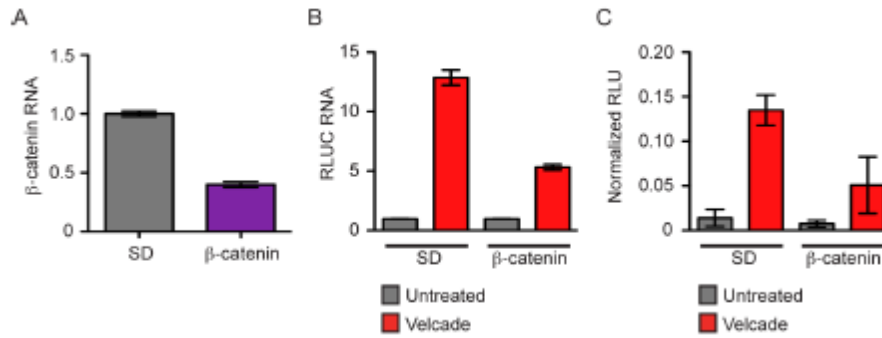


**Figure 2.6.  $\beta$ -catenin knockdown reduces the magnitude of Velcade-induced activation of latent HIV-1.** HeLa#14 cells were transiently transfected in triplicate with a pool of three  $\beta$ -catenin specific GIPZ lentiviral shRNAs or with the SD shRNA control. Transfection efficiencies were, on average, 74% (data not shown) as determined by the number of transfected cells expressing GFP, which is present in the shRNA expression constructs. **A.** Forty-eight hours post-transfection,  $\beta$ -catenin mRNA levels were analyzed via reverse transcription-quantitative PCR.  $\beta$ -catenin expression values were calculated via  $\Delta\Delta C(t)$  method with the values normalized to the expression level of GAPDH in each transfected sample.  $\beta$ -catenin expression level was arbitrarily set to 1 in the SD sample (negative control). **B and C.** Forty-eight hours post-transfection, cells were treated with 15 nM Velcade or left untreated. Forty-eight hours post-treatment, RLUC RNA levels (**B**) and RLUC activity (**C**) were analyzed. RLUC RNA levels were analyzed via reverse transcription-quantitative PCR and RNA expression values were calculated via  $\Delta\Delta C(t)$  method with the values normalized to the expression level of GAPDH in each sample. RLUC expression level was arbitrarily set to 1 in the untreated samples (negative control). RLUC activity was analyzed and RLUs were normalized to protein concentration and then to the number of transfected cells (# of GFP<sup>+</sup> cells). Error bars indicate standard error of the mean. The figure represents average values from three independent experiments. Abbreviations: SD (scrambled duplex); GAPDH (glyceraldehydes 3-phosphate dehydrogenase); RLUC (*Renilla* luciferase); GFP (green fluorescence protein).

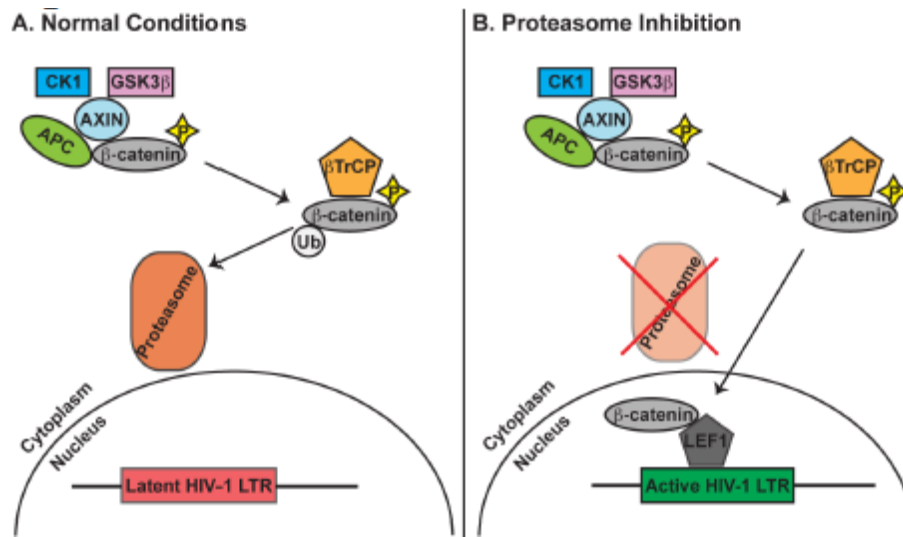


**Figure 2.7. Potential pathway through which PIs activate latent HIV-1 transcription. A.** Under normal circumstances in the absence of Wnt signaling,  $\beta$ -catenin is phosphorylated by casein kinase 1 $\alpha$  (CK1) and glycogen synthase kinase 3 $\beta$  (GSK3 $\beta$ ) of the APC/Axin1 destruction complex. Phosphorylated  $\beta$ -catenin is then recognized by E3 ubiquitin ligase(s), which induces the ubiquitination of  $\beta$ -catenin and its subsequent degradation by the proteasome. **B.** Upon proteasome inhibition, phosphorylated  $\beta$ -catenin is no longer degraded making it available for nuclear translocation. Once in the nucleus,  $\beta$ -catenin binds its co-transcription factor LEF1 (lymphoid enhancer-binding factor 1), which has binding sites in the HIV-1 5' LTR promoter region, resulting in the activation of latent HIV-1 transcription.

### **Chapter 3: Characterization of the Activity of Proteasome Inhibitors as HIV-1 Latency Antagonists**

#### **Abstract**

Existing highly active antiretroviral therapy (HAART) effectively controls viral replication in human immunodeficiency virus type 1 (HIV-1) infected individuals but cannot completely eradicate the infection due to the persistence of latently infected cells. One strategy that is being actively pursued to eliminate the latent arm of HIV-1 infection involves therapies combining latency antagonists with HAART. However, discordant pharmacokinetics between these types of drugs can potentially create sites of active viral replication within certain tissues that might be impervious to HAART. In an effort to identify novel cellular regulators of HIV-1 latency, a preliminary reverse genetic screen was performed which indicated that the proteasome might be involved in the maintenance of the latent state. This prompted testing to determine if proteasome inhibitors (PIs) could act as latency antagonists. Experiments demonstrated that PIs effectively activated latent HIV-1 in several model systems, including primary T cell model systems, thereby defining PIs as a new class of HIV-1 latency antagonists. Expanding upon experiments from previous reports, it was also confirmed that PIs inhibit HIV-1 replication. Moreover, it was possible to show that PIs act as bifunctional antagonists of HIV-1 latency and replication in a single cycle of infection. Thus, the data indicate that PIs induce viral gene expression from latent provirus while promoting the production of defective virions. Such bifunctional antagonists have the capacity to ensure precise tissue overlap of anti-latency and anti-replication activities, which is of significant importance in the consideration of future drug therapies aimed at viral clearance.





## **Introduction**

Human immunodeficiency virus type 1 (HIV-1) infection is presently incurable necessitating life-long drug treatment [354]. HIV-1 is able to persist within its cellular host by entering a reversible dormant state, termed latency, which provides protection from the immune system and antiviral pharmaceuticals. Consequently, latent HIV-1 is able to persist indefinitely awaiting activation, upon which it can reestablish a productive infection in the absence of highly active antiretroviral therapy (HAART) (latency reviewed in [426]).

Currently, one strategy to abolish latent infection involves treating patients with a latency antagonist concomitantly with HAART to prevent new infections and the reestablishment of the latent reservoir upon the activation of latent virus [310, 311, 426-429]. A major reservoir of latent infection *in vivo* is within memory CD4<sup>+</sup> T cells [430] but other cell types have been reported to harbor latent HIV-1 as well, including cells of myeloid origin. Additionally, latently infected cells can be found in tissues that are resistant to effective penetration of at least some HAART drugs [431-438]. For instance, the brain is known to house latently infected cells [431, 438-442] while the blood-brain barrier (BBB) can restrict the entry of many antiretroviral drugs into the brain [443-449]. In light of this, it may be important to not only treat patients with both latency activators and HAART simultaneously, but to ensure their concurrent delivery to the same tissue and cellular compartments.

The 26S proteasome is composed of two regulatory 19S subunits that abut a catalytic 20S core subunit and as a whole is responsible for the degradation of ubiquitinated proteins in the cell [385]. Interestingly, the proteasome is involved in promoting HIV-1 replication via its specific degradation of the APOBEC3 family of HIV-1 restriction factors in the presence of the

viral protein Vif (reviewed in [450]). Surprisingly, as delineated previously in Chapter 2 and here in this study, it was also found that the proteasome is involved in maintaining HIV-1 latency. The fact that the proteasome positively influences both HIV-1 replication and latency makes it a unique, single drug target whose inhibition has the potential to elicit dual antiviral effects. The development of a drug that exhibits bifunctional antagonism of both aspects of the viral life cycle would help to address concerns regarding the insufficient penetration of HAART into some tissues harboring latently infected cells.

In this report, evidence that proteasome inhibitors (PIs) hinder both HIV-1 latency and replication is presented. Here, it is shown that PIs activate latent HIV-1 in several *in vitro* model systems, including two primary human CD4<sup>+</sup> T cell model systems. Consequently, PIs represent a new class of HIV-1 latency antagonists. Additionally, this study confirms that PIs inhibit HIV-1 replication. Finally, it is demonstrated that PIs activate latent HIV-1 and subsequently reduce progeny virion infectivity in a single round of infection. These results introduce a novel proof-of-concept that effective bifunctional HIV-1 antagonists can be developed.

## **Materials and Methods**

### **Plasmid Constructs**

The construct present in HeLa#14 cells (labeled as RLUC/RFP) is an HIV-1<sub>NL4-3</sub>-based construct harboring *Renilla luciferase* (RLUC) in the *env* position and *red fluorescence protein* (RFP) in the *nef* position [366]. The construct present in 24ST1NLESG cells (labeled as SEAP/GFP) is an HIV-1<sub>NL4-3</sub>-based construct harboring *secreted alkaline phosphatase* (SEAP) in the *env* position and *green fluorescence protein* (GFP) in the *nef* position [451]. Both the RLUC/RFP and the SEAP/GFP constructs have a 2.5-kb deletion in *pol* and a 1.0-kb deletion in *env* to render the vectors replication-incompetent. Additionally, the *vpu* start codon in both constructs is mutated for robust marker gene expression [366] [451]. The Bcl-2 expression vector pEB-FLV [452] was a kind gift from Dr. Robert F. Siliciano. The gGnΔ construct is an HIV-1<sub>NL4-3</sub>-based construct that is replication-incompetent. PCR fragments containing the 3' region of *env*, the complete coding sequence for *Gaussia luciferase* (GLUC), the T2A sequence, the complete coding sequence for *enhanced green fluorescence protein* (EGFP), and the 5' region of *nef* were fused together by SOEing PCR. The T2A sequence ensures that GLUC is expressed as a single peptide by promoting a ribosomal 'skip' [453, 454]. The fused PCR fragment was inserted into the HIV-1<sub>NL4-3</sub> construct via BamHI-XhoI restriction sites. A 903-bp deletion in *env* was made by inserting a PCR fragment, containing the 3' region of *vpr* including a mutation in the start codon of *env* (ATG → ACG) and the 5' region of *env* up to position 6344, into the pHIV-1<sub>NL4-3</sub> construct via EcoRI-NheI restriction sites. The Gn construct is an HIV-1<sub>NL4-3</sub>-based construct that is replication-competent. PCR fragments containing the 3' region of *env*, the complete coding sequence for *EGFP*, the T2A sequence, and the 5' region of *nef* were fused together by SOEing PCR. The T2A sequence here

ensures that EGFP is expressed as a single peptide [453, 454]. The fused PCR fragment was inserted into the HIV-1<sub>NL4-3</sub> construct via BamH1-Xho1 restriction sites.

### **Cells and Culture Media**

The following cell lines were obtained through the AIDS Research and Reference Reagent Program, Division of AIDS, NIAID, NIH: OM-10.1 from Dr. Salvatore Butera (36-40), and U373-MAGI-CXCR4CEM from Dr. Michael Emerman (41). OM-10.1 cells, primary human activated CD4<sup>+</sup> T cells, primary human resting CD4<sup>+</sup> T cells, primary human CD4<sup>+</sup> TCM-like cells, and primary human CD4<sup>+</sup> Bcl-2 transduced cells were cultured in RPMI 1640 GlutaMAX, HEPES medium (Life Technologies, Grand Island, NY) supplemented with 10% FBS (Thermo Scientific Hyclone, Logan, UT), 2X MEM Non-essential amino acids solution (Life Technologies, Grand Island, NY), and 100 U/ml penicillin-100 µg/ml streptomycin solution (Life Technologies, Grand Island, NY). HeLa#14 cells were cultured in MEM GlutaMAX medium (Life Technologies, Grand Island, NY) supplemented with 10% FetalClone III Serum (Thermo Scientific Hyclone, Logan, UT), 2X MEM Non-essential amino acids solution, and 100 U/ml penicillin-100 µg/ml streptomycin solution. U373-MAGI-CXCR4CEM cells were cultured in DMEM, high glucose GlutaMAX medium (Life Technologies, Grand Island, NY) supplemented with 10% FBS, 2X MEM Non-essential amino acids solution, 0.2 mg/ml G418 (Sigma-Aldrich, St. Louis, MO), 0.1 mg/ml hygromycin B (Sigma-Aldrich, St. Louis, MO), and 1.0 µg/ml puromycin (Sigma-Aldrich, St. Louis, MO). HeLaT4 cells and HEK293T cells were cultured in DMEM, high glucose GlutaMAX medium supplemented with 10% FetalClone III Serum, 2X MEM Non-essential amino acids solution, and 100 U/ml penicillin-100 µg/ml streptomycin solution.

## **Development of Latently Infected Primary Human CD4+ T Cell Models: TCM-like Cells and Bcl-2**

### **Transduced Cells**

Leukocyte enriched blood samples from healthy adult human donors were purchased from the New York Blood Center. To obtain a purified population of peripheral blood mononuclear cells (PBMCs), buffy coats were isolated from the blood by a Ficoll gradient using Histopaque-1077 (Sigma-Aldrich, St. Louis, MO). Also, red blood cells were lysed using ACK lysing buffer (Lonza, Inc., Allendale, NJ). Primary human CD4+ TCM-like cells were prepared as previously described (42) with the modification that naïve CD4+ T cells were separated from PBMCs using the Dynabeads Untouched™ Human CD4+ T Cells kit (Life Technologies, Grand Island, NY) according to the manufacturer's instructions with the additional antibodies mouse IgG anti-human CD25 (BD Biosciences, Franklin Lakes, NJ) and mouse IgG anti-human CD45RO (BD Biosciences, Franklin Lakes, NJ) for the specific removal of activated and memory CD4+ T cells, respectively. Primary human Bcl-2-transduced CD4+ T cells were prepared as previously described (33) with the modification that cells were activated using the Dynabeads Human T-Activator CD3/CD28 kit (Life Technologies, Grand Island, NY) according to the manufacturer's instructions in the presence of 30U/ml interleukin-2 (IL-2) (Peprotech, Rocky Hill, NJ). Vesicular stomatitis virus envelope pseudotyped virions used to establish a latent viral infection in TCM-like cells or in Bcl-2-transduced cells were produced in HEK293T cells transfected with the gGnΔ construct and the packaging plasmid pMD.G (43) using polyethyleneimine linear (molecular weight of 25kDa) (Polysciences Inc., Warrington, PA). Forty-eight hours post-transfection, viral supernatants were collected and concentrated 50X using Retro-Concentin (System Biosciences, Mountain View, CA) according to the manufacturer's instructions. TCM-like cells or Bcl-2-transduced cells were infected via spinoculation as previously described (44) with the modifications that infections

were carried out in 24-well plates and in the presence of 8 µg/ml polybrene (Sigma-Aldrich, St. Louis, MO). Infected cells were cultured for an extended period of time to establish a latent infection (33, 42).

### **PI Treatment to Analyze Latent HIV-1 Activation**

Twenty-four hours prior to treatment, HeLa#14 cells were seeded in 24-well plates at  $5 \times 10^4$  cells per well. Cells were then treated in triplicate with 4.5 µM clasto-Lactacystin β-lactone (CLBL) (Sigma-Aldrich, St. Louis, MO), 450 nM MG-132 (Cayman Chemicals, Ann Arbor, MI), 7 nM Velcade (Selleckchem, Houston, TX), 2 µM suberoylanilide hydroxamic acid (SAHA) (Selleckchem, Houston, TX) (positive control), or 0.25% DMSO (negative control). Forty-eight hours post-treatment, the cells were lysed, protein concentration was measured via standard Bradford assay and RLUC activity was measured as described above.

24ST1NLESG cells were plated in 24-well plates at  $5 \times 10^5$  cells per well. Immediately, cells were treated in triplicate with 4.5 µM CLBL, 450 nM MG-132, 7 nM Velcade, 2 µM SAHA (positive control), or 0.25% DMSO (negative control). CLBL and SAHA treated cells were analyzed 48 hours post-treatment while MG-132, Velcade, and DMSO treated cells were analyzed 72 hours post-treatment. SEAP activity in the culture supernatant was measured using the Phospha-Light Secreted Alkaline Phosphatase Reporter Gene Assay System (ABI, Foster City, CA) according to the manufacturer's instructions. Luminescence was measured on the Turner Biosystems 20/20n Luminometer using default settings.

OM-10.1 cells were plated in 6-well plates at  $2.5 \times 10^6$  cells per well. Immediately, cells were treated in duplicate with 4.5 µM CLBL, 450 nM MG-132, 7 nM Velcade, 2 µM SAHA (positive

control), or 0.25% DMSO (negative control). Seventy-two hours post-treatment, HIV-1 capsid protein (p24) concentration in the culture supernatant was analyzed via p24 ELISA using the HIV-1 p24 Antigen Capture Kit (AIDS & Cancer Virus Program, NCI-Frederick, MD) according to their instructions. Secondary antibody peroxidase activity was determined via colorimetric analysis using the Coulter Microplate Reader set to read at 450 nm with a reference reading at 650 nm.

TCM-like cells and Bcl-2 transduced cells, latently infected with the gGnΔ construct, were plated in 96-well plates at  $1 \times 10^5$  cells per well. Immediately, cells were treated with 5 μM CLBL, 250 nM MG-132, 10 nM Velcade, Dynabeads Human T-Activator CD3/CD28 beads according to the manufacturer's instructions in the presence of 30 U/ml IL-2 (positive control), or were left untreated (negative control). Forty-eight hours post-treatment, GLUC activity in the culture supernatant was measured using the BioLux Gaussia luciferase Flex Assay Kit (New England Biolabs, Ipswich, MA) according to the manufacturer's instructions. Luminescence was measured on the Promega GloMax 20/20 Luminometer with a 10 second integration setting. Additionally, PI-treated cells were fixed with a 1% formaldehyde solution for 5 minutes and then GFP mean channel fluorescence values were determined using the BD Biosciences Accuri C6 Flow Cytometer.

### **PI Treatment to Analyze T Cell Activation Status**

Human PBMCs were isolated from healthy donor leukocyte enriched blood samples as described above. CD4<sup>+</sup> T cells were isolated using the Dynabeads Untouched™ Human CD4<sup>+</sup> T Cells kit according to the manufacturer's instructions. The cells were plated in a 96-well plate at  $1 \times 10^5$

cells per well and then left untreated (negative control), treated with 500 nM MG-132, or activated using the Dynabeads Human T-Activator CD3/CD28 kit according to the manufacturer's instructions in the presence of 30 U/ml IL-2 (positive control). Forty-eight hours post-treatment, cells were incubated with 20  $\mu$ l of mouse IgG FITC-conjugated anti-human CD25 antibody (BD Biosciences, Franklin Lakes, NJ) for 30 minutes at 4°C. The percentage of CD25+ cells in each of the samples was then determined using the BD Biosciences Accuri C6 Flow Cytometer.

### **PI Treatment to Analyze HIV-1 Replication Kinetics**

Human PBMCs were isolated from healthy donor leukocyte enriched blood samples as described above. CD4+ T cells were isolated using the Dynabeads Untouched™ Human CD4+ T Cells kit according to the manufacturer's instructions. The CD4+ T cells were then activated using the Dynabeads Human T-Activator CD3/CD28 kit according to the manufacturer's instructions in the presence of 30 U/ml IL-2 and were cultured an additional 3 days in the presence of IL-2. The cells were then plated in 24-well plates at  $2 \times 10^6$  cells per well. Immediately, 0.5 ml (corresponding to MOI ~0.2) of Gn virus stock was added to each well and the cells were spinoculated as previously described (44) in the presence of 8  $\mu$ g/ml polybrene. Six hours post-spinoculation, the infections were terminated and either 500 nM MG-132 was added to the cultures immediately, or the cultures were left untreated as a positive control (PC). Forty-eight hours post-treatment, viral supernatants were collected and p24 concentrations were measured via p24 ELISA using the HIV-1 p24 Antigen Capture Kit according to their instructions. Secondary antibody peroxidase activity was determined via colorimetric analysis using the Coulter Microplate Reader set to read at 450nm with a reference reading at 650 nm. HeLaT4 cells were



then seeded in 24-well plates at  $2 \times 10^5$  cells per well 24 hours prior to infection. Viral supernatants were diluted 10-fold and then 0.5 ml of diluted supernatants were added to each well in triplicate. The HeLaT4 cells were then spinoculated in the presence of polybrene as described above. Infections were terminated 6 hours post-spinoculation. Forty-eight hours post-infection, cells were fixed with a 1% formaldehyde solution for 5 minutes and then GFP+ cell numbers were analyzed using the BD Biosciences Accuri C6 Flow Cytometer.

### **PI Treatment to Analyze Antagonism of HIV-1 Latency and Replication in a Single Round of Infection**

OM-10.1 cells were treated with either 50 ng/ml TNF $\alpha$  (Sigma-Aldrich, St. Louis, MO) to stimulate the production of positive control (PC) viral particles, or with 5  $\mu$ M CLBL, to stimulate the production of viral particles under the influence of proteasomal inhibition. Seventy-two hours post-treatment, virus-containing supernatants were collected and p24 concentrations were measured via p24 ELISA using the HIV-1 p24 Antigen Capture Kit according to their instructions. Secondary antibody peroxidase activity was determined via colorimetric analysis using the Coulter Microplate Reader set to read at 450 nm with a reference reading at 650 nm. Twenty-four hours prior to infection, U373-MAGI-CXCR4CEM cells were seeded in 12-well plates at  $1 \times 10^5$  cells per well. Viral supernatants were diluted to a p24 concentration of 200 ng/ml and then 300  $\mu$ l of the diluted viral supernatants were used to infect U373-MAGI-CXCR4CEM cells in duplicate in the presence of 8  $\mu$ g/ml polybrene at 37°C. Infections were terminated within 5 hours. Forty-eight hours post-infection, cells were lysed, protein concentration was measured via standard Bradford assay and  $\beta$ -galactosidase activity was measured using the  $\beta$ -Galactosidase Enzyme Assay System with Reporter Lysis Buffer (Promega, Madison, WI)

according to the manufacturer's instructions. Colorimetric analysis was performed using the Nanodrop 2000 Spectrophotometer set to read at 420 nm.

## **Results**

### **PIs activate latent HIV-1 gene expression.**

As seen in Chapter 2, the siRNA screen in HeLa#14 cells [455] implicated the ubiquitin-proteasome system as having a role in maintaining HIV latency, namely through proteasome subunit, alpha type, 7 (PSMA7), a subunit of the 20S catalytic core particle of the 26S proteasome [385]. While we showed that the activity of Velcade, a proteasome inhibitor, worked at least partly through  $\beta$ -catenin stabilization, we sought to test the activity of it and two other proteasome inhibitors in three different cell models as well as in two primary cell models. First, we utilized the tissue culture-based latency models HeLa#14, 24ST1NLESG [451], and OM-10.1 [388-392]. 24ST1NLESG cells are a clonal population of SupT1 cells (a human CD4<sup>+</sup> T cell line) that are latently infected with an HIV-1<sub>NL4-3</sub>-based reporter construct SEAP/GFP. Briefly, the vector is rendered replication-incompetent via deletions in *pol* and *env* while green fluorescence protein (GFP) is expressed as an early gene product from the *nef* position and secreted alkaline phosphatase (SEAP) is expressed as a late gene product from the *env* position (Fig. 3.1) [451]. OM-10.1 cells are a clonal population of HL-60 promyelocytes that are latently infected with the replication-competent HIV-1<sub>LAV</sub> strain [388-392]. We treated HeLa#14 cells, 24ST1NLESG cells, and OM-10.1 cells with the PIs clasto-Lactacystin  $\beta$ -lactone (CLBL), Velcade, and MG-132, each of which inhibit the chymotrypsin-like activity of the 20S proteasome core particle [381, 386], and then analyzed latent proviral gene expression. PI concentrations and treatment durations were optimized in each system to effectively reduce cytotoxicity to low levels (data not shown). All three PIs were able to induce HeLa#14 cell RLUC expression (Fig.

3.2A), 24ST1NLESG cell SEAP expression (Fig. 3.2B), and OM-10.1 cell HIV-1 capsid protein (p24) expression (Fig. 3.2C) indicating activation of latent virus.

Next, we studied the effects of proteasome inhibition on proviral gene expression in two latent HIV-1 primary human CD4<sup>+</sup> T cell models. To start, HIV-1 virions were produced using a replication-incompetent HIV-1<sub>NL4-3</sub>-based reporter construct gGnΔ in which *Gaussia* luciferase (GLUC) and GFP are expressed as early gene products from the *nef* position (Fig. 3.1). This reporter virus was then used to establish a latent HIV-1 infection in primary human CD4<sup>+</sup> T cells, isolated from peripheral blood mononuclear cells (PBMCs) collected from healthy donors, via two distinct methods. The first involved the infection of non-polar CD4<sup>+</sup> T cells, which are considered to be the *in vitro* counterparts of latently infected central memory T cells *in vivo* [456]. Naïve human CD4<sup>+</sup> T cells were isolated, activated in a non-polarizing environment, infected with the gGnΔ virus, and then cultured for an extended period of time to establish a latent infection. These cells are referred to as T<sub>CM</sub>-like cells [456]. The second method involved the use of primary human CD4<sup>+</sup> T cells transduced with a Bcl-2 expression vector, which mimic both central memory and effector memory T cells [452]. The Bcl-2 transduced cells were activated, infected with the gGnΔ virus, and cultured for an extended period of time to permit the establishment of viral latency [452]. The latently infected T<sub>CM</sub>-like primary and Bcl-2 transduced human CD4<sup>+</sup> T cells were treated with PIs and analyzed for latent viral gene expression 48 hours later. Despite the expected donor-to-donor variability, PI treatment, on average, induced the expression of GFP (Fig. 3.3 A and B) and GLUC (Fig. 3.3 C and D) in both latent, primary human CD4<sup>+</sup> T cell models, with MG-132 and Velcade yielding the highest activation levels. We also examined the activation status of uninfected primary human resting CD4<sup>+</sup> T cells following exposure to MG-132. Resting human CD4<sup>+</sup> T cells cultured in the presence

of MG-132 for 48 hours did not become activated, as evidenced by a lack of expression of the T cell activation marker CD25 (Fig. 3.4). These results are in concert with previous studies, which indicated that PIs do not activate primary human T cells [457, 458].

Of note, the primary latent cell models discussed above were utilized instead of cells directly isolated from HIV-1 infected patients for a specific reason. Generally, when using patient samples for latency activation studies, the addition of allogeneic, MHC mismatched CD4<sup>+</sup> T cells is required to expand viral outgrowth upon latent viral reactivation [306, 310, 459-462]. The addition of allogeneic cells themselves might contribute to the activation of latent virus in patient sample systems and therefore, the latently infected primary cell models described above were chosen for testing the antagonist activity of PIs. Nevertheless, confidence in PIs' potential efficacy *in vivo* is boosted by the fact that significant activation of latent virus was demonstrated in all five model systems treated with PIs.

#### **PIs inhibit HIV-1 replication.**

Previous reports indicate that PIs can inhibit HIV-1 replication [463-466]. To examine PI-mediated replication inhibition, virions were generated via transfection of the replication-competent HIV-1<sub>NL4-3</sub>-based reporter construct Gn, in which GFP is expressed as an early gene product from the *nef* position, (Fig. 3.1) into HEK293T cells. The reporter virus was used to infect activated primary human CD4<sup>+</sup> T cells isolated from PBMCs collected from healthy donors. Six hours post-infection, cells were either treated with 500 nM MG-132 or left untreated for 48 hours. The resultant virus-containing supernatants were then collected and used to infect HeLaT4 cells in order to analyze viral infectivity. Forty-eight hours post-infection, the number of

infected (GFP<sup>+</sup>) HeLaT4 cells were counted and normalized to the p24 concentrations of inoculating viral supernatants. Approximately two times fewer HeLaT4 cells were infected from viral supernatants collected from infected, MG-132-treated primary CD4<sup>+</sup> T cells than from viral supernatants collected from infected, untreated primary CD4<sup>+</sup> T cells in just a single round of infection (Fig. 3.5). These results support the previous findings indicating that PIs inhibit HIV-1 replication, through interfering with release and maturation of virions. It is also likely that PIs enable the restriction factor APOBEC3G to be active, by preventing its vif-mediated proteasomal degradation [464-466].

### **Pis are bifunctional antagonists of HIV-1.**

The results demonstrating that PIs can both activate latent HIV-1 gene expression and inhibit HIV-1 replication suggested the feasibility of antagonizing both latency and replication in a single round of infection. To test this, the PI CLBL was employed to induce virion production from latently infected cells followed by an analysis of the infectivity of the resultant virions. Latently infected OM-10.1 cells were treated with either TNF $\alpha$ , to stimulate the production of positive control (PC) virus, or with CLBL, to stimulate the production of virus under the influence of proteasome inhibition. Seventy-two hours post-treatment, virus-containing supernatants were collected and p24 concentrations were measured. Figure 3.6A illustrates the magnitude of the induction of p24 production observed following the treatment of OM-10.1 cells with these two activators. Due to the fact that TNF $\alpha$  induces a significantly higher titer of virus than CLBL, viral supernatants were diluted to equal p24 concentrations and then used to infect U373-MAGI-CXCR4<sub>CEM</sub> cells to analyze viral infectivity. U373-MAGI-CXCR4<sub>CEM</sub> cells are human glioblastoma cells that have been transduced to constitutively express CD4 and CXCR4.

Additionally, they express  $\beta$ -Galactosidase ( $\beta$ -Gal) from an HIV-1 LTR promoter (Tat-inducible expression) and as such, are regularly used to obtain HIV-1 titers [467]. Forty-eight hours post-infection, we analyzed  $\beta$ -Gal activity in infected cell lysates. As shown in Figure 3.6B, cells infected with virions produced from CLBL-stimulated OM-10.1 cells (PI virus) expressed five times less  $\beta$ -Gal than cells infected with the same amount of PC virus, indicating that virus produced from PI-treated cells exhibit reduced infectivity.

## **Discussion**

This report demonstrates that PIs have the ability to activate latent HIV-1 in three tissue culture model systems and two primary cell model systems of HIV-1 latency identifying PIs as a new class of HIV-1 latency antagonists. We have also confirmed that proteasome inhibition in producer cells, whether they are productively infected or latently infected with HIV-1, results in the production of virions that exhibit reduced infectivity. Taken together, our results represent a novel proof-of-concept that a single pharmaceutical drug can antagonize both HIV-1 latency and replication simultaneously.

The previous finding that the downregulation of PSMA7, a catalytic subunit of the proteasome [385], activated HIV-1 gene expression was initially surprising considering that proteasome activity is required for the activation of NF $\kappa$ B, known to participate in HIV-1 transcription (reviewed in [379]). However, a review of the literature revealed two gene expression profiling studies that supported this finding. One study analyzed the gene expression profile in latently infected ACH-2 cells and found that 15 proteasome genes were upregulated in the latent state prior to viral reactivation [468]. The other study, which analyzed gene expression profiles in productively infected and latently infected cells, found that seven

proteasome genes were downregulated in productively infected H9 cells in comparison to uninfected cells [469]. This information in accordance with our results led us to formulate the hypothesis that the proteasome is involved in maintaining HIV-1 latency. Therefore, several PIs were tested for their ability to activate latent HIV-1 gene expression in different HIV-1 latency model systems. As shown in Figures 3.2 and 3.3, PIs activated latent HIV-1 gene expression in all three tissue culture models and both primary cell models tested. The variability in the degree of gene expression activation between inhibitors and model systems could be attributed to differences in the pharmacokinetics of each drug within each model system. Variability might also be affected by the specific model system and mode of reporter gene analysis. For example, late gene products were analyzed in the tissue culture model systems (RLUC, SEAP, and p24) while early gene products were analyzed in the primary cell model systems (GLUC and GFP). In addition, a degree of variability is expected when comparing results in primary cells obtained from different donors [470, 471]. Nevertheless, the results revealed that PIs consistently activate latent HIV-1 gene expression in several different model systems, including primary cell models, identifying PIs as a new class of HIV-1 latency antagonists. Of note, previous findings were confirmed [457, 458] showing that PIs do not activate primary human resting CD4<sup>+</sup> T cells *in vitro* (Fig. 3.4), which is an important consideration in order to avoid promoting a “cytokine storm” during treatment. In corroboration, studies have indicated that PIs are safe for use *in vivo* as the PI Velcade is FDA approved for the treatment of multiple myelomas, leukemias, and lymphomas [380-383, 472].

There are potential explanations for PI-mediated activation of latent HIV-1. First, there is increasing evidence that the 26S proteasome and/or individual 19S and 20S proteasome subparticles can regulate transcription both proteolytically and non-proteolytically, as protein



components of the proteasome have been found in the nucleus [473]. Interestingly, a study found that the 26S proteasome is associated with the HIV-1 LTR and controls basal transcription proteolytically in the absence of Tat in HeLa-LTR-Luc cells [474, 475]. Therefore, it is possible that PIs facilitate the activation of latent HIV-1 by inhibiting the degradation of and stabilizing factors that are involved in prompting viral transcription. For example, it was recently shown that the proteasome partially downregulates the expression of Cyclin T1, a subunit of the P-TEFb complex, in resting memory human CD4<sup>+</sup> T cells [476]. The P-TEFb complex is essential for HIV-1 transcriptional elongation as a cofactor of Tat (reviewed in [379]). It is theorized that low levels of Cyclin T1 contribute to the establishment of latency in resting memory CD4<sup>+</sup> T cells because they are less likely capable of supporting processive viral transcription [476]. Hence, PIs might promote the activation of latent HIV-1 transcription by stabilizing the Cyclin T1 component of the P-TEFb complex. It will be of great interest to explore the mechanism(s) of PI-induced activation of latent HIV-1 in more detail.

Experiments were also performed confirming that PIs inhibit HIV-1 replication. PI effects upon viral replication were examined in two ways, the first by treating freshly infected primary CD4<sup>+</sup> T cells with PIs and analyzing the infectivity of virion output (Fig. 3.5) and the second by analyzing the infectivity of virions produced as a consequence of PI-mediated activation of latent HIV-1 gene expression (Fig. 3.6 A and B). In both cases, treating replication-competent virus-producing cells with PIs reduced virion infectivity 2 to 5-fold in a single round of infection (Figs. 3.5 and 6B, respectively). Therefore, it is expected that continuous PI treatment over several rounds of infection would result in an exponential decline in HIV-1 replication. The results shown here are also in concert with results obtained from several previous studies. A3.01 cells infected with HIV-1<sub>NL4-3</sub> and subsequently treated with MG-132 have been shown to exhibit

a 15-fold reduction in viral output and the output virions exhibited a 50-fold reduction in infectivity in C8166 cells. It should be noted that they treated their cells with a concentration of MG-132 that was 100 times higher than the concentration used here (40-50  $\mu$ M), which could explain the fact that they observed a much higher-fold reduction in infectivity [464]. Moreover, it has been shown that activated PBMCs (collected from healthy donors) infected with HIV-1<sub>BAL</sub> in the presence of Velcade and/or MG-132 exhibit an approximate 10-fold reduction in both viral supernatant reverse transcriptase concentration and proviral copy number in target cells [465]. Finally, three genome-wide knock-down screens performed to identify cellular modulators of HIV-1 replication identified the proteasome complex as an enriched gene ontology functional group whose downregulation inhibited HIV-1 replication [463].

There are also potential explanations for PI-mediated HIV-1 replication inhibition. The bulk of evidence supports the involvement of the APOBEC3 family of cellular viral restriction factors, among which APOBEC3G and 3F (A3G/F) are the most potent against HIV-1 replication. A3G/F are cytidine deaminases that have been shown to inhibit HIV-1 replication by inducing viral genome hypermutation as well as by causing defects in the efficiency of reverse transcription and integration. In order to inhibit viral replication, A3G/F must be expressed in virus-producing cells and packaged into nascent virions. From there, they are able to inhibit viral replication in subsequent target cells (reviewed in [450]). A3G causes viral genome hypermutation during reverse transcription by deaminating cytidine residues in the minus strand of viral DNA, which results in G→A mutations in the plus strand of viral DNA during synthesis [477-480]. Additionally, A3G was shown to impair primer tRNA processing during reverse transcription, which not only affects the progression of reverse transcription but also results in the creation of viral DNA ends that are unfit for integration into cellular DNA [481-

483]. However, under normal conditions, HIV-1 is protected from the effects of A3G/F by the viral protein Vif, which binds to and targets A3G/F for proteasomal degradation precluding its incorporation into HIV-1 virions [466, 484-488]. Numerous studies have shown that PIs increase intracellular levels of A3G in infected cells by inhibiting its degradation even in the presence of Vif [466, 484-486, 488]. One study found that A3G was incorporated into virions produced from MG-132 treated virus-producing 293T cells and those virions exhibited an approximate 5-fold reduction in infectivity [466]. A3G/F are expressed in primary CD4<sup>+</sup> T cells and OM-10.1 cells [450], both of which were used to produce virus during treatment with PIs in this study. Therefore, it is a strong possibility that the PI-mediated inhibition of HIV-1 replication observed here was in large measure mediated by A3G/F. It will be interesting to delineate the involvement of A3G/F in PI-mediated inhibition of HIV-1 replication, as well as potential alternative mechanism(s) in future studies.

Overall, the data presented in this report validate the concept that effective inhibition of both HIV-1 latency and replication is attainable through the use of a single drug. The clinical importance of this concept is best understood when considering the fact that latency activators such as various HDAC inhibitors have failed in clinical trials to effectively expedite the decay rate of the latent reservoir in patients [310, 311, 426-429]. This phenomenon could be explained by the fact that antiretroviral drugs, administered concomitantly with latency activators, exhibit diverse pharmacokinetics amongst themselves and within different tissues. As such, an uneven distribution of antiviral activities in the body that do not coincide with latency antagonist activities might provide an opportunity for the establishment of fresh latent infection in certain tissues. In that scenario, a strategy to purge latent virus via the simultaneous delivery of latency

antagonists and antivirals might inadvertently extend the half-life of the latent reservoir instead of accelerate its decay.

There is evidence of differential antiretroviral drug efficacy within viral pools in secondary lymphoid tissue compartments in patients. For instance, a study observed only mild viral inhibition in the secondary lymphoid tissues of patients on ART regimens made up of two or three reverse transcriptase inhibitors [489]. Also, macrophages have been shown to require the highest therapeutic concentrations of protease inhibitors attainable *in vivo* to inhibit virus production in humans [490]. Moreover, macrophages have been shown to harbor latent HIV-1 in sanctuary tissues, such as the brain [431, 438-442], that can be impervious to at least some antiretroviral drugs. For instance, differences in the development of drug resistance between viral isolates from the blood and isolates from the cerebrospinal fluid in patients on HAART indicate that antiretroviral drug penetration into the CNS is not sufficient [443]. Many antiretroviral drugs do not effectively penetrate the BBB [443-449]. The testes represent another potential sanctuary site from which latently infected cells have been isolated [490, 491] but in which the blood-testes barrier restricts the entry of some antiretroviral drugs [490, 492]. Therefore, tissues that are poorly penetrated by antiretroviral drugs represent potential sites in which re-activated latent virus might infect new cells and re-seed the latent reservoir. In fact, viral replication in patients resulting in more than 50 HIV-1 RNA copies/ml of blood plasma has been shown to decrease the decay rate of the latent reservoir [493, 494]. Consequently, in the effort to eliminate latent infection in patients, it is imperative to not only deliver latency antagonists and antiretroviral drugs simultaneously, but to deliver them to the same tissue and cellular compartments. Hence, the development of a single, bifunctional antagonist of both HIV-1 latency and replication is ideal.

Fundamentally, this concept can be applied to the future development of innovative anti-HIV-1 pharmaceuticals capable of clearing latent virus. It is not limited to the use of PIs, as one can imagine employing combinatorial chemistry between different HIV-1 latency activators and replication inhibitors to create novel classes of bifunctional HIV-1 antagonists. However, a PI may very well be a viable option for evaluating the efficacy of an HIV-1 bifunctional antagonist in patients. As previously mentioned, Velcade is already approved by the FDA for the treatment of multiple myeloma and another PI, Marizomib, is currently being evaluated in clinical trials for the treatment of patients with lymphomas, leukemias, and multiple myeloma [380, 381]. The most common adverse effects associated with Velcade include gastrointestinal effects, fatigue, thrombocytopenia, and peripheral neuropathy, with the latter two being the most clinically significant [383, 472]. However, thrombocytopenia was found to wane between cycles of treatment with Velcade [472] and peripheral neuropathy was found to be effectively managed with dose changes [382]. Perhaps even more promising, early phase I clinical trial results with Marizomib have revealed that at less than half the dose of Velcade, Marizomib is more effective and far less toxic. In fact, peripheral neuropathy and thrombocytopenia have not been observed [382]. Importantly, Marizomib is characterized by a very small size that allows it to pass the BBB [381] which could be quite important in purging the latent reservoir in patients. Thus, PIs have exhibited substantial efficacies and manageable toxicities in patients with multiple myeloma and therefore, PIs could be considered feasible candidates for an assessment of the efficacy of HIV-1 bifunctional antagonists in infected patients. Also, PIs target a cellular factor, which significantly increases the genetic threshold for the development of drug resistance.

In this study, PIs are shown to represent a new class of HIV-1 latency antagonists. Additionally, previous reports of PI-mediated HIV-1 replication inhibition were confirmed.

Therefore, the findings demonstrate the feasibility of developing dual antagonists of HIV-1 latency and replication. This is a novel concept that can be applied to the development of pioneering anti-HIV-1 pharmaceuticals with the potential to substantially impact the goal of purging HIV-1 from infected individuals.

## Figures

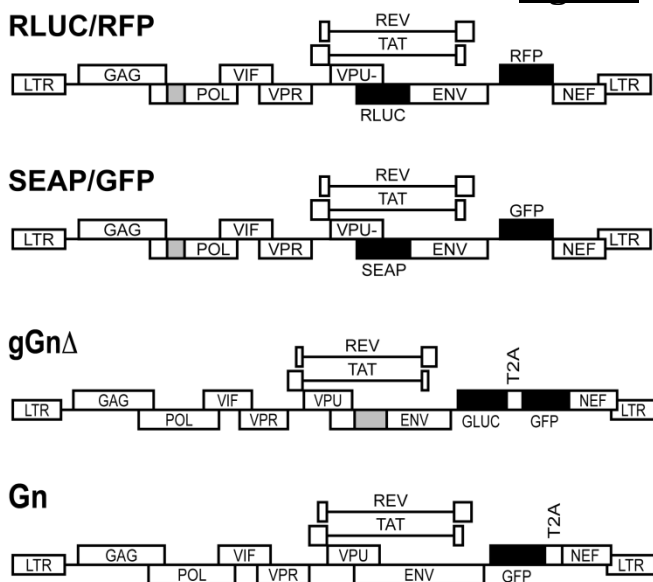


**Figure 3.1. HIV-1 constructs.** This figure depicts HIV-1 constructs utilized throughout this study.

The *vpu* gene start codon in both the RLUC/RFP and SEAP/GFP constructs is mutated for robust reporter gene expression. Gray boxes represent deletions within viral genes, which render those constructs replication-incompetent. The black boxes indicate reporter gene insertions. T2A sequences ensure that two proteins are expressed as single polypeptides and not fusions (34, 35). Please note that the Gn construct is fully replication-competent.

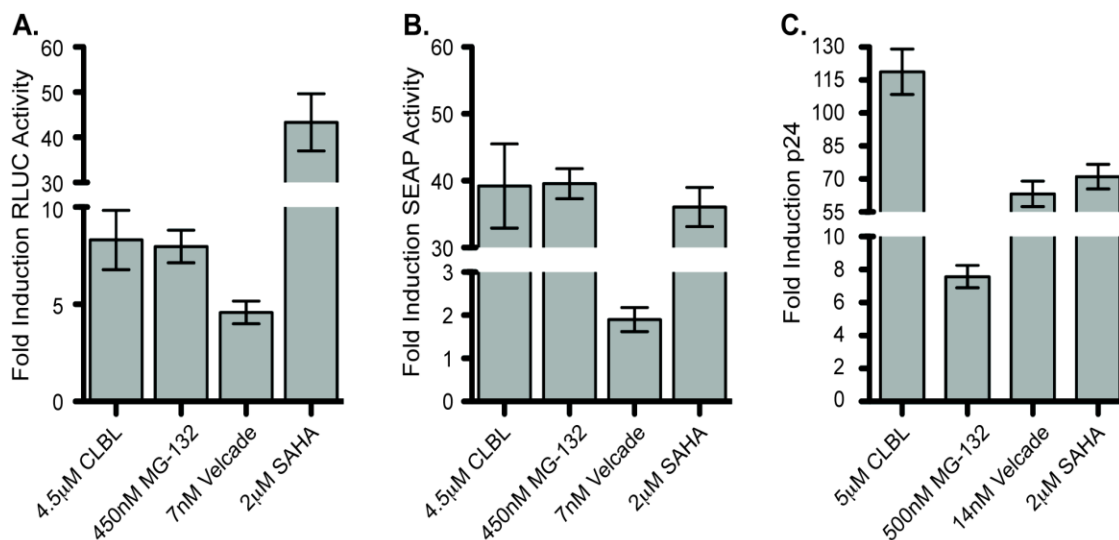


**Figure 3.2. PIs activate latent HIV-1 gene expression in tissue culture model systems. A.**

HeLa#14 cells were treated for 48 hours with PIs as indicated and RLUC activity was measured.

RLUs were normalized to protein concentrations and the values shown depict the average fold change in RLUC activity relative to DMSO (negative control) treated samples. **B.** 24ST1NLESG

cells were treated with CLBL for 48 hours and MG-132 and Velcade for 72 hours at the indicated concentrations, and SEAP activity was analyzed. RLUs were normalized to the number of live cells and the values shown illustrate the average fold change in SEAP activity relative to DMSO (negative control) treated samples. **C.** OM-10.1 cells were treated for 72 hours with PIs as

indicated and p24 levels in the supernatant were analyzed via p24 ELISA. p24 levels (ng/mL) were calculated using standard curve values and the values shown represent the average fold change in p24 production relative to DMSO (negative control) treated samples. Error bars

indicate SEM. Cells treated with suberoylanilide hydroxamic acid (SAHA) served as a positive control. The figure represents average values from three independent experiments.



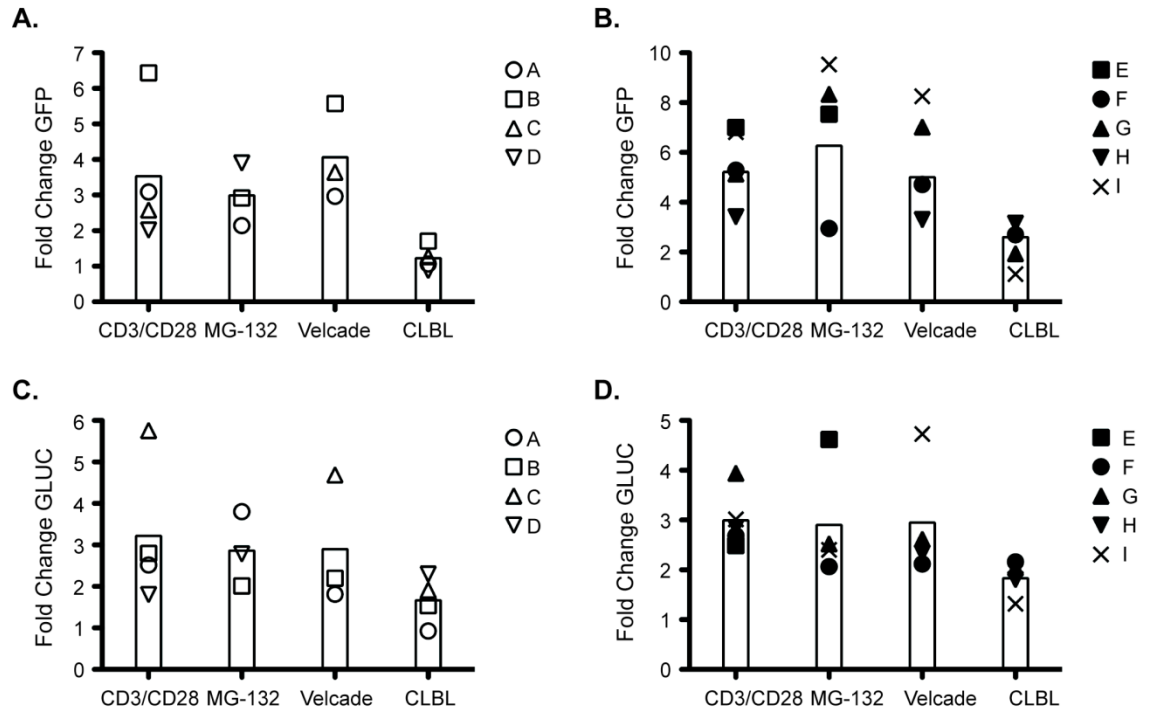


**Figure 3.3. PIs activate latent HIV-1 in primary human  $CD4^+$  T cell models.** **A.** Latently infected  $T_{CM}$ -like cells and **B.** latently infected Bcl-2-transduced  $CD4^+$  T cells were treated for 48 hours with PIs CLBL (5  $\mu$ M), MG-132 (250 nM), and Velcade (10 nM). Flow cytometry was performed and the values shown indicate the fold change in GFP expression relative to unstimulated cell (negative control) sample values. **C.** Latently infected  $T_{CM}$ -like cells and **D.** latently infected Bcl-2-transduced  $CD4^+$  T cells were treated for 48 hours with PIs (same concentrations as above) followed by measurement of GLUC activity. RLU were normalized to the number of live cells and the values shown indicate the fold change in GLUC activity relative to unstimulated cell (negative control) sample values. In all experiments, the vertical open bars represent average values from all healthy donors while symbols represent individual donor results; each donor result represents a single experiment. Cells treated with CD3/CD28 activating beads served as positive controls. All cells treated with PIs were simultaneously treated with Raltegravir to prevent the integration of unintegrated viral genomes.

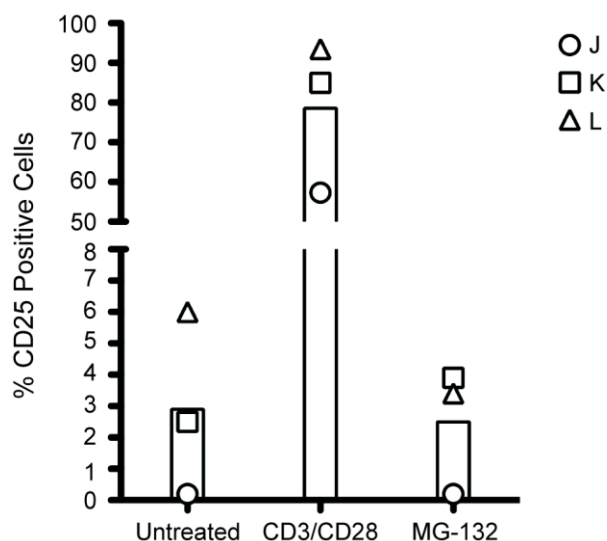


**Figure 3.4. Expression of CD25 early activation marker in primary human resting CD4<sup>+</sup> T Cells**

**treated with MG-132.** Resting CD4<sup>+</sup> T cells isolated from healthy donor PBMCs were treated with 500 nM MG-132. Forty-eight hours post-treatment, cells were incubated with FITC-conjugated CD25 antibody and the percentage of CD25<sup>+</sup> cells in each sample was determined via flow cytometry. Untreated PBMCs served as a negative control and PBMCs treated with CD3/CD28 activating beads served as a positive control. The vertical open bars represent average values from all healthy donors while symbols represent individual donor results; each donor result represents a single experiment.

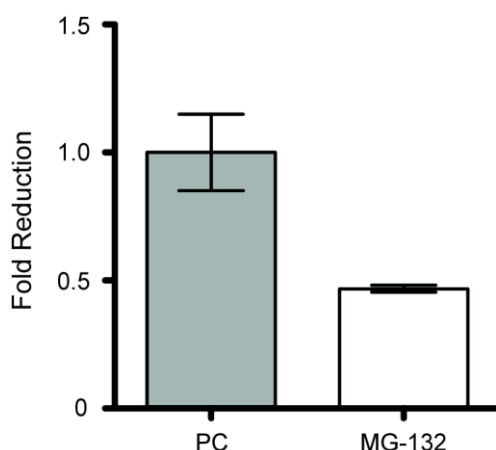


**Figure 3.5. PI-treatment of productively infected primary human CD4<sup>+</sup> T Cells results in the production of HIV-1 virions with reduced infectivity.** CD4<sup>+</sup> T cells isolated from healthy donor PBMCs were activated and infected with replication-competent Gn virus. Six hours post-infection, cells were either treated with 500 nM MG-132 or left untreated as a positive control (PC). Forty-eight hours post-infection, virus-containing supernatants were collected, p24 concentrations were measured, and then the supernatants were used to infect  $2 \times 10^5$  HeLaT4 cells. Forty-eight hours post-infection, GFP<sup>+</sup> cell numbers were analyzed via flow cytometry. GFP<sup>+</sup> cell numbers were first normalized to the number of live cells and then to the p24 (ng/ml) concentration of the inoculating viral supernatant. Values shown depict the fold reduction in the number of cells infected with MG-132-treated viral supernatants in comparison to the number of cells infected with untreated (PC) viral supernatants (arbitrarily set to 1). Error bars indicate standard deviation. These results are representative of three independent experiments which utilized primary cells isolated from different healthy donors and which consistently resulted in comparable data.

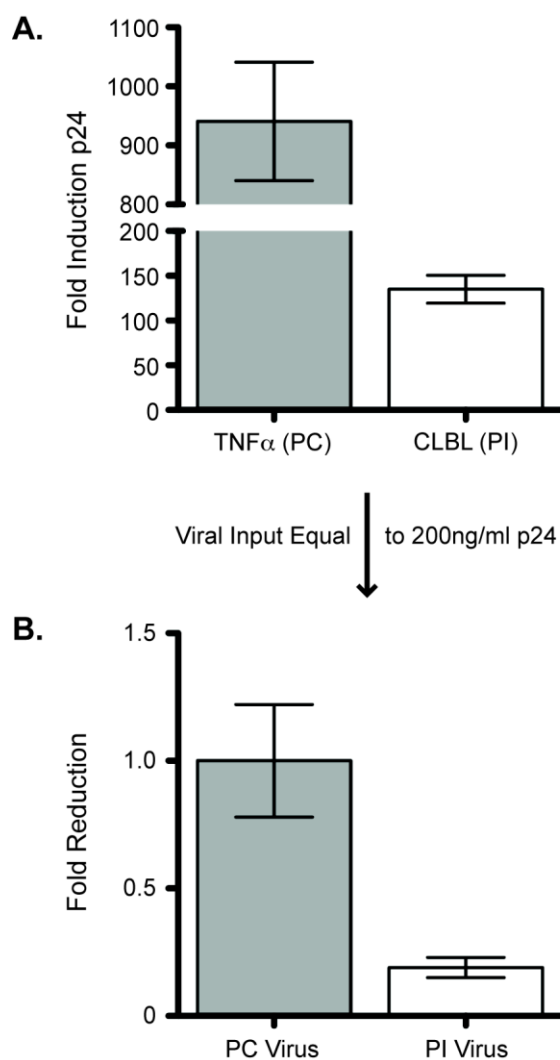


**Figure 3.6. HIV-1 virions produced as a result of PI-mediated activation of latent viral gene expression exhibit reduced infectivity.** **A.** OM-10.1 cells were treated with 50 ng/ml TNF $\alpha$  to stimulate the production of positive control (PC) viral particles or with 5  $\mu$ M CLBL to stimulate the production of viral particles under the influence of proteasome inhibition (PI). Seventy-two hours post-treatment, viral-supernatants were collected and p24 levels were analyzed via p24 ELISA. p24 levels (ng/mL) were calculated using standard curve values and the values shown represent the average fold change in p24 production relative to DMSO (negative control) treated samples. **B.** PC and PI virus-containing supernatants were diluted to a p24 concentration

of 200 ng/ml and used to infect  $1 \times 10^5$  U373-MAGI-CXCR4<sub>CEM</sub> cells. Forty-eight hours post-infection,  $\beta$ -Gal activity was measured.  $\beta$ -Gal activity was calculated using standard curve values and then normalized to protein concentrations. Values shown depict the average fold reduction in  $\beta$ -Gal activity in PI-treated virus-infected cells in comparison to PC virus-infected cells (arbitrarily set to 1). Error bars indicate SEM. The figure represents average values from three independent experiments.

## **Chapter 4: Inhibition of a Specific Ubiquitin-Proteasome Pathway Activates Latent HIV**

### **Abstract**

HIV-1 persists indefinitely in infected individuals including those being effectively treated with antiretroviral therapy (ART). Extensive research indicates that latently infected memory CD4<sup>+</sup> T cells represent an important source of this enduring infection. One strategy that has emerged to eliminate the latent arm of the infection involves the development and use of latency-reversing agents (LRAs) to activate latent virus, ideally promoting immune recognition and clearance of the infected cells or cell death due to cytopathic effects of expressed viral proteins. For the strategy to succeed, it is important to develop potent LRAs with a high degree of specificity as they would likely exhibit fewer off-target effects. Previously, we found that proteasome inhibitors (PIs) displayed LRA activity. Although PIs are not highly specific, their LRA activity indicated that it might be possible to exploit the high degree of specificity of the ubiquitin-proteasome system (UPS) to develop targeted LRAs. Here we describe a small molecule that inhibits the E3 ubiquitin ligase  $\beta$ -TrCP, an essential component of a particular UPS pathway, and exhibits potent LRA activity in both a primary cell model system of latency and patient samples. Moreover, we show that this E3 ligase inhibitor can act in complementary fashion with at least two other LRAs representing novel drug combinations.

## **Introduction**

An important approach to eliminate the latent arm of HIV-1 infection involves the development of effective latency reversing agents (LRAs). LRAs which can activate latent virus with a high degree of specificity are likely to have fewer off-target effects and be significantly less toxic than drugs lacking specificity. Thus, it is important to develop LRAs that can reactivate latent virus with greater precision.

Previously, we obtained results indicating that the ubiquitin-proteasome system (UPS) is involved in the maintenance of HIV-1 latency, which presents the potential to develop relatively specific antagonists of HIV-1 latency. It has become clear that the UPS plays an important role in gene expression utilizing both its proteolytic and nonproteolytic activities [361]. Ubiquitin-dependent protein turnover is a highly regulated, multistep process. In general, proteins targeted for proteolysis by the multi-component 26S proteasome, which is composed of two regulatory 19S subunits that abut a catalytic 20S core subunit, must be modified with at least a tetra-ubiquitin (Ub) chain. Generally, the first Ub is typically conjugated to a lysine on the target substrate, and the additional Ubs are attached at lysine 48 of Ub. Three proteins are required for poly-Ub conjugation. They are E1 (Ub-activating enzyme), E2 (Ub-conjugating enzyme), and E3 (Ub ligase enzyme). There are 2 E1s, ~40 E2s, and over 600 E3s, and the combinatorial utilization of the three classes of protein confers a great deal of specificity to substrate ubiquitylation and subsequent turnover [339]. Because of the great diversity of E3 ligases, they are the most important factor in the UPS for conferring specificity to substrate ubiquitylation and subsequent turnover.

It was previously shown that signaling through the Wnt pathway can upregulate HIV-1 gene expression [425] and that the E3 ubiquitin ligase  $\beta$ -TrCP plays an important role in

regulation through the Wnt pathway. This prompted us to test if GS143, a small molecule inhibitor of  $\beta$ -TrCP that was previously developed as an inhibitor of NF $\kappa$ B signaling, exhibited LRA activity [495, 496]. It was found that GS143 is a specific and potent LRA with both a primary cell model of latency and patient samples. Moreover, GS143 acts in complementary fashion with at least two different classes of LRAs, representing novel LRA combinations.



## **Materials and Methods**

### **Culture media.**

All non-adherent cells were cultured in RPMI 1640 GlutaMAX, HEPES medium (Thermo Fisher Scientific) supplemented with 10% BioTC-Fetal Bovine Serum, (LDP), MEM Non-essential amino acids solution (Thermo Fisher Scientific), and 100 U/ml penicillin-100 µg/ml streptomycin solution (Thermo Fisher Scientific). Adherent cells were cultured in DMEM GlutaMAX medium (Thermo Fisher Scientific) supplemented with 10% BioTC-Fetal Bovine Serum, (LDP), MEM Non-essential amino acids solution (Thermo Fisher Scientific), and 100 U/ml penicillin plus 100 µg/ml streptomycin solution (Thermo Fisher Scientific).

### **Reagents.**

The following reagents were used: polyethyleneimine (PEI) linear MW 25 kDa (Polysciences), Retro-concentin (System Biosciences), Raltegravir (Selleckchem), polybrene, Histopaque®-1077 (Sigma-Aldrich), Trizol reagent, the SuperScript® IV First-Strand Synthesis System, TaqMan® Gene Expression Master Mix Dynabeads® Untouched™ Human CD4 T Cells Kit (Thermo Fisher Scientific). For activation-marker staining, FITC Mouse Anti-Human CD25 (#555431, BD Pharmingen, San Jose, CA), Anti-Human HLA-DR FITC conjugate (#MHLDR01, Life Technologies, Grand Island, NY), and CD69 Antibody, FITC conjugate (#MA1-10275, Life Technologies, Grand Island, NY) were used.

### **HIV-1 RNA quantitation.**

Relative HIV-1 mRNA amounts were determined by modifying the method described by Bullen et al [334]. Total RNA from  $3 \times 10^5$  resting T cells or  $2.5 \times 10^6$  patient cells were isolated using Trizol reagent and cDNAs were produced from the RNAs with random hexamer using the

SuperScript® IV First-Strand Synthesis System (Thermo Fisher Scientific). qPCR was performed with TaqMan® Gene Expression Master Mix using primers CAGATGCTGCATATAAGCAGCTG and TTTTTTTTTTTTTTTTTTTTGAAGCAC and probe FAM-CCTGTACTGGGTCTCTCTGG-Iowa black. Duplicate reactions were set up for each sample. After 50~60 cycles of amplification, each  $2^{-Ct}$  average from the duplicate was normalized by the cell number. Obtained values were then normalized to values obtained from the mock treated cells.

### **Cell Treatments**

The following drugs were used in cell treatment experiments: ionomycin, phorbol myristate acetate (PMA) prostratin, ingenol-3-angelate, N,N'-Hexamethylene bis(acetamide) (HMBA), TNF $\alpha$  (Sigma-Aldrich), anti-CD3/anti-CD28 coated magnetic beads (Thermo Fisher), recombinant human interleukin-2 (PeproTech), chidamide, pyroxamide, (+)-JQ1 (Cayman Chemical), bryostatin-1 (Calbiochem), Velcade (Selleck Chemical) and GS143 (Tocris).

### **Primary cell isolation**

PBMCs were isolated from healthy donor leukocytes (New York Blood Center) using Ficoll separation: 10 mL of blood was mixed with 20 mL 1x PBS pH 7.4, after which 15 mL Histopaque®-1077 (Sigma-Aldrich) a solution of polysucrose and sodium diatrizoate with a density of 1.077 g/mL, was added to the bottom of the tube. It was then centrifuged at 800x g for 20 minutes with the brake set at 5 using a Sorvall Legend X1R, after which the buffy coats were collected, the volume brought up to 45 mL with 1x PBS pH 7.4, and spun at 300x g for 10 minutes, and then washed again with PBS and spun. Residual red blood cells were removed by resuspension in 2 mL ACK Lysing Buffer (Thermo Fisher), an ammonium-chloride-potassium solution, and incubated for 2 minutes at room temperature, then washed twice with 1x PBS pH 7.4.

Dynabeads Untouched Human CD4 T Cells kit (Thermo Fisher) was used to isolate primary resting CD4<sup>+</sup> T-cells via negative selection:  $2 \times 10^8$  PBMCs were resuspended in 2 mL isolation buffer (1x PBS pH 7.4, 2% FBS, 2 mM EDTA), 400  $\mu$ L FBS, 400  $\mu$ L mouse IgG antibody mix recognizing CD8, CD14, CD16a and CD16b, CD19, CD36, CD56, CDw123, and CD235a, and 5  $\mu$ L mouse IgG anti-CD25 (Thermo Fisher), and anti-CD25 antibody to remove activated CD4<sup>+</sup> T-cells, mixed, and incubated for 20 minutes at 4°C. 10 mL isolation buffer was added to the cells and then they were centrifuged at 350x g for 8 minutes at 4°C. Supernatant was discarded and the cells resuspended in 2 mL isolation buffer. 2 mL of 20 mg/mL Depletion MyOne Dynabeads (super-paramagnetic polymer beads 1  $\mu$ m in diameter coated with monoclonal human IgG4 anti-mouse IgG antibody recognizing all mouse IgG subclasses and Fc-specific) were mixed with 2 mL isolation buffer and placed on a magnet for 1 minute, the supernatant discarded, removed from the magnet and resuspended in 2 mL isolation buffer. The beads were then mixed with the cells and incubated for 15 minutes at room temperature with gentle tilting. 10 mL isolation buffer was added to the cells and thoroughly mixed by pipetting ~10 times using a pipette with a narrow tip opening, avoiding foaming. The tube was placed on a magnet for 2 minutes and the supernatant transferred to a new tube. Then 10 mL isolation buffer was added to the tube containing the beads, and mixed as above by pipetting, then placed on the magnet for 2 minutes and supernatant removed to a new tube. Both supernatant-containing tubes were placed on the magnet one final time for 2 minutes, to remove any residual beads, then the supernatants were collected and pooled together.

### **Cell surface staining**

$2 \times 10^5$  resting CD4<sup>+</sup> T-cells were resuspended in 100  $\mu$ L media in 96-well plates, treated at 37°C for 48 hours with: CD3/CD28 beads and 100 U/mL IL-2, 5-20  $\mu$ M GS143, 0.5  $\mu$ M prostratin, 5 nM

bryostatin-1, or 5 nM ingenol-3-angelate, GS143 10  $\mu$ M both alone and with either JQ1 5  $\mu$ M or chidamide 5  $\mu$ M, then collected and washed with 2 mL staining buffer (1x PBS pH 7.4, 2% FBS, 2 mM EDTA), resuspended in 100  $\mu$ L buffer and incubated for 30 min at 4°C with either of the following FITC-conjugated antibodies: HLA-DR (Class II), CD69 (Thermo Fisher), or CD25 (BD Biosciences). They were then washed with 1 mL staining buffer and centrifuged at 600x g for 10 minutes, three times, before being resuspended in 1x PBS pH 7.4 and fixed with 1% formaldehyde for 5 minutes, then washed with 1 mL 1x PBS pH 7.4 and resuspended in 100  $\mu$ L 1x PBS pH 7.4. They were then analyzed using an Accuri C6 Flow Cytometer (BD Biosciences) to look at the percentage of cells positive for FITC signal.

### **Toxicity**

5x10<sup>4</sup> resting CD4<sup>+</sup> T-cells were resuspended in 100  $\mu$ L media in 96-well plates and treated with the same compounds as above, along with: 2.5-5  $\mu$ M chidamide and 0.5-5  $\mu$ M JQ1 both alone and in combination with 10  $\mu$ M GS143, for 48 hours at 37°C, then cell viability was assessed using the CellTiter-Glo Luminescent Cell Viability Assay (Promega): the plate was incubated at room temperature for 30 minutes, then 100  $\mu$ L assay solution was added to every well, then the plate placed in a GloMax Discover (Promega) where it was shaken for 2 minutes, incubated at room temperature for 10 minutes, and the luminescent signal detected with an integration time of 1 second.

### **Primary cell model**

Virus was produced using polyethyleneimine (PEI) (Polysciences) transfection. More specifically, six 100 mM tissue culture plates of 90% confluent HEK293T were split 1:2. The next day, transfection mix was prepared for each plate using 1 mL Opti-MEM Reduced Serum Media (Thermo Fisher Scientific), 12  $\mu$ g of gGn-p6\* virus plasmid, 3  $\mu$ g pcCNA-VPXsiv, and 45  $\mu$ g PEI.

This mix was incubated for 15 minutes at room temperature and then added to the cells. 48 hours later the media was harvested, filtered through a 0.45  $\mu\text{m}$  filter, and mixed with Retroconcentin (System Biosciences) and incubated at 4°C. 48 hours later the viral mix was spun at 1500x g for 30 minutes at 4°C; the viral pellet was resuspended in RPMI-1640 and frozen in liquid nitrogen.

$4 \times 10^6$  resting CD4+ T-cells were resuspended in 500  $\mu\text{L}$  concentrated gGn-p6\* virus with 16  $\mu\text{g}/\text{mL}$  polybrene, in 24-well plates, and spun at 1200x g for 1.5 hours at room temperature, then put in a 37°C incubator for 2 hours. Afterwards, RPMI-1640 media with FBS was added, and the cells then transferred to the H80 feeder cell line, and incubated overnight. The following day the cells were washed with fresh media, resuspended and placed on H80 cells. After 48 hours of coculturing, the infected resting cells were then removed, resuspended in 96-well plates, and incubated with select compounds for 24-48 hours, while remaining in coculture.

### **GFP reading**

After 48 hours of treatment, the infected resting CD4+ T-cells were fixed in 1% formaldehyde for 5 minutes at room temperature, washed and resuspended in 100  $\mu\text{L}$  1x PBS pH 7.4 and then analyzed with Accuri C6 Flow Cytometer (BD Biosciences) to look at mean channel fluorescence of GFP; gating by size and granularity was used to exclude any lifted H80 cells.

### **Patient samples**

Buffy coats were separated from 180 ml whole blood by 1,200x g centrifugation and resting CD4+ T-cells were isolated using the same procedure for healthy donor samples.  $2.5 \sim 5 \times 10^6$  resting CD4+ T-cells in 500  $\mu\text{L}$  media were treated with each LRA for 24 hours and total RNA was then isolated.

## **Results**

### **Primary cell model of HIV-1 used for initial screening.**

Fig. 4.1 depicts the previously described primary model cell system utilized for the initial testing of GS143, the inhibitor of the E3 ligase  $\beta$ -TrCP, for LRA activity [497]. A replication-competent (RC) HIV-1 vector virus, gGn-p6\*, was utilized for infection. Gn-p6\* harbors an SIV Vpx binding site within the p6 domain allowing complementation with Vpx protein, which promotes more efficient infection of resting CD4+ T cells. To establish latent virus infection, resting CD4+ T cells were isolated from healthy donors followed by infection via spinoculation with Vpx-complemented gGn-p6\*. We find that this procedure typically provides for the establishment of latent virus infection in 10 to 15% of the resting CD4+ T cells within 3 days.

### **Testing of GS143, the small molecule inhibitor of $\beta$ -TrCP, for LRA activity using the primary cell model of latency.**

Latent virus infection was established as described above. Latently infected cells were treated for 48 hours with GS143 at concentrations ranging from 5 to 40  $\mu$ M followed by analysis for GFP marker expression via flow cytometry (Fig. 4.2). Mean channel fluorescence measurements indicate that GS143 significantly upregulates GFP expression particularly at concentrations ranging from 5 to 20  $\mu$ M suggesting that GS143 is a potent LRA especially when compared to the positive controls including treatment with potent T cell activators including PMA plus ionomycin, anti-CD3/anti-CD28 (aCD3/aCD28) coated magnetic beads, or PHA. GS143 also demonstrated comparable activity to proteasome inhibitor Velcade, which we previously demonstrated to be a robust LRA (Fig 4.2, [498]).

The effect of GS143 upon HIV-1 mRNA expression was measured. The same protocol as described above was employed to establish a latent virus infection followed by treatment with

the indicated LRAs (Fig. 4.3). HIV-1 mRNA was measured via RT-qPCR as previously described [334]. GS143 alone produced a potent signal compared to the PMA plus ionomycin positive control in support of the results obtained via monitoring GFP expression (Fig. 4.2). The effect of GS143 was compared to three previously described LRAs including chidamide, a recently described histone deacetylase inhibitor with LRA activity [497], JQ1, a bromodomain inhibitor, and bryostatin, a PKC agonist. As can be ascertained, GS143 LRA activity compared quite favorably with all of these LRAs in efficacy yielding the greatest activity.

#### **T-cell activation and toxicity profile of GS143.**

In order to determine the safety profile of GS143, we investigated its effects on non-infected resting CD4+ T-cells from healthy donors. The cells were isolated via Ficoll separation and purified by negative selection with antibody-coated magnetic beads to remove all non-resting cells. They were then incubated with the indicated compounds for 48 hours and assayed. Toxicity was determined using the CellTiter-Glo Luminescent Cell Viability Assay (Promega), which measures cell number as a function of cellular ATP. As seen in Fig. 4.4, GS143 did not exhibit significant toxicity at 5 and 10  $\mu$ M and displayed only mild toxicity at 20  $\mu$ M. Similar results were seen for JQ1, a previously characterized LRA, and chidamide, a recently identified histone deacetylase inhibitor LRA [497]. Likewise, combinations of these drugs with 10  $\mu$ M GS143 showed mild effects on toxicity (Fig. 4.4). Also, LRAs from the PKC agonist class including prostratin, bryostatin-1, and ingenol-3-angelate were tested. Interestingly it was found that there was an increased signal suggesting they induce T-cell activation and/or cellular proliferation.

The T-cell activation profile was examined after treatment with GS143 to ensure that the LRA activity being exhibited by GS143 was not due to an indirect effect upon T cell

activation. After treatment of resting CD4<sup>+</sup> T cells from healthy donors with drug, they were examined for expression of the activation markers HLA-DR, CD69, and CD25 (Fig. 4.5). Magnetic beads coated with antibodies to CD3 and CD28, along with IL-2 treatment, were used to fully activate the cells and served as a positive control. No effect was observed upon expression of these markers by treatment with 10  $\mu$ M GS148, alone or in concert with JQ1 or chidamide. However, with the PKC agonists we found a large increase in CD69 expression and mild increase in CD25, indicating at least partial T-cell activation, in line with the results seen above when testing toxicity.

#### **GS143 effect upon HIV-1 mRNA expression utilizing patient samples.**

Next, GS143 was tested for LRA activity with patient samples. Samples were obtained from patients undergoing antiretroviral therapy who gave informed consent and were 21 to 65 years of age with CD4<sup>+</sup> T cell counts greater than 350 per  $\mu$ L and viral loads below 50 copies per ml. Resting CD4<sup>+</sup> T cells were isolated from patient blood followed by treatment with GS143 for 24 hours after which mRNA was isolated and HIV-1 mRNA quantified via RT-qPCR [334]. Treatment with GS143 resulted in a significant increase in viral RNA levels at all concentrations tested compared to the level of activation obtained with the potent positive control PMA plus ionomycin (Fig. 4.6). There was significant patient to patient variation; however, this was expected as observed by others when testing other LRA utilizing patient samples [499].

#### **GS143 in combination with previously identified LRAs.**

Initially, GS143 was tested in combination using the primary cell model of latency delineated earlier. As described earlier, primary resting CD4<sup>+</sup> T cells were infected with the gGn-p6\* and cocultured with H80 cells for three days to let the provirus enter a latent state (Fig. 4.1). Afterwards, the cells were treated with the indicated compounds for 48 hours and the



mean channel fluorescence measured by flow cytometry (Fig. 4.7). GS143 was tested in combination with previously described LRAs since as we and others previously noted it ultimately might be necessary to utilize LRA combinations to obtain sufficient efficacy [335, 336, 500]. Four out of five combinations displayed strong complementary effects (Fig. 4.7), including combinations with the previously well-described LRAs JQ1, and bryostatin [291, 336]. Of particular note were the potent effects of two histone deacetylase inhibitors (HDACis) chidamide and pyroxamide, which were also quite active when combined with GS143. It is noteworthy that these HDACis contain a benzamide functional group and a pyridyl cap. On the other hand, hexamethylene bisacetamide (HMBA) which releases P-TEFb from 7SK snRNA [327] and ionomycin alone exhibited only a modest effect, as previously shown in several primary cell latency models [333, 501] and did not show any synergy with GS143. TNF $\alpha$  alone demonstrated modest activation, as reported before [333] and had a mildly additive effect with GS143.

We also tested whether the combination of GS143 and other LRAs work in an additive or synergistic fashion. After treatment with the different compounds for 48 hours and measuring GFP mean channel fluorescence, synergy was determined using the Bliss independence method as previously described [292]. As seen in Fig. 4.8,  $\Delta fa_{xy} > 0$  indicates synergy;  $\Delta fa_{xy} = 0$  indicates additive effects;  $\Delta fa_{xy} < 0$  indicates antagonism. Each set of symbols represents an experiment using cells from a different healthy donor, and statistical significance was determined for each set of values for a particular combination. Other than the lowest dose of GS143 (5  $\mu$ M) plus chidamide, all other combinations showed some degree of synergy, with both doses of JQ1 showing the greatest synergy for each concentration of GS143.

Combinations of GS143 were then tested with patient samples. Since the number of HIV-infected resting CD4<sup>+</sup> T cells that can be isolated from patient samples is somewhat limiting,

the experiment focused upon studying GS143 in combination with two of the LRAs (Fig 4.9). Chidamide and JQ1 were selected due to their different mechanisms of action and their strong activity in the cell model (Fig. 4.7 and 8). Moreover, both chidamide and JQ1 exhibited promising toxicity and activation profiles (Fig. 4.4 and 5). The protein kinase C agonists were ruled out because of their activation profile suggesting that they activate resting CD4+ T cells indicating that they would ultimately not be ideal LRAs for clinical use (Fig 4.5) [298]. GS143 in combination with either JQ1 or chidamide had complementary activity as seen in the primary cell model. These are novel LRA combinations that have the potential for significant clinical interest.

## **Discussion**

Proteasome inhibitors exhibit HIV-1 LRA activity [498], but they have relatively broad effects upon inhibition of the ubiquitin-proteasome system. However, the UPS displays a high degree of specificity conferred by numerous specific UPS pathways using different combinations of E1, E2, and E3 ligases [339, 502]. In particular, there are more than 600 E3 ligases, which presents the possibility of developing highly specific LRAs that target an individual E3 ligase playing a role in maintaining HIV-1 latency. Since it had been previously reported that the Wnt pathway is involved in regulating HIV-1 expression and the UPS pathway employing the E3 ligase  $\beta$ -TrCP modulates Wnt signaling, GS143, which inhibits  $\beta$ -TrCP action, was tested for LRA activity [425, 496, 503]. Using both a primary model of latency and patient samples to assess latency reversal, it was shown that GS143 is a strong LRA. Moreover, GS143 can act in complementary fashion with other classes of LRAs.

A clear advantage of focusing on inhibition of an E3 ligase is that the E3 ligases are the primary mediators of specificity for the UPS. Additionally, it has been reported that it is possible to develop inhibitors of the E3 ligases that block only a subset of the proteins they target for degradation; therefore, targeting an E3 ligase provides for a great degree of specificity. For example, GS143 was originally developed to inhibit NF $\kappa$ B signaling by blocking ubiquitylation and subsequent degradation of I $\kappa$ B, yet GS143 did not affect the turnover of  $\beta$ -catenin, another target of  $\beta$ -TrCP [496]. Another potential advantage of the further drug development of GS143 is that it is not reversing latency through activation of NF $\kappa$ B which alleviates a possible concern because of NF $\kappa$ B's prominent role in immune signaling [504]. It will be interesting to uncover which particular factor mediating latency reversal is being affected by GS143 inhibition of  $\beta$ -TrCP.

It is obviously important to ascertain if a potentially novel LRA can affect latent provirus in patient samples. Nevertheless, the model system being utilized here has demonstrated good predictive power in discerning if a novel LRA would also display activity with patient samples. For example, GS143 as well chidamide, an HDACi with a benzamide functional group and pyridyl cap, were first tested with the model system [497] and were both subsequently shown to act as LRAs with patient samples (Fig. 4.9). Additionally, other LRAs including JQ1 and PKC agonists were also active in the model system whereas SAHA which was previously shown to be active in other model systems but not with patient samples was not active with the model system utilized here [497]. Thus, this model system may be particularly useful for preclinical development before advancing to patient samples.

GS143 acted in a complementary fashion with JQ1 and chidamide with both the model system and patient samples. As our laboratory and others previously proposed, it may ultimately be necessary to employ LRA combinations to obtain suitable efficacy to produce sufficient latent virus clearance, so it was reassuring to find that GS143 worked in concert with two potentially clinically important LRAs. As noted in the results section, we decided to focus upon GS143 combinations with chidamide and JQ1 because of their promising activity, toxicity and activation profiles (Fig. 4.4 and 5). In contrast treatment with PKC agonists resulted in strong upregulation of one activation marker and partial activation of another, so we eschewed examining combinations using PKC agonists with patient samples.

In summary, GS143 represents a first in class LRA by virtue of its ability to act as a HIV-1 latency antagonist by inhibiting a specific E3 ligase, namely,  $\beta$ -TrCP. The results support the concept that modulating a specific UPS pathway involved in regulating HIV-1 latency can produce not only a potent LRA but one with potentially less toxic side effects owing to its

specificity. Thus, further drug development of a small molecule such as GS143 in an effort to clear persistent HIV-1 infection is clearly warranted.

## Figures

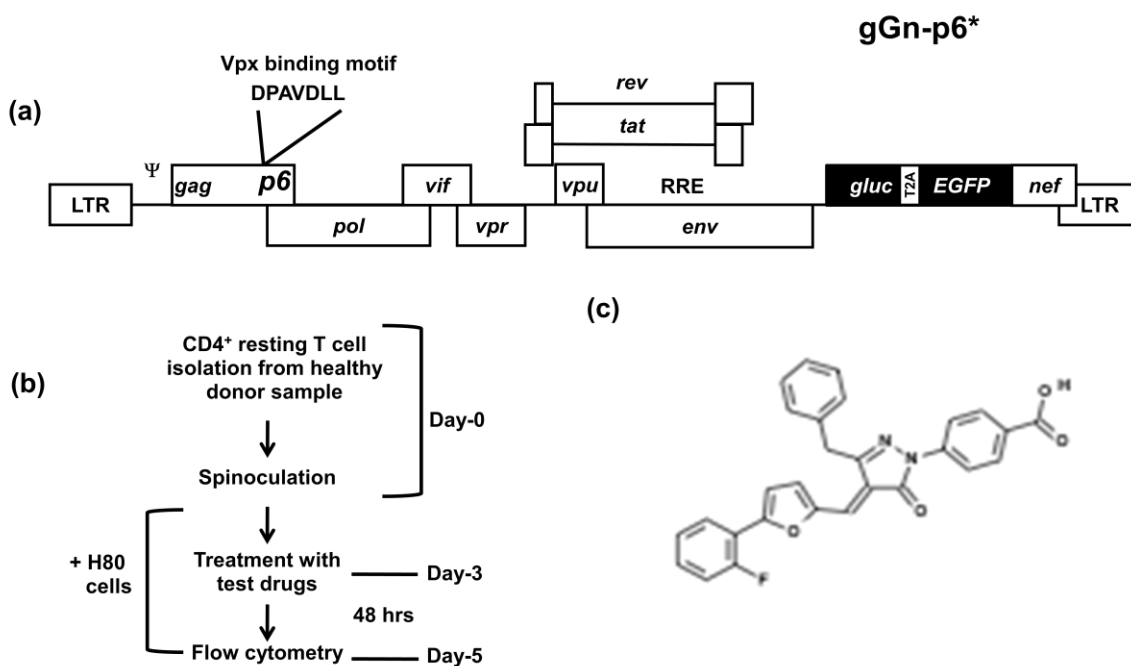


**Figure 4.1. Protocol for establishing latent virus infection in primary resting CD4<sup>+</sup> T cells. (a)**

Construct gGn-p6\* is a replication competent vector with the Vpx binding motif (DPAVDLL) inserted within p6 as indicated. Abbreviations: *gluc* – *Gaussia* luciferase gene; T2A – T2A peptide promoting “ribosomal skipping”; *EGFP* – enhanced green fluorescent protein gene. (b) Primary resting CD4<sup>+</sup> T cells were isolated from leukocyte-enriched healthy donor samples using a Ficoll gradient and negative selection. The isolated T cells were infected by spinoculation with gGn-p6\* virus containing Vpx protein. Three days post infection cultures were treated with test compounds followed 48 h later by flow cytometric analyses. Where indicated, resting cells were co-cultured with the H80 glioma cell line at day-1 post infection. (c) Structural formula of GS143.

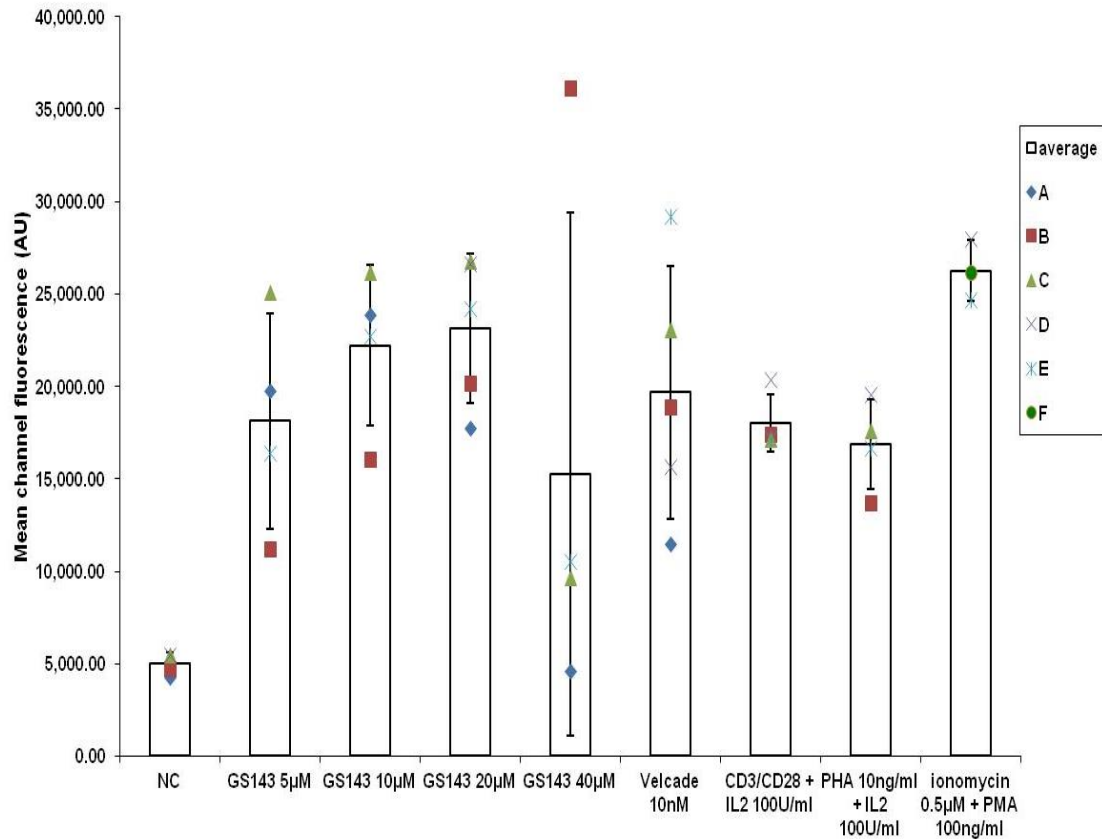


**Figure 4.2. Activation of latent virus in the primary cell model by GS143.** Resting T cells

infected with gGn-p6\* were treated with indicated concentration of GS143, Velcade, anti-CD3/anti-CD28 beads plus IL-2 100 U/mL, phytohaemagglutinin (PHA) plus IL2, or ionomycin plus phorbol 12-myristate 13-acetate (PMA). GFP mean channel fluorescence from the infected cells were measured 48 hours later. Each value is obtained from four or five healthy donor samples indicated with symbols shown on the upper right. The bars represent the averages obtained. NC stands for negative control. Error bars show standard deviations. AU stands for arbitrary units.

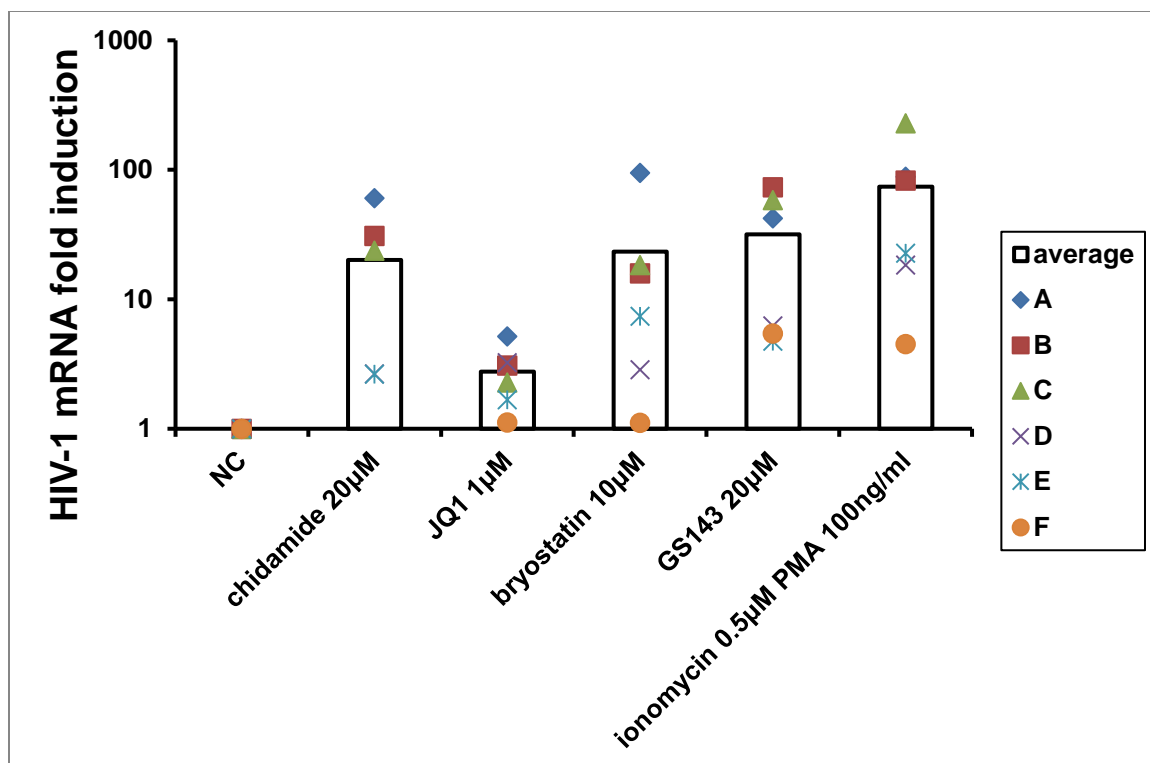


**Figure 4.3. HIV-1 mRNA induction by GS143 and representative LRAs with the primary resting CD4+ T cell model.** HIV-1 mRNA expression in the resting cell model was measured via RT-qPCR after treatment with the indicated LRAs. RNA measurements were normalized to the negative control. Each symbol corresponds to results obtained with resting CD4+ T cells isolated from different healthy donors. Each data point is the average of two PCR reactions. Averages are shown by open columns.



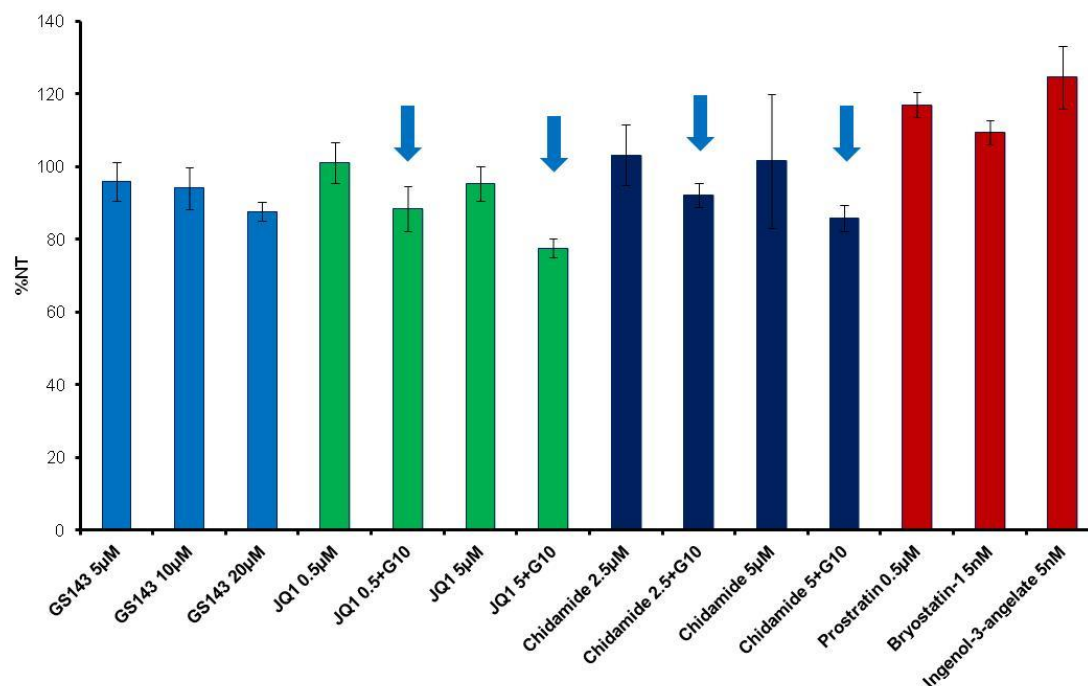


**Figure 4.4. Toxicity profile of GS143 alone and in combination.** Primary resting CD4<sup>+</sup> T-cells were treated with the indicated compounds for 48 hours and then assayed with the CellTiter-Glo Luminescent Cell Viability Assay (Promega). Arrows indicate combinations of LRA with GS143 10  $\mu$ M. The values are displayed as a percentage of the negative control. Shown is the average of three experiments from three healthy donors.

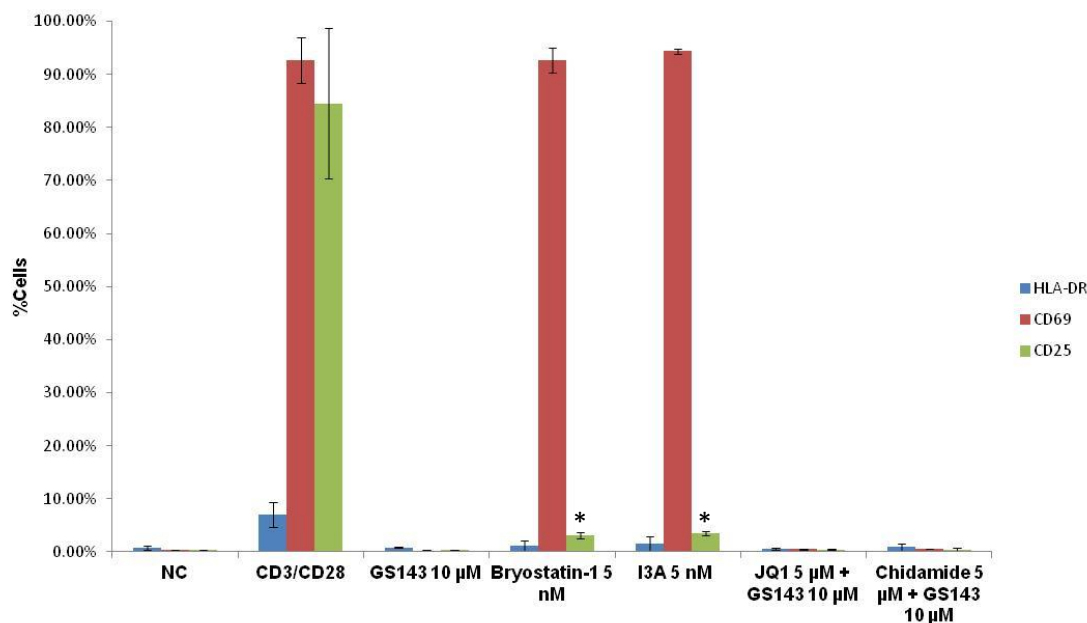


**Figure 4.5. Activation profile of GS143 alone and in combination.** Primary resting CD4<sup>+</sup> T-cells were treated with the indicated compounds for 48 hours, then incubated with fluorescently-tagged antibodies specific to the indicated T-cell activation markers and analyzed by flow cytometry. Significance was determined using one-tailed paired t-test: \* $p < 0.05$ . CD3/CD28 – treatment with 100 U/mL and beads coated with antibodies against CD3/CD28. I3A – ingenol-3-angelate. Shown is the average of three experiments from three healthy donors.

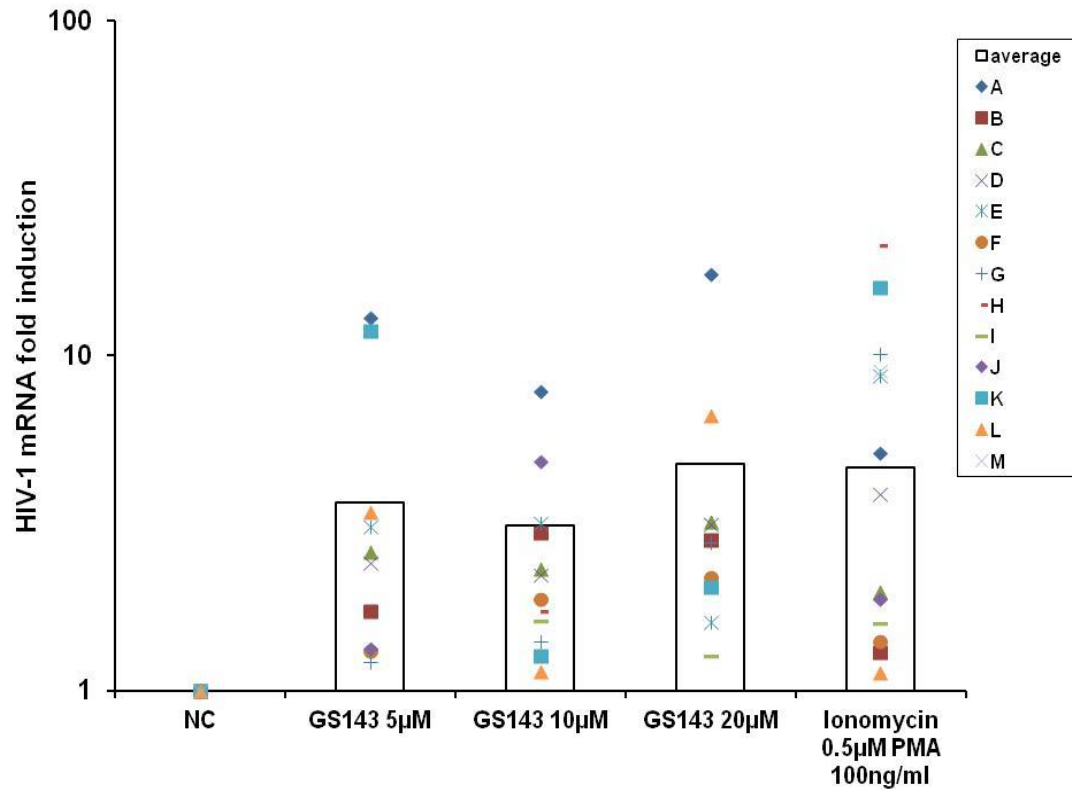


**Figure 4.6. HIV-1 expression induced by GS143 in resting CD4+ T cells isolated from patients on suppressive ART.** Resting CD4+ T cells were isolated from patient blood. The resting CD4+ T cells were then treated with GS143 or Ionomycin plus PMA for 24 hours. Total RNA was then isolated, and HIV-1 mRNA was quantified via RT-qPCR as previously described. The signals were normalized to the mock treated negative control. Each symbol corresponds to a specific patient as shown in upper right of the figure. Averages of all patients are indicated by the open columns.

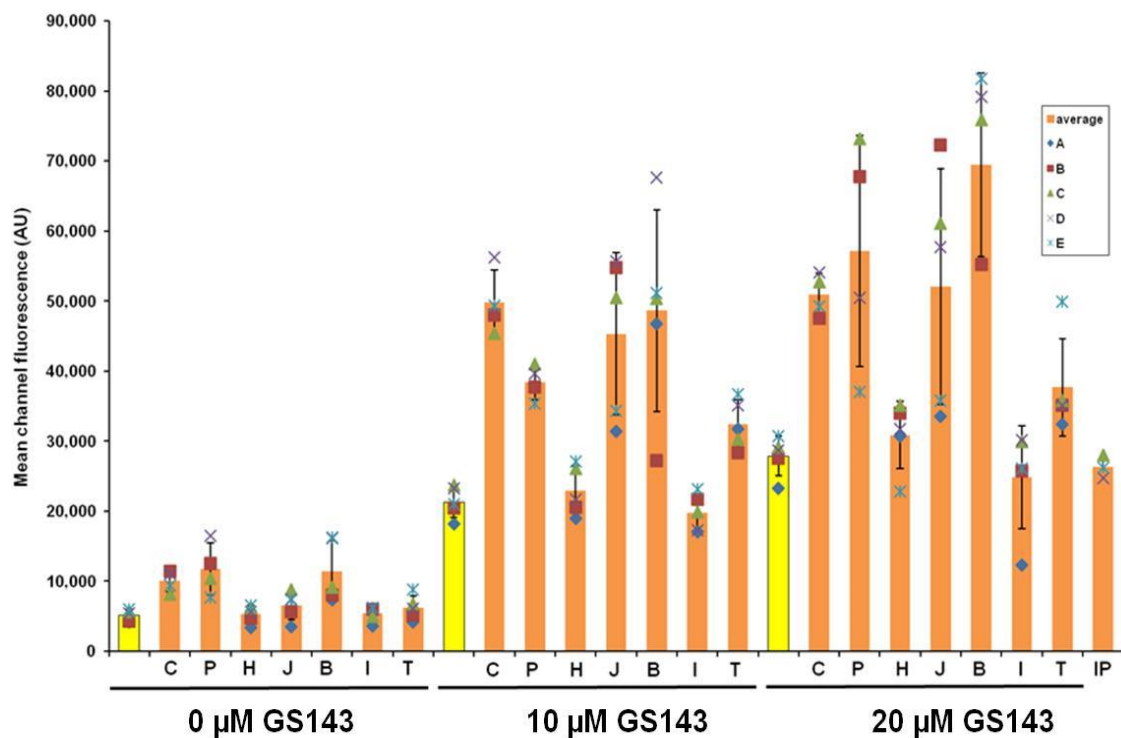


**Figure 4.7. GS143 combinational drug assay on HIV-1 activation in resting T cell.** Resting T cells infected with gGn-p6\* were treated with indicated concentration of GS143, or its combination with LRAs. C, P, H, J, B, I, T, and IP stand for 20 µM chidamide, 20 µM pyroxamide, 1 mM HMBA, 1 µM JQ1, 10 nM bryostatin, 0.5 µM ionomycin, 20 ng/ml TNFα, and 0.5 µM ionomycin plus 100ng/ml PMA, respectively. GFP mean channel fluorescence from the infected cells were measured 48 hours later. Each value is obtained from four or five healthy donor samples indicated with symbols. NC stands for negative control. Error bars show standard deviations. AU abbreviates arbitral unit. The yellow bars represent the untreated negative control or treatment with GS143 at the indicated concentration.

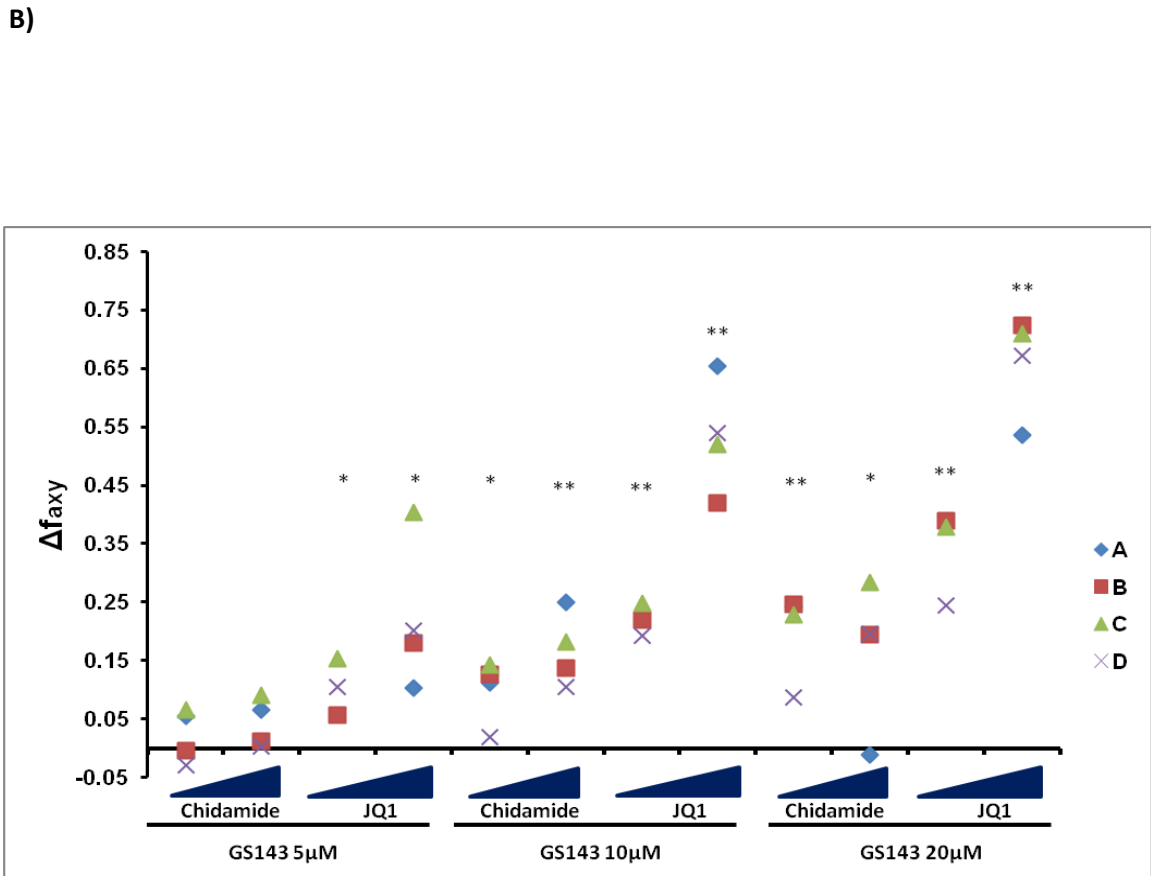
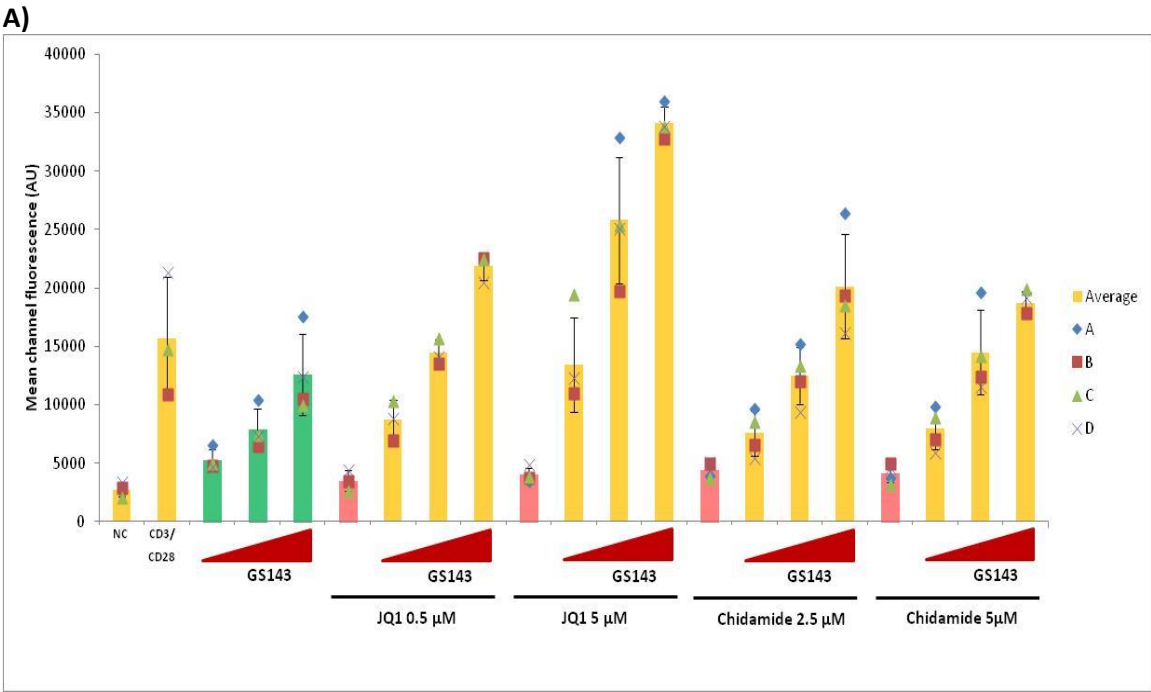


**Figure 4.8. Synergy of GS143 with JQ1 or chidamide.** Primary resting CD4+ T-cells infected with gGn-p6\* were treated with the indicated compounds for 48 hours. A) Mean channel fluorescence (MCF). NC = no treatment control. CD3/CD28 = treatment with IL-2 100 U/mL and magnetic beads coated with antibodies to CD3 and CD28. Dose escalations of GS143 correspond to 5  $\mu$ M, 10  $\mu$ M, and 20  $\mu$ M. Bars indicate average with error bars displaying standard deviation. Each value is obtained from three or four healthy donor samples. B) Synergy was calculated using the Bliss independence model as in [17] using the data from (A). The equation  $\Delta fa_{xy} = fa_{xyO} - fa_{xyP}$  was used, where  $\Delta fa_{xy} > 0$  indicated synergy.  $fa_{xyP}$  indicates the predicted fraction affected by a combination of drugs x and y, given each drug used individually:  $fa_{xyP} = fa_x + fa_y - (fa_x)(fa_y)$ . The fraction affected  $fa_x = (MCF \text{ drug x} - MCF \text{ NC}) / (MCF \text{ CD3/CD28} - MCF \text{ NC})$ ; however, since some of our combinations give a signal stronger than the positive control aCD3/aCD28, we used [highest MCF + 1] in each experiment to serve as a 'positive control'.  $fa_{xyO}$  indicates the observed fraction affected with a combination of drugs x and y. Dose escalations correspond to 2.5  $\mu$ M and 5  $\mu$ M chidamide, and 0.5  $\mu$ M and 5  $\mu$ M JQ1. The data shown is from four experiments using the cells of three or four separate healthy donors. Values above the x-axis (0) indicate synergy, while those below indicate antagonism. Significance was calculated using one-tail paired t-test: \* $p < 0.05$ , \*\* $p < 0.01$ .

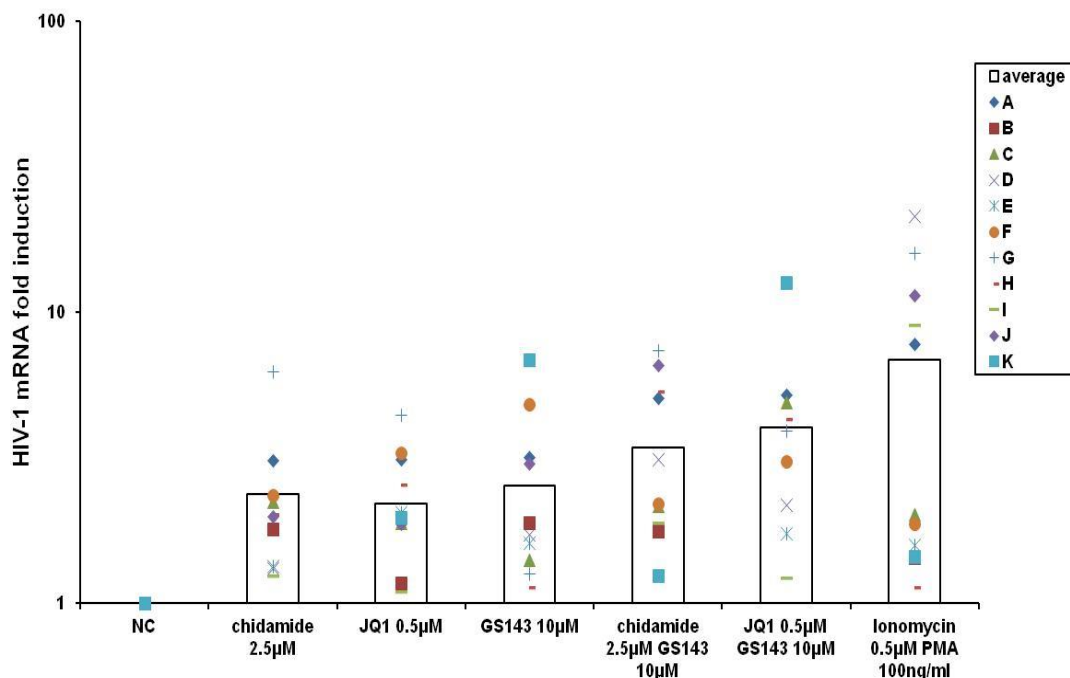


**Figure 4.9. HIV-1 expression induced by representative LRAs, or those combinations with GS143, in resting CD4+ T cells isolated from patients on suppressive ART.** Resting CD4+ T cells were isolated from patient blood. The resting CD4+ T cells were then treated with chidamide, MS-275, JQ1, those combinations with GS143, or Ionomycin plus PMA for 24 hours. Total RNA was then isolated, and HIV-1 mRNA was quantified via RT-qPCR as previously described [6]. The signals were normalized to the mock treated negative control. Each symbol corresponds to a specific patient as shown in upper right of the figure. Averages of all patients are indicated by the open columns. P-values were calculated with two-tailed paired t-test.

## **Concluding Remarks**

In this work, our group utilized a large genetic screen which directed us to look at the ubiquitin-proteasome system and its involvement in HIV-1 latency. We found that global proteasome inhibition with clinically available compounds lead to reversal of the latent state, using both cell lines as well as primary cell models of latency. One of the downstream effectors of proteasome inhibition was found to be  $\beta$ -catenin, a transcription factor which can directly bind the HIV-1 5'-LTR to promote expression: inhibiting the proteasome likewise inhibited the turnover of  $\beta$ -catenin, allowing it to accumulate.

$\beta$ -catenin is regulated through constitutive degradation by the proteasome via ubiquitylation by the E3 ligase  $\beta$ -Trcp. This fact, along with the high representation in the screen of various UPS components including several E3 ligases, led us to consider the possibility of using the UPS for a more targeted reversal of HIV-1 latency. All major LRAs act in a general fashion by activating or inhibiting entire pathways which affect gene expression. Two of the biggest LRA classes are perfect examples of this: PKC agonists ultimately reverse latency through activation of NF $\kappa$ B, an important transcription factor in many pathways including those heavily linked to oncogenesis, while HDAC inhibitors can affect global gene expression; this can be seen in practice with several HDAC inhibitors, such as vorinostat and romidepsin, being used as anti-cancer agents, with adverse effects including nausea, fatigue, and decreases in white and red blood cell counts, and liver toxicity [505].

We view the UPS as the perfect target for specific latency reversal due to the inherent specificity already in the system: combinations of E2 and E3 ligases allow the cell to regulate the degradation of specific proteins. We thus searched for inhibitors of E3 ligases which can lead to latency reversal. Fortunately, while there are few such inhibitors available, targeting the UPS is a



fast and growing area of research. Our search led us to GS143, as it was found to be an inhibitor of  $\beta$ -Trcp-induced ubiquitylation of NF $\kappa$ B. While it didn't affect levels of  $\beta$ -catenin, it did lead to remarkably robust latency reversal, both in a primary cell model as well as samples taken from aviremic HIV+ patients. It also worked in combination with two representative LRAs – chidamide, an HDAC inhibitor, and JQ1, a bromodomain protein inhibitor and activator of P-TEFb. We thus proved that specific inhibition of a UPS pathway can reverse HIV latency, adding a new drug target to the LRA research kit.

Ideally, GS143 derivatives could be candidates for clinical trials aimed at latency reversal in HIV+ patients. In our experiments, we showed that the efficacy of GS143 can rival the positive control of T-cell activation, and that it can work in combination with other LRAs; we also showed that it does not cause T-cell activation, an important consideration for LRAs as global activation of T-cells can be life-threatening. We believe that this efficacy and its unique mechanism of action make it worthy of clinical investigation. To date, all current clinical trials evaluating LRAs have been unable to show a reduction in reservoir size, even if treatment results in increases in viral load. These trials have included various classes of HDAC inhibitors, the PKC agonist bryostatin, disulfiram, and immune modulators such as IL-7 and Toll-like receptor agonists [506]. One potential explanation is a possible effect of HDAC inhibitors on CD8+ T-cell function: several studies have found that they can impair cytokine production and proliferation of antigen-specific CD8+ T-cells [298, 507, 508], though some studies have found HDAC inhibitors can cause viral protein production sufficient enough to provoke CD8+ T-cell-mediated killing [509, 510]. Without a strong CD8+ T-cell response, reactivated latent cells won't be cleared by the immune system. Another issue could be simply that these compounds are not powerful LRAs *in vivo* and are thus not reactivating enough of the latent reservoir strongly enough to elicit significant cell death. GS143 was shown to be a very strong LRA and thus its derivatives may be

able to achieve robust enough reactivation *in vivo* to overcome this hurdle; similarly, it was shown to act strongly in combination with other LRA classes, so multi-drug therapy is also a possible avenue which has not been clinically tested yet.

Finding the exact mechanism of action of GS143 is not critical to clinical development, although it would be helpful – and to this end we have been performing Western blots against known targets of  $\beta$ -Trcp to see if their levels are increased upon treatment; if a hit is found, the next step would be chromatin immunoprecipitation to look for enrichment of the protein hit at the HIV-1 5'-LTR. Regardless, we could employ x-ray crystallography looking at the GS143: $\beta$ -Trcp complex to see exactly what parts of the molecule are important for its activity. This information could help with, though it's not required for, performing medicinal chemistry to optimize the compound through structure-activity relationship analysis for increased activity, reduced toxicity, and also to determine solubility which would define the route of administration. The next step would be animal studies with these GS143 derivatives to determine toxicity, pharmacokinetics, and pharmacodynamics; similar experiments would then be needed in healthy, uninfected humans before moving into HIV+ patients. We believe that GS143 marks the start of a new class of LRA compounds that are worthy of further investigation and development.

## **Bibliography**

1. Barre-Sinoussi, F., et al., *Isolation of a t-lymphotropic retrovirus from a patient at risk for acquired immune deficiency syndrome (aids)*. Science, 1983. **220**(4599): p. 868-71.
2. Gallo, R.C., et al., *Isolation of human t-cell leukemia virus in acquired immune deficiency syndrome (aids)*. Science, 1983. **220**(4599): p. 865-7.
3. UNAIDS.org, *Global aids update*. 2016.
4. Gebo, K.A., et al., *Contemporary costs of hiv healthcare in the haart era*. AIDS, 2010. **24**(17): p. 2705-15.
5. Nakagawa, F., et al., *Projected lifetime healthcare costs associated with hiv infection*. PLoS One, 2015. **10**(4): p. e0125018.
6. Turner, B.G. and M.F. Summers, *Structural biology of hiv*. J Mol Biol, 1999. **285**(1): p. 1-32.
7. Wilen, C.B., J.C. Tilton, and R.W. Doms, *Hiv: Cell binding and entry*. Cold Spring Harb Perspect Med, 2012. **2**(8).
8. Hu, W.S. and S.H. Hughes, *Hiv-1 reverse transcription*. Cold Spring Harb Perspect Med, 2012. **2**(10).
9. Bukrinsky, M.I. and O.K. Haffar, *Hiv-1 nuclear import: In search of a leader*. Front Biosci, 1999. **4**: p. D772-81.
10. Bukrinsky, M.I., et al., *Active nuclear import of human immunodeficiency virus type 1 preintegration complexes*. Proc Natl Acad Sci U S A, 1992. **89**(14): p. 6580-4.
11. Schroder, A.R., et al., *Hiv-1 integration in the human genome favors active genes and local hotspots*. Cell, 2002. **110**(4): p. 521-9.
12. Garber, M.E. and K.A. Jones, *Hiv-1 tat: Coping with negative elongation factors*. Curr Opin Immunol, 1999. **11**(4): p. 460-5.
13. Zhou, Q., et al., *Transcription elongation factor p-tefb mediates tat activation of hiv-1 transcription at multiple stages*. EMBO J, 1998. **17**(13): p. 3681-91.
14. Pollard, V.W. and M.H. Malim, *The hiv-1 rev protein*. Annu Rev Microbiol, 1998. **52**: p. 491-532.
15. Sundquist, W.I. and H.G. Krausslich, *Hiv-1 assembly, budding, and maturation*. Cold Spring Harb Perspect Med, 2012. **2**(7): p. a006924.
16. Strebel, K., *Hiv accessory proteins versus host restriction factors*. Curr Opin Virol, 2013. **3**(6): p. 692-9.
17. Le Rouzic, E. and S. Benichou, *The vpr protein from hiv-1: Distinct roles along the viral life cycle*. Retrovirology, 2005. **2**: p. 11.
18. Bour, S. and K. Strebel, *The hiv-1 vpu protein: A multifunctional enhancer of viral particle release*. Microbes Infect, 2003. **5**(11): p. 1029-39.
19. Foster, J.L. and J.V. Garcia, *Hiv-1 nef: At the crossroads*. Retrovirology, 2008. **5**: p. 84.
20. Hladik, F. and M.J. McElrath, *Setting the stage: Host invasion by hiv*. Nat Rev Immunol, 2008. **8**(6): p. 447-57.
21. Pope, M. and A.T. Haase, *Transmission, acute hiv-1 infection and the quest for strategies to prevent infection*. Nat Med, 2003. **9**(7): p. 847-52.
22. Brenner, B.G., et al., *High rates of forward transmission events after acute/early hiv-1 infection*. J Infect Dis, 2007. **195**(7): p. 951-9.
23. Hollingsworth, T.D., R.M. Anderson, and C. Fraser, *Hiv-1 transmission, by stage of infection*. J Infect Dis, 2008. **198**(5): p. 687-93.

24. Centlivre, M., et al., *In hiv-1 pathogenesis the die is cast during primary infection*. AIDS, 2007. **21**(1): p. 1-11.
25. Mehandru, S., et al., *Lack of mucosal immune reconstitution during prolonged treatment of acute and early hiv-1 infection*. PLoS Med, 2006. **3**(12): p. e484.
26. Mehandru, S., et al., *Primary hiv-1 infection is associated with preferential depletion of cd4+ t lymphocytes from effector sites in the gastrointestinal tract*. J Exp Med, 2004. **200**(6): p. 761-70.
27. Connor, R.I., et al., *Change in coreceptor use correlates with disease progression in hiv-1-infected individuals*. J Exp Med, 1997. **185**(4): p. 621-8.
28. Limper, A.H., et al., *Fungal infections in hiv/aids*. Lancet Infect Dis, 2017.
29. Chaisson, R.E., et al., *Impact of opportunistic disease on survival in patients with hiv infection*. AIDS, 1998. **12**(1): p. 29-33.
30. Moore, R.D. and R.E. Chaisson, *Natural history of opportunistic disease in an hiv-infected urban clinical cohort*. Ann Intern Med, 1996. **124**(7): p. 633-42.
31. Selik, R.M., E.T. Starcher, and J.W. Curran, *Opportunistic diseases reported in aids patients: Frequencies, associations, and trends*. AIDS, 1987. **1**(3): p. 175-82.
32. Henrard, D.R., et al., *Natural history of hiv-1 cell-free viremia*. JAMA, 1995. **274**(7): p. 554-8.
33. Katzenstein, T.L., et al., *Longitudinal serum hiv rna quantification: Correlation to viral phenotype at seroconversion and clinical outcome*. AIDS, 1996. **10**(2): p. 167-73.
34. Deeks, S.G., et al., *Immune activation set point during early hiv infection predicts subsequent cd4+ t-cell changes independent of viral load*. Blood, 2004. **104**(4): p. 942-7.
35. Lavreys, L., et al., *Higher set point plasma viral load and more-severe acute hiv type 1 (hiv-1) illness predict mortality among high-risk hiv-1-infected african women*. Clin Infect Dis, 2006. **42**(9): p. 1333-9.
36. Quinn, T.C., et al., *Viral load and heterosexual transmission of human immunodeficiency virus type 1. Rakai project study group*. N Engl J Med, 2000. **342**(13): p. 921-9.
37. Fideli, U.S., et al., *Virologic and immunologic determinants of heterosexual transmission of human immunodeficiency virus type 1 in africa*. AIDS Res Hum Retroviruses, 2001. **17**(10): p. 901-10.
38. Fraser, C., et al., *Variation in hiv-1 set-point viral load: Epidemiological analysis and an evolutionary hypothesis*. Proc Natl Acad Sci U S A, 2007. **104**(44): p. 17441-6.
39. Blanquart, F., et al., *Viral genetic variation accounts for a third of variability in hiv-1 set-point viral load in europe*. PLoS Biol, 2017. **15**(6): p. e2001855.
40. Alizon, S., et al., *Phylogenetic approach reveals that virus genotype largely determines hiv set-point viral load*. PLoS Pathog, 2010. **6**(9): p. e1001123.
41. Ndhlovu, Z.M., et al., *Magnitude and kinetics of cd8+ t cell activation during hyperacute hiv infection impact viral set point*. Immunity, 2015. **43**(3): p. 591-604.
42. Riou, C., et al., *Differential impact of magnitude, polyfunctional capacity, and specificity of hiv-specific cd8+ t cell responses on hiv set point*. J Virol, 2014. **88**(3): p. 1819-24.
43. Roberts, L., et al., *Genital tract inflammation during early hiv-1 infection predicts higher plasma viral load set point in women*. J Infect Dis, 2012. **205**(2): p. 194-203.
44. Perelson, A.S., et al., *Decay characteristics of hiv-1-infected compartments during combination therapy*. Nature, 1997. **387**(6629): p. 188-91.
45. Perelson, A.S., *Modelling viral and immune system dynamics*. Nat Rev Immunol, 2002. **2**(1): p. 28-36.
46. Clavel, F. and A.J. Hance, *Hiv drug resistance*. N Engl J Med, 2004. **350**(10): p. 1023-35.

47. Cihlar, T. and A.S. Ray, *Nucleoside and nucleotide hiv reverse transcriptase inhibitors: 25 years after zidovudine*. Antiviral Res, 2010. **85**(1): p. 39-58.
48. de Bethune, M.P., *Non-nucleoside reverse transcriptase inhibitors (nnrtis), their discovery, development, and use in the treatment of hiv-1 infection: A review of the last 20 years (1989-2009)*. Antiviral Res, 2010. **85**(1): p. 75-90.
49. Rabi, S.A., et al., *Multi-step inhibition explains hiv-1 protease inhibitor pharmacodynamics and resistance*. J Clin Invest, 2013. **123**(9): p. 3848-60.
50. Bierman, W.F., et al., *Hiv monotherapy with ritonavir-boosted protease inhibitors: A systematic review*. AIDS, 2009. **23**(3): p. 279-91.
51. Perez-Valero, I. and J.R. Arribas, *Protease inhibitor monotherapy*. Curr Opin Infect Dis, 2011. **24**(1): p. 7-11.
52. Messiaen, P., et al., *Clinical use of hiv integrase inhibitors: A systematic review and meta-analysis*. PLoS One, 2013. **8**(1): p. e52562.
53. Dorr, P., et al., *Maraviroc (uk-427,857), a potent, orally bioavailable, and selective small-molecule inhibitor of chemokine receptor ccr5 with broad-spectrum anti-human immunodeficiency virus type 1 activity*. Antimicrob Agents Chemother, 2005. **49**(11): p. 4721-32.
54. Gulick, R.M., et al., *Five-year safety evaluation of maraviroc in hiv-1-infected treatment-experienced patients*. J Acquir Immune Defic Syndr, 2014. **65**(1): p. 78-81.
55. Haqqani, A.A. and J.C. Tilton, *Entry inhibitors and their use in the treatment of hiv-1 infection*. Antiviral Res, 2013. **98**(2): p. 158-70.
56. Lalezari, J.P., et al., *Enfuvirtide, an hiv-1 fusion inhibitor, for drug-resistant hiv infection in north and south america*. N Engl J Med, 2003. **348**(22): p. 2175-85.
57. Rodger, A.J., et al., *Sexual activity without condoms and risk of hiv transmission in serodifferent couples when the hiv-positive partner is using suppressive antiretroviral therapy*. JAMA, 2016. **316**(2): p. 171-81.
58. Cohen, M.S., et al., *Prevention of hiv-1 infection with early antiretroviral therapy*. N Engl J Med, 2011. **365**(6): p. 493-505.
59. Group, I.S.S., et al., *Initiation of antiretroviral therapy in early asymptomatic hiv infection*. N Engl J Med, 2015. **373**(9): p. 795-807.
60. Plana, M., et al., *Immunological benefits of antiretroviral therapy in very early stages of asymptomatic chronic hiv-1 infection*. AIDS, 2000. **14**(13): p. 1921-33.
61. Sun, Y., et al., *The investigation of cd4+t-cell functions in primary hiv infection with antiretroviral therapy*. Medicine (Baltimore), 2017. **96**(28): p. e7430.
62. Lifson, A.R., et al., *Improved quality of life with immediate versus deferred initiation of antiretroviral therapy in early asymptomatic hiv infection*. AIDS, 2017. **31**(7): p. 953-963.
63. Gunthard, H.F., et al., *Antiretroviral drugs for treatment and prevention of hiv infection in adults: 2016 recommendations of the international antiviral society-usa panel*. JAMA, 2016. **316**(2): p. 191-210.
64. Margolis, A.M., et al., *A review of the toxicity of hiv medications*. J Med Toxicol, 2014. **10**(1): p. 26-39.
65. Stolbach, A., et al., *A review of the toxicity of hiv medications ii: Interactions with drugs and complementary and alternative medicine products*. J Med Toxicol, 2015. **11**(3): p. 326-41.
66. Evans-Jones, J.G., et al., *Recognition of risk for clinically significant drug interactions among hiv-infected patients receiving antiretroviral therapy*. Clin Infect Dis, 2010. **50**(10): p. 1419-21.

67. Priyanka, P., et al., *Recognition of possible risk factors for clinically significant drug-drug interactions among indian people living with hiv receiving highly active antiretroviral therapy and concomitant medications*. Int J Risk Saf Med, 2017. **29**(1-2): p. 25-55.
68. Greub, G., et al., *Intermittent and sustained low-level hiv viral rebound in patients receiving potent antiretroviral therapy*. AIDS, 2002. **16**(14): p. 1967-9.
69. Havlir, D.V., et al., *Prevalence and predictive value of intermittent viremia with combination hiv therapy*. JAMA, 2001. **286**(2): p. 171-9.
70. Mira, J.A., et al., *Transient rebounds of low-level viraemia among hiv-infected patients under haart are not associated with virological or immunological failure*. Antivir Ther, 2002. **7**(4): p. 251-6.
71. Nettles, R.E., et al., *Intermittent hiv-1 viremia (blips) and drug resistance in patients receiving haart*. JAMA, 2005. **293**(7): p. 817-29.
72. Lee, P.K., et al., *Hiv-1 viral load blips are of limited clinical significance*. J Antimicrob Chemother, 2006. **57**(5): p. 803-5.
73. Manavi, K., *The significance of low-level plasma hiv viral load on cobas taqman hiv-1 assays for patients with undetectable plasma viral load on cobas amplicor monitor version 1.5*. HIV Clin Trials, 2008. **9**(4): p. 283-6.
74. Garrett, N.J., et al., *Comparison of the rate and size of hiv-1 viral load blips with roche cobas taqman hiv-1 versions 1.0 and 2.0 and implications for patient management*. J Clin Virol, 2012. **53**(4): p. 354-5.
75. Nettles, R.E. and T.L. Kieffer, *Update on hiv-1 viral load blips*. Curr Opin HIV AIDS, 2006. **1**(2): p. 157-61.
76. Grennan, J.T., et al., *Magnitude of virologic blips is associated with a higher risk for virologic rebound in hiv-infected individuals: A recurrent events analysis*. J Infect Dis, 2012. **205**(8): p. 1230-8.
77. Easterbrook, P.J., et al., *The natural history and clinical significance of intermittent viraemia in patients with initial viral suppression to < 400 copies/ml*. AIDS, 2002. **16**(11): p. 1521-7.
78. Moore, A.L., et al., *Raised viral load in patients with viral suppression on highly active antiretroviral therapy: Transient increase or treatment failure?* AIDS, 2002. **16**(4): p. 615-8.
79. Di Mascio, M., et al., *Viral blip dynamics during highly active antiretroviral therapy*. J Virol, 2003. **77**(22): p. 12165-72.
80. Di Mascio, M., et al., *Dynamics of intermittent viremia during highly active antiretroviral therapy in patients who initiate therapy during chronic versus acute and early human immunodeficiency virus type 1 infection*. J Virol, 2004. **78**(19): p. 10566-73.
81. Jones, L.E. and A.S. Perelson, *Modeling the effects of vaccination on chronically infected hiv-positive patients*. J Acquir Immune Defic Syndr, 2002. **31**(4): p. 369-77.
82. Jones, L.E. and A.S. Perelson, *Opportunistic infection as a cause of transient viremia in chronically infected hiv patients under treatment with haart*. Bull Math Biol, 2005. **67**(6): p. 1227-51.
83. Jones, L.E. and A.S. Perelson, *Transient viremia, plasma viral load, and reservoir replenishment in hiv-infected patients on antiretroviral therapy*. J Acquir Immune Defic Syndr, 2007. **45**(5): p. 483-93.
84. Rong, L. and A.S. Perelson, *Modeling latently infected cell activation: Viral and latent reservoir persistence, and viral blips in hiv-infected patients on potent therapy*. PLoS Comput Biol, 2009. **5**(10): p. e1000533.

85. Rong, L. and A.S. Perelson, *Asymmetric division of activated latently infected cells may explain the decay kinetics of the hiv-1 latent reservoir and intermittent viral blips*. Math Biosci, 2009. **217**(1): p. 77-87.
86. Conway, J.M. and D. Coombs, *A stochastic model of latently infected cell reactivation and viral blip generation in treated hiv patients*. PLoS Comput Biol, 2011. **7**(4): p. e1002033.
87. Meyaard, L., et al., *Programmed death of t cells in hiv-1 infection*. Science, 1992. **257**(5067): p. 217-9.
88. Finkel, T.H., et al., *Apoptosis occurs predominantly in bystander cells and not in productively infected cells of hiv- and siv-infected lymph nodes*. Nat Med, 1995. **1**(2): p. 129-34.
89. Jekle, A., et al., *In vivo evolution of human immunodeficiency virus type 1 toward increased pathogenicity through cxcr4-mediated killing of uninfected cd4 t cells*. J Virol, 2003. **77**(10): p. 5846-54.
90. Doitsh, G., et al., *Abortive hiv infection mediates cd4 t cell depletion and inflammation in human lymphoid tissue*. Cell, 2010. **143**(5): p. 789-801.
91. Doitsh, G., et al., *Cell death by pyroptosis drives cd4 t-cell depletion in hiv-1 infection*. Nature, 2014. **505**(7484): p. 509-14.
92. Munoz-Arias, I., et al., *Blood-derived cd4 t cells naturally resist pyroptosis during abortive hiv-1 infection*. Cell Host Microbe, 2015. **18**(4): p. 463-70.
93. Moon, H.S. and J.S. Yang, *Role of hiv vpr as a regulator of apoptosis and an effector on bystander cells*. Mol Cells, 2006. **21**(1): p. 7-20.
94. Yang, Y., et al., *Monocytes treated with human immunodeficiency virus tat kill uninfected cd4(+) cells by a tumor necrosis factor-related apoptosis-induced ligand-mediated mechanism*. J Virol, 2003. **77**(12): p. 6700-8.
95. Ahr, B., et al., *Apoptosis of uninfected cells induced by hiv envelope glycoproteins*. Retrovirology, 2004. **1**: p. 12.
96. Grau-Exposito, J., et al., *A novel single-cell fish-flow assay identifies effector memory cd4+ t cells as a major niche for hiv-1 transcription in hiv-infected patients*. MBio, 2017. **8**(4).
97. Douek, D.C., et al., *Hiv preferentially infects hiv-specific cd4+ t cells*. Nature, 2002. **417**(6884): p. 95-8.
98. Mattapallil, J.J., et al., *Massive infection and loss of memory cd4+ t cells in multiple tissues during acute siv infection*. Nature, 2005. **434**(7037): p. 1093-7.
99. Li, Q., et al., *Peak siv replication in resting memory cd4+ t cells depletes gut lamina propria cd4+ t cells*. Nature, 2005. **434**(7037): p. 1148-52.
100. Brenchley, J.M., et al., *Cd4+ t cell depletion during all stages of hiv disease occurs predominantly in the gastrointestinal tract*. J Exp Med, 2004. **200**(6): p. 749-59.
101. Guadalupe, M., et al., *Severe cd4+ t-cell depletion in gut lymphoid tissue during primary human immunodeficiency virus type 1 infection and substantial delay in restoration following highly active antiretroviral therapy*. J Virol, 2003. **77**(21): p. 11708-17.
102. Guadalupe, M., et al., *Viral suppression and immune restoration in the gastrointestinal mucosa of human immunodeficiency virus type 1-infected patients initiating therapy during primary or chronic infection*. J Virol, 2006. **80**(16): p. 8236-47.
103. Asmuth, D.M., et al., *Tissue pharmacologic and virologic determinants of duodenal and rectal gut immune reconstitution in hiv-infected patients initiating antiretroviral therapy*. The Journal of Infectious Diseases, 2017.

104. Brenchley, J.M., et al., *Microbial translocation is a cause of systemic immune activation in chronic hiv infection*. Nat Med, 2006. **12**(12): p. 1365-71.
105. Nazli, A., et al., *Exposure to hiv-1 directly impairs mucosal epithelial barrier integrity allowing microbial translocation*. PLoS Pathog, 2010. **6**(4): p. e1000852.
106. Marchetti, G., et al., *Microbial translocation is associated with sustained failure in cd4+ t-cell reconstitution in hiv-infected patients on long-term highly active antiretroviral therapy*. AIDS, 2008. **22**(15): p. 2035-8.
107. Baroncelli, S., et al., *Microbial translocation is associated with residual viral replication in haart-treated hiv+ subjects with <50copies/ml hiv-1 rna*. J Clin Virol, 2009. **46**(4): p. 367-70.
108. Marchetti, G., et al., *Microbial translocation predicts disease progression of hiv-infected antiretroviral-naive patients with high cd4+ cell count*. AIDS, 2011. **25**(11): p. 1385-94.
109. Hunt, P.W., et al., *Gut epithelial barrier dysfunction and innate immune activation predict mortality in treated hiv infection*. J Infect Dis, 2014. **210**(8): p. 1228-38.
110. Wolthers, K.C., et al., *T cell telomere length in hiv-1 infection: No evidence for increased cd4+ t cell turnover*. Science, 1996. **274**(5292): p. 1543-7.
111. Palmer, L.D., et al., *Telomere length, telomerase activity, and replicative potential in hiv infection: Analysis of cd4+ and cd8+ t cells from hiv-discordant monozygotic twins*. J Exp Med, 1997. **185**(7): p. 1381-6.
112. Kaufmann, D.E., et al., *Upregulation of ctla-4 by hiv-specific cd4+ t cells correlates with disease progression and defines a reversible immune dysfunction*. Nat Immunol, 2007. **8**(11): p. 1246-54.
113. Trautmann, L., et al., *Upregulation of pd-1 expression on hiv-specific cd8+ t cells leads to reversible immune dysfunction*. Nat Med, 2006. **12**(10): p. 1198-202.
114. Kelley, C.F., et al., *Incomplete peripheral cd4+ cell count restoration in hiv-infected patients receiving long-term antiretroviral treatment*. Clin Infect Dis, 2009. **48**(6): p. 787-94.
115. Price, P., et al., *Immune dysfunction and immune restoration disease in hiv patients given highly active antiretroviral therapy*. J Clin Virol, 2001. **22**(3): p. 279-87.
116. Falasca, F., et al., *Evaluation of hiv-DNA and inflammatory markers in hiv-infected individuals with different viral load patterns*. BMC Infect Dis, 2017. **17**(1): p. 581.
117. van den Dries, L., et al., *Immune activation in prolonged cart-suppressed hiv patients is comparable to that of healthy controls*. Virology, 2017. **509**: p. 133-139.
118. Guaraldi, G., et al., *Premature age-related comorbidities among hiv-infected persons compared with the general population*. Clin Infect Dis, 2011. **53**(11): p. 1120-6.
119. Antiretroviral Therapy Cohort, C., *Survival of hiv-positive patients starting antiretroviral therapy between 1996 and 2013: A collaborative analysis of cohort studies*. Lancet HIV, 2017.
120. Tozzi, V., et al., *Prevalence and risk factors for human immunodeficiency virus-associated neurocognitive impairment, 1996 to 2002: Results from an urban observational cohort*. J Neurovirol, 2005. **11**(3): p. 265-73.
121. Navia, B.A., et al., *The aids dementia complex: li. Neuropathology*. Ann Neurol, 1986. **19**(6): p. 525-35.
122. Navia, B.A., B.D. Jordan, and R.W. Price, *The aids dementia complex: I. Clinical features*. Ann Neurol, 1986. **19**(6): p. 517-24.
123. Clifford, D.B. and B.M. Ances, *Hiv-associated neurocognitive disorder*. Lancet Infect Dis, 2013. **13**(11): p. 976-86.



124. Hua, X., et al., *Disrupted cerebral metabolite levels and lower nadir cd4 + counts are linked to brain volume deficits in 210 hiv-infected patients on stable treatment.* Neuroimage Clin, 2013. **3**: p. 132-42.
125. Zhuang, Y., et al., *Combination antiretroviral therapy improves cognitive performance and functional connectivity in treatment-naive hiv-infected individuals.* J Neurovirol, 2017.
126. Robertson, K.R., et al., *Neurocognitive effects of treatment interruption in stable hiv-positive patients in an observational cohort.* Neurology, 2010. **74**(16): p. 1260-6.
127. Mellors, J.W., et al., *Plasma viral load and cd4+ lymphocytes as prognostic markers of hiv-1 infection.* Ann Intern Med, 1997. **126**(12): p. 946-54.
128. Mellors, J.W., et al., *Prognosis in hiv-1 infection predicted by the quantity of virus in plasma.* Science, 1996. **272**(5265): p. 1167-70.
129. Lyles, R.H., et al., *Natural history of human immunodeficiency virus type 1 viremia after seroconversion and proximal to aids in a large cohort of homosexual men. Multicenter aids cohort study.* J Infect Dis, 2000. **181**(3): p. 872-80.
130. Goujard, C., et al., *Cd4 cell count and hiv DNA level are independent predictors of disease progression after primary hiv type 1 infection in untreated patients.* Clin Infect Dis, 2006. **42**(5): p. 709-15.
131. Williams, J.P., et al., *Hiv-1 DNA predicts disease progression and post-treatment virological control.* Elife, 2014. **3**: p. e03821.
132. Tierney, C., et al., *Prognostic value of baseline human immunodeficiency virus type 1 DNA measurement for disease progression in patients receiving nucleoside therapy.* J Infect Dis, 2003. **187**(1): p. 144-8.
133. Rouzioux, C., et al., *Early levels of hiv-1 DNA in peripheral blood mononuclear cells are predictive of disease progression independently of hiv-1 rna levels and cd4+ t cell counts.* J Infect Dis, 2005. **192**(1): p. 46-55.
134. Fourati, S., et al., *Factors associated with a low hiv reservoir in patients with prolonged suppressive antiretroviral therapy.* J Antimicrob Chemother, 2014. **69**(3): p. 753-6.
135. Borrow, P., et al., *Virus-specific cd8+ cytotoxic t-lymphocyte activity associated with control of viremia in primary human immunodeficiency virus type 1 infection.* J Virol, 1994. **68**(9): p. 6103-10.
136. Koup, R.A., et al., *Temporal association of cellular immune responses with the initial control of viremia in primary human immunodeficiency virus type 1 syndrome.* J Virol, 1994. **68**(7): p. 4650-5.
137. Kiepiela, P., et al., *Cd8+ t-cell responses to different hiv proteins have discordant associations with viral load.* Nat Med, 2007. **13**(1): p. 46-53.
138. Almeida, J.R., et al., *Superior control of hiv-1 replication by cd8+ t cells is reflected by their avidity, polyfunctionality, and clonal turnover.* J Exp Med, 2007. **204**(10): p. 2473-85.
139. Lifson, A.R., et al., *Long-term human immunodeficiency virus infection in asymptomatic homosexual and bisexual men with normal cd4+ lymphocyte counts: Immunologic and virologic characteristics.* J Infect Dis, 1991. **163**(5): p. 959-65.
140. Sheppard, H.W., et al., *The characterization of non-progressors: Long-term hiv-1 infection with stable cd4+ t-cell levels.* AIDS, 1993. **7**(9): p. 1159-66.
141. Rodes, B., et al., *Differences in disease progression in a cohort of long-term non-progressors after more than 16 years of hiv-1 infection.* AIDS, 2004. **18**(8): p. 1109-16.
142. Buchbinder, S.P., et al., *Long-term hiv-1 infection without immunologic progression.* AIDS, 1994. **8**(8): p. 1123-8.

143. Migueles, S.A., et al., *Hiv-specific cd8+ t cell proliferation is coupled to perforin expression and is maintained in nonprogressors*. Nat Immunol, 2002. **3**(11): p. 1061-8.
144. Betts, M.R., et al., *Hiv nonprogressors preferentially maintain highly functional hiv-specific cd8+ t cells*. Blood, 2006. **107**(12): p. 4781-9.
145. O'Connor, G.M., et al., *Natural killer cells from long-term non-progressor hiv patients are characterized by altered phenotype and function*. Clin Immunol, 2007. **124**(3): p. 277-83.
146. Costa, P., et al., *Low expression of inhibitory natural killer receptors in cd8 cytotoxic t lymphocytes in long-term non-progressor hiv-1-infected patients*. AIDS, 2003. **17**(2): p. 257-60.
147. Yamada, T. and A. Iwamoto, *Comparison of proviral accessory genes between long-term nonprogressors and progressors of human immunodeficiency virus type 1 infection*. Arch Virol, 2000. **145**(5): p. 1021-7.
148. Deacon, N.J., et al., *Genomic structure of an attenuated quasi species of hiv-1 from a blood transfusion donor and recipients*. Science, 1995. **270**(5238): p. 988-91.
149. Kirchhoff, F., et al., *Brief report: Absence of intact nef sequences in a long-term survivor with nonprogressive hiv-1 infection*. N Engl J Med, 1995. **332**(4): p. 228-32.
150. Salvi, R., et al., *Grossly defective nef gene sequences in a human immunodeficiency virus type 1-seropositive long-term nonprogressor*. J Virol, 1998. **72**(5): p. 3646-57.
151. Premkumar, D.R., et al., *The nef gene from a long-term hiv type 1 nonprogressor*. AIDS Res Hum Retroviruses, 1996. **12**(4): p. 337-45.
152. Casartelli, N., et al., *Structural defects and variations in the hiv-1 nef gene from rapid, slow and non-progressor children*. AIDS, 2003. **17**(9): p. 1291-301.
153. Saksela, K., G. Cheng, and D. Baltimore, *Proline-rich (ppxpp) motifs in hiv-1 nef bind to sh3 domains of a subset of src kinases and are required for the enhanced growth of nef+ viruses but not for down-regulation of cd4*. EMBO J, 1995. **14**(3): p. 484-91.
154. Lum, J.J., et al., *Vpr r77q is associated with long-term nonprogressive hiv infection and impaired induction of apoptosis*. J Clin Invest, 2003. **111**(10): p. 1547-54.
155. Fischer, A., et al., *Is the vpr r77q mutation associated with long-term non-progression of hiv infection?* AIDS, 2004. **18**(9): p. 1346-7.
156. Jacquot, G., et al., *Characterization of the molecular determinants of primary hiv-1 vpr proteins: Impact of the q65r and r77q substitutions on vpr functions*. PLoS One, 2009. **4**(10): p. e7514.
157. Caly, L., et al., *Impaired nuclear import and viral incorporation of vpr derived from a hiv long-term non-progressor*. Retrovirology, 2008. **5**: p. 67.
158. Dean, M., et al., *Genetic restriction of hiv-1 infection and progression to aids by a deletion allele of the ckr5 structural gene. Hemophilia growth and development study, multicenter aids cohort study, multicenter hemophilia cohort study, san francisco city cohort, alive study*. Science, 1996. **273**(5283): p. 1856-62.
159. Eugen-Olsen, J., et al., *Heterozygosity for a deletion in the ckr-5 gene leads to prolonged aids-free survival and slower cd4 t-cell decline in a cohort of hiv-seropositive individuals*. AIDS, 1997. **11**(3): p. 305-10.
160. Romiti, M.L., et al., *Prognostic value of a ccr5 defective allele in pediatric hiv-1 infection*. Mol Med, 2000. **6**(1): p. 28-36.
161. Misrahi, M., et al., *Ccr5 chemokine receptor variant in hiv-1 mother-to-child transmission and disease progression in children. French pediatric hiv infection study group*. JAMA, 1998. **279**(4): p. 277-80.
162. Martin, M.P., et al., *Genetic acceleration of aids progression by a promoter variant of ccr5*. Science, 1998. **282**(5395): p. 1907-11.

163. Clegg, A.O., et al., *Ccr5 promoter polymorphisms, ccr5 59029a and ccr5 59353c, are under represented in hiv-1-infected long-term non-progressors. The australian long-term non-progressor study group.* AIDS, 2000. **14**(2): p. 103-8.
164. Ometto, L., et al., *Polymorphisms in the ccr5 promoter region influence disease progression in perinatally human immunodeficiency virus type 1-infected children.* J Infect Dis, 2001. **183**(5): p. 814-8.
165. Reynes, J., et al., *Cd4 t cell surface ccr5 density as a host factor in hiv-1 disease progression.* AIDS, 2001. **15**(13): p. 1627-34.
166. Morawetz, R.A., et al., *Genetic polymorphism of ccr5 gene and hiv disease: The heterozygous (ccr5/delta ccr5) genotype is neither essential nor sufficient for protection against disease progression. Swiss hiv cohort.* Eur J Immunol, 1997. **27**(12): p. 3223-7.
167. Land, A.M., et al., *Human immunodeficiency virus (hiv) type 1 proviral hypermutation correlates with cd4 count in hiv-infected women from kenya.* J Virol, 2008. **82**(16): p. 8172-82.
168. Kourteva, Y., et al., *Apobec3g expression and hypermutation are inversely associated with human immunodeficiency virus type 1 (hiv-1) burden in vivo.* Virology, 2012. **430**(1): p. 1-9.
169. Madlala, P., et al., *Association of polymorphisms in the ledgf/p75 gene (psip1) with susceptibility to hiv-1 infection and disease progression.* AIDS, 2011. **25**(14): p. 1711-9.
170. Ballana, E., et al., *Rare ledgf/p75 genetic variants in white long-term nonprogressor hiv+ individuals.* AIDS, 2012. **26**(4): p. 527-8.
171. Messiaen, P., et al., *Characterization of ledgf/p75 genetic variants and association with hiv-1 disease progression.* PLoS One, 2012. **7**(11): p. e50204.
172. Flores-Villanueva, P.O., et al., *Control of hiv-1 viremia and protection from aids are associated with hla-bw4 homozygosity.* Proc Natl Acad Sci U S A, 2001. **98**(9): p. 5140-5.
173. Lopez-Vazquez, A., et al., *Interaction between kir3dl1 and hla-b\*57 supertype alleles influences the progression of hiv-1 infection in a zambian population.* Hum Immunol, 2005. **66**(3): p. 285-9.
174. Migueles, S.A., et al., *Hla b\*5701 is highly associated with restriction of virus replication in a subgroup of hiv-infected long term nonprogressors.* Proc Natl Acad Sci U S A, 2000. **97**(6): p. 2709-14.
175. Navis, M., et al., *Viral replication capacity as a correlate of hla b57/b5801-associated nonprogressive hiv-1 infection.* J Immunol, 2007. **179**(5): p. 3133-43.
176. Bailey, J.R., et al., *Maintenance of viral suppression in hiv-1-infected hla-b\*57+ elite suppressors despite ctl escape mutations.* J Exp Med, 2006. **203**(5): p. 1357-69.
177. Okulicz, J.F., et al., *Clinical outcomes of elite controllers, viremic controllers, and long-term nonprogressors in the us department of defense hiv natural history study.* J Infect Dis, 2009. **200**(11): p. 1714-23.
178. Andrade, A., et al., *Cd4+ t cell depletion in an untreated hiv type 1-infected human leukocyte antigen-b\*5801-positive patient with an undetectable viral load.* Clin Infect Dis, 2008. **46**(8): p. e78-82.
179. Greenough, T.C., J.L. Sullivan, and R.C. Desrosiers, *Declining cd4 t-cell counts in a person infected with nef-deleted hiv-1.* N Engl J Med, 1999. **340**(3): p. 236-7.
180. Hunt, P.W., et al., *Relationship between t cell activation and cd4+ t cell count in hiv-seropositive individuals with undetectable plasma hiv rna levels in the absence of therapy.* J Infect Dis, 2008. **197**(1): p. 126-33.
181. Boufassa, F., et al., *Cd4 dynamics over a 15 year-period among hiv controllers enrolled in the anrs french observatory.* PLoS One, 2011. **6**(4): p. e18726.

182. Lamine, A., et al., *Replication-competent hiv strains infect hiv controllers despite undetectable viremia (anrs ep36 study)*. AIDS, 2007. **21**(8): p. 1043-5.
183. Chen, H., et al., *Cd4+ t cells from elite controllers resist hiv-1 infection by selective upregulation of p21*. J Clin Invest, 2011. **121**(4): p. 1549-60.
184. Saez-Cirion, A., et al., *Hiv controllers exhibit potent cd8 t cell capacity to suppress hiv infection ex vivo and peculiar cytotoxic t lymphocyte activation phenotype*. Proc Natl Acad Sci U S A, 2007. **104**(16): p. 6776-81.
185. Hersperger, A.R., et al., *Perforin expression directly ex vivo by hiv-specific cd8 t-cells is a correlate of hiv elite control*. PLoS Pathog, 2010. **6**(5): p. e1000917.
186. Bailey, J.R., et al., *Neutralizing antibodies do not mediate suppression of human immunodeficiency virus type 1 in elite suppressors or selection of plasma virus variants in patients on highly active antiretroviral therapy*. J Virol, 2006. **80**(10): p. 4758-70.
187. Lambotte, O., et al., *Heterogeneous neutralizing antibody and antibody-dependent cell cytotoxicity responses in hiv-1 elite controllers*. AIDS, 2009. **23**(8): p. 897-906.
188. Pereyra, F., et al., *Genetic and immunologic heterogeneity among persons who control hiv infection in the absence of therapy*. J Infect Dis, 2008. **197**(4): p. 563-71.
189. Johansson, S.E., et al., *Nk cell function and antibodies mediating adcc in hiv-1-infected viremic and controller patients*. Viral Immunol, 2011. **24**(5): p. 359-68.
190. Ackerman, M.E., et al., *Polyfunctional hiv-specific antibody responses are associated with spontaneous hiv control*. PLoS Pathog, 2016. **12**(1): p. e1005315.
191. Chun, T.W., et al., *Re-emergence of hiv after stopping therapy*. Nature, 1999. **401**(6756): p. 874-5.
192. Davey, R.T., Jr., et al., *Hiv-1 and t cell dynamics after interruption of highly active antiretroviral therapy (haart) in patients with a history of sustained viral suppression*. Proc Natl Acad Sci U S A, 1999. **96**(26): p. 15109-14.
193. Lodi, S., et al., *Immunovirologic control 24 months after interruption of antiretroviral therapy initiated close to hiv seroconversion*. Arch Intern Med, 2012. **172**(16): p. 1252-5.
194. Li, J.Z., et al., *The size of the expressed hiv reservoir predicts timing of viral rebound after treatment interruption*. AIDS, 2016. **30**(3): p. 343-53.
195. Steingrover, R., et al., *Hiv-1 viral rebound dynamics after a single treatment interruption depends on time of initiation of highly active antiretroviral therapy*. AIDS, 2008. **22**(13): p. 1583-8.
196. Hocqueloux, L., et al., *Long-term immunovirologic control following antiretroviral therapy interruption in patients treated at the time of primary hiv-1 infection*. AIDS, 2010. **24**(10): p. 1598-601.
197. Saez-Cirion, A., et al., *Post-treatment hiv-1 controllers with a long-term virological remission after the interruption of early initiated antiretroviral therapy anrs visconti study*. PLoS Pathog, 2013. **9**(3): p. e1003211.
198. Stohr, W., et al., *Duration of hiv-1 viral suppression on cessation of antiretroviral therapy in primary infection correlates with time on therapy*. PLoS One, 2013. **8**(10): p. e78287.
199. Hurst, J., et al., *Immunological biomarkers predict hiv-1 viral rebound after treatment interruption*. Nat Commun, 2015. **6**: p. 8495.
200. Harper, M.E., et al., *Detection of lymphocytes expressing human t-lymphotropic virus type iii in lymph nodes and peripheral blood from infected individuals by in situ hybridization*. Proc Natl Acad Sci U S A, 1986. **83**(3): p. 772-6.
201. Ho, D.D., T. Moudgil, and M. Alam, *Quantitation of human immunodeficiency virus type 1 in the blood of infected persons*. N Engl J Med, 1989. **321**(24): p. 1621-5.

202. Psallidopoulos, M.C., et al., *Integrated proviral human immunodeficiency virus type 1 is present in cd4+ peripheral blood lymphocytes in healthy seropositive individuals*. J Virol, 1989. **63**(11): p. 4626-31.
203. Simmonds, P., et al., *Human immunodeficiency virus-infected individuals contain provirus in small numbers of peripheral mononuclear cells and at low copy numbers*. J Virol, 1990. **64**(2): p. 864-72.
204. Chun, T.W., et al., *In vivo fate of hiv-1-infected t cells: Quantitative analysis of the transition to stable latency*. Nat Med, 1995. **1**(12): p. 1284-90.
205. Chun, T.W., et al., *Quantification of latent tissue reservoirs and total body viral load in hiv-1 infection*. Nature, 1997. **387**(6629): p. 183-8.
206. Finzi, D., et al., *Identification of a reservoir for hiv-1 in patients on highly active antiretroviral therapy*. Science, 1997. **278**(5341): p. 1295-300.
207. Wong, J.K., et al., *Recovery of replication-competent hiv despite prolonged suppression of plasma viremia*. Science, 1997. **278**(5341): p. 1291-5.
208. Siliciano, J.D., et al., *Long-term follow-up studies confirm the stability of the latent reservoir for hiv-1 in resting cd4+ t cells*. Nat Med, 2003. **9**(6): p. 727-8.
209. Palmer, S., et al., *New real-time reverse transcriptase-initiated pcr assay with single-copy sensitivity for human immunodeficiency virus type 1 rna in plasma*. Journal of Clinical Microbiology, 2003. **41**(10): p. 4531-4536.
210. Chun, T.W., et al., *Early establishment of a pool of latently infected, resting cd4+ t cells during primary hiv-1 infection*. Proc Natl Acad Sci U S A, 1998. **95**: p. 8869-8873.
211. Zack, J.A., et al., *Hiv-1 entry into quiescent primary lymphocytes: Molecular analysis reveals a labile, latent viral structure*. Cell, 1990. **61**(2): p. 213-22.
212. Stevenson, M., et al., *Hiv-1 replication is controlled at the level of t cell activation and proviral integration*. EMBO J, 1990. **9**(5): p. 1551-60.
213. Bukrinsky, M.I., et al., *Quiescent t lymphocytes as an inducible virus reservoir in hiv-1 infection*. Science, 1991. **254**(5030): p. 423-7.
214. Pierson, T.C., et al., *Molecular characterization of preintegration latency in human immunodeficiency virus type 1 infection*. J Virol, 2002. **76**(17): p. 8518-31.
215. Stevenson, M., et al., *Integration is not necessary for expression of human immunodeficiency virus type 1 protein products*. J Virol, 1990. **64**(5): p. 2421-5.
216. Wu, Y. and J.W. Marsh, *Selective transcription and modulation of resting t cell activity by preintegrated hiv DNA*. Science, 2001. **293**(5534): p. 1503-6.
217. Lassen, K.G., J.R. Bailey, and R.F. Siliciano, *Analysis of human immunodeficiency virus type 1 transcriptional elongation in resting cd4+ t cells in vivo*. J Virol, 2004. **78**(17): p. 9105-14.
218. Schnittman, S.M., et al., *Preferential infection of cd4+ memory t cells by human immunodeficiency virus type 1: Evidence for a role in the selective t-cell functional defects observed in infected individuals*. Proc Natl Acad Sci U S A, 1990. **87**(16): p. 6058-62.
219. Pierson, T., et al., *Characterization of chemokine receptor utilization of viruses in the latent reservoir for human immunodeficiency virus type 1*. J Virol, 2000. **74**(17): p. 7824-33.
220. Brenchley, J.M., et al., *T-cell subsets that harbor human immunodeficiency virus (hiv) in vivo: Implications for hiv pathogenesis*. J Virol, 2004. **78**(3): p. 1160-8.
221. Chomont, N., et al., *Hiv reservoir size and persistence are driven by t cell survival and homeostatic proliferation*. Nat Med, 2009. **15**(8): p. 893-900.

222. Buzon, M.J., et al., *Hiv-1 persistence in cd4+ t cells with stem cell-like properties*. Nat Med, 2014. **20**(2): p. 139-42.
223. Dunay, G.A., et al., *Assessment of the hiv-1 reservoir in cd4+ regulatory t cells by a droplet digital pcr based approach*. Virus Res, 2017.
224. Massanella, M. and D.D. Richman, *Measuring the latent reservoir in vivo*. J Clin Invest, 2016. **126**(2): p. 464-72.
225. Henrich, T.J., S.G. Deeks, and S.K. Pillai, *Measuring the size of the latent human immunodeficiency virus reservoir: The present and future of evaluating eradication strategies*. J Infect Dis, 2017. **215**(suppl\_3): p. S134-S141.
226. Descours, B., et al., *Cd32a is a marker of a cd4 t-cell hiv reservoir harbouring replication-competent proviruses*. Nature, 2017. **543**(7646): p. 564-567.
227. Raposo, R.A., et al., *Ifitm1 targets hiv-1 latently infected cells for antibody-dependent cytolysis*. JCI Insight, 2017. **2**(1): p. e85811.
228. Bui, J.K., et al., *Proviruses with identical sequences comprise a large fraction of the replication-competent hiv reservoir*. PLoS Pathog, 2017. **13**(3): p. e1006283.
229. Lee, G.Q., et al., *Clonal expansion of genome-intact hiv-1 in functionally polarized th1 cd4+ t cells*. J Clin Invest, 2017. **127**(7): p. 2689-2696.
230. Wiegand, A., et al., *Single-cell analysis of hiv-1 transcriptional activity reveals expression of proviruses in expanded clones during art*. Proc Natl Acad Sci U S A, 2017. **114**(18): p. E3659-E3668.
231. Bruner, K.M., et al., *Defective proviruses rapidly accumulate during acute hiv-1 infection*. Nat Med, 2016. **22**(9): p. 1043-9.
232. Pollack, R.A., et al., *Defective hiv-1 proviruses are expressed and can be recognized by cytotoxic t lymphocytes, which shape the proviral landscape*. Cell Host Microbe, 2017. **21**(4): p. 494-506 e4.
233. Imamichi, H., et al., *Defective hiv-1 proviruses produce novel protein-coding rna species in hiv-infected patients on combination antiretroviral therapy*. Proc Natl Acad Sci U S A, 2016. **113**(31): p. 8783-8.
234. Rainwater-Lovett, K., et al., *Paucity of intact non-induced provirus with early, long-term antiretroviral therapy of perinatal hiv infection*. PLoS One, 2017. **12**(2): p. e0170548.
235. Hermankova, M., et al., *Analysis of human immunodeficiency virus type 1 gene expression in latently infected resting cd4+ t lymphocytes in vivo*. J Virol, 2003. **77**(13): p. 7383-92.
236. Eriksson, S., et al., *Comparative analysis of measures of viral reservoirs in hiv-1 eradication studies*. PLoS Pathog, 2013. **9**(2): p. e1003174.
237. Ho, Y.C., et al., *Replication-competent noninduced proviruses in the latent reservoir increase barrier to hiv-1 cure*. Cell, 2013. **155**(3): p. 540-51.
238. Hosmane, N.N., et al., *Proliferation of latently infected cd4+ t cells carrying replication-competent hiv-1: Potential role in latent reservoir dynamics*. J Exp Med, 2017. **214**(4): p. 959-972.
239. Persaud, D., et al., *Continued production of drug-sensitive human immunodeficiency virus type 1 in children on combination antiretroviral therapy who have undetectable viral loads*. J Virol, 2004. **78**(2): p. 968-79.
240. Mens, H., et al., *Investigating signs of recent evolution in the pool of proviral hiv type 1 DNA during years of successful haart*. AIDS Res Hum Retroviruses, 2007. **23**(1): p. 107-15.

241. Persaud, D., et al., *Slow human immunodeficiency virus type 1 evolution in viral reservoirs in infants treated with effective antiretroviral therapy*. AIDS Res Hum Retroviruses, 2007. **23**(3): p. 381-90.
242. Kieffer, T.L., et al., *Genotypic analysis of hiv-1 drug resistance at the limit of detection: Virus production without evolution in treated adults with undetectable hiv loads*. J Infect Dis, 2004. **189**(8): p. 1452-65.
243. Evering, T.H., et al., *Absence of hiv-1 evolution in the gut-associated lymphoid tissue from patients on combination antiviral therapy initiated during primary infection*. PLoS Pathog, 2012. **8**(2): p. e1002506.
244. Joos, B., et al., *Hiv rebounds from latently infected cells, rather than from continuing low-level replication*. Proc Natl Acad Sci U S A, 2008. **105**(43): p. 16725-30.
245. Hutter, G., et al., *Long-term control of hiv by ccr5 delta32/delta32 stem-cell transplantation*. N Engl J Med, 2009. **360**(7): p. 692-8.
246. Allers, K., et al., *Evidence for the cure of hiv infection by ccr5delta32/delta32 stem cell transplantation*. Blood, 2011. **117**(10): p. 2791-9.
247. Kordelas, L., et al., *Shift of hiv tropism in stem-cell transplantation with ccr5 delta32 mutation*. N Engl J Med, 2014. **371**(9): p. 880-2.
248. Henrich, T.J., et al., *Antiretroviral-free hiv-1 remission and viral rebound after allogeneic stem cell transplantation: Report of 2 cases*. Ann Intern Med, 2014. **161**(5): p. 319-27.
249. Henrich, T.J., et al., *Long-term reduction in peripheral blood hiv type 1 reservoirs following reduced-intensity conditioning allogeneic stem cell transplantation*. J Infect Dis, 2013. **207**(11): p. 1694-702.
250. Holland, H.K., et al., *Allogeneic bone marrow transplantation, zidovudine, and human immunodeficiency virus type 1 (hiv-1) infection. Studies in a patient with non-hodgkin lymphoma*. Ann Intern Med, 1989. **111**(12): p. 973-81.
251. Avettand-Fenoel, V., et al., *Failure of bone marrow transplantation to eradicate hiv reservoir despite efficient haart*. AIDS, 2007. **21**(6): p. 776-7.
252. Woolfrey, A.E., et al., *Generation of hiv-1-specific cd8+ cell responses following allogeneic hematopoietic cell transplantation*. Blood, 2008. **112**(8): p. 3484-7.
253. Koelsch, K.K., et al., *Impact of allogeneic hematopoietic stem cell transplantation on the hiv reservoir and immune response in 3 hiv-infected individuals*. J Acquir Immune Defic Syndr, 2017. **75**(3): p. 328-337.
254. Henrich, T.J., et al., *Human immunodeficiency virus type 1 persistence following systemic chemotherapy for malignancy*. J Infect Dis, 2017. **216**(2): p. 254-262.
255. Persaud, D., et al., *Absence of detectable hiv-1 viremia after treatment cessation in an infant*. N Engl J Med, 2013. **369**(19): p. 1828-35.
256. Luzuriaga, K., et al., *Viremic relapse after hiv-1 remission in a perinatally infected child*. N Engl J Med, 2015. **372**(8): p. 786-8.
257. Butler, K.M., et al., *Rapid viral rebound after 4 years of suppressive therapy in a seronegative hiv-1 infected infant treated from birth*. Pediatr Infect Dis J, 2014.
258. Frange, P., et al., *Hiv-1 virological remission lasting more than 12 years after interruption of early antiretroviral therapy in a perinatally infected teenager enrolled in the french anrs epf-co10 paediatric cohort: A case report*. Lancet HIV, 2016. **3**(1): p. e49-54.
259. Wang, G.P., et al., *Hiv integration site selection: Analysis by massively parallel pyrosequencing reveals association with epigenetic modifications*. Genome Res, 2007. **17**(8): p. 1186-94.

260. Jordan, A., P. Defechereux, and E. Verdin, *The site of hiv-1 integration in the human genome determines basal transcriptional activity and response to tat transactivation*. EMBO J, 2001. **20**(7): p. 1726-38.
261. Han, Y., et al., *Orientation-dependent regulation of integrated hiv-1 expression by host gene transcriptional readthrough*. Cell Host Microbe, 2008. **4**(2): p. 134-46.
262. Lenasi, T., X. Contreras, and B.M. Peterlin, *Transcriptional interference antagonizes proviral gene expression to promote hiv latency*. Cell Host Microbe, 2008. **4**(2): p. 123-33.
263. Marban, C., et al., *Recruitment of chromatin-modifying enzymes by ctip2 promotes hiv-1 transcriptional silencing*. EMBO J, 2007. **26**(2): p. 412-23.
264. du Chene, I., et al., *Suv39h1 and hp1gamma are responsible for chromatin-mediated hiv-1 transcriptional silencing and post-integration latency*. EMBO J, 2007. **26**(2): p. 424-35.
265. Pearson, R., et al., *Epigenetic silencing of human immunodeficiency virus (hiv) transcription by formation of restrictive chromatin structures at the viral long terminal repeat drives the progressive entry of hiv into latency*. J Virol, 2008. **82**(24): p. 12291-303.
266. Imai, K., H. Togami, and T. Okamoto, *Involvement of histone h3 lysine 9 (h3k9) methyltransferase g9a in the maintenance of hiv-1 latency and its reactivation by bix01294*. J Biol Chem, 2010. **285**(22): p. 16538-45.
267. Friedman, J., et al., *Epigenetic silencing of hiv-1 by the histone h3 lysine 27 methyltransferase enhancer of zeste 2*. J Virol, 2011. **85**(17): p. 9078-89.
268. Keedy, K.S., et al., *A limited group of class i histone deacetylases acts to repress human immunodeficiency virus type 1 expression*. J Virol, 2009. **83**(10): p. 4749-56.
269. Kauder, S.E., et al., *Epigenetic regulation of hiv-1 latency by cytosine methylation*. PLoS Pathog, 2009. **5**(6): p. e1000495.
270. Blazkova, J., et al., *Paucity of hiv DNA methylation in latently infected, resting cd4+ t cells from infected individuals receiving antiretroviral therapy*. J Virol, 2012. **86**(9): p. 5390-2.
271. Verdin, E., P. Paras, Jr., and C. Van Lint, *Chromatin disruption in the promoter of human immunodeficiency virus type 1 during transcriptional activation*. EMBO J, 1993. **12**(8): p. 3249-59.
272. Jadowsky, J.K., et al., *Negative elongation factor is required for the maintenance of proviral latency but does not induce promoter-proximal pausing of rna polymerase ii on the hiv long terminal repeat*. Mol Cell Biol, 2014. **34**(11): p. 1911-28.
273. Lusic, M., et al., *Regulation of hiv-1 gene expression by histone acetylation and factor recruitment at the ltr promoter*. EMBO J, 2003. **22**(24): p. 6550-61.
274. Treand, C., et al., *Requirement for swi/snf chromatin-remodeling complex in tat-mediated activation of the hiv-1 promoter*. EMBO J, 2006. **25**(8): p. 1690-9.
275. Pereira, L.A., et al., *A compilation of cellular transcription factor interactions with the hiv-1 ltr promoter*. Nucleic Acids Res, 2000. **28**(3): p. 663-8.
276. Weil, R. and A. Israel, *Deciphering the pathway from the tcr to nf-kappab*. Cell Death Differ, 2006. **13**(5): p. 826-33.
277. Macian, F., *Nfat proteins: Key regulators of t-cell development and function*. Nat Rev Immunol, 2005. **5**(6): p. 472-84.
278. Pazin, M.J., et al., *Nf-kappa b-mediated chromatin reconfiguration and transcriptional activation of the hiv-1 enhancer in vitro*. Genes Dev, 1996. **10**(1): p. 37-49.
279. Kim, Y.K., et al., *T-cell receptor signaling enhances transcriptional elongation from latent hiv proviruses by activating p-tefb through an erk-dependent pathway*. J Mol Biol, 2011. **410**(5): p. 896-916.



280. Williams, S.A., et al., *Nf-kappab p50 promotes hiv latency through hdac recruitment and repression of transcriptional initiation*. EMBO J, 2006. **25**(1): p. 139-49.
281. He, G. and D.M. Margolis, *Counterregulation of chromatin deacetylation and histone deacetylase occupancy at the integrated promoter of human immunodeficiency virus type 1 (hiv-1) by the hiv-1 repressor yy1 and hiv-1 activator tat*. Mol Cell Biol, 2002. **22**(9): p. 2965-73.
282. Tyagi, M. and J. Karn, *Cbf-1 promotes transcriptional silencing during the establishment of hiv-1 latency*. EMBO J, 2007. **26**(24): p. 4985-95.
283. Tyagi, M., R.J. Pearson, and J. Karn, *Establishment of hiv latency in primary cd4+ cells is due to epigenetic transcriptional silencing and p-tefb restriction*. J Virol, 2010. **84**(13): p. 6425-37.
284. Han, Y., et al., *Resting cd4+ t cells from human immunodeficiency virus type 1 (hiv-1)-infected individuals carry integrated hiv-1 genomes within actively transcribed host genes*. J Virol, 2004. **78**(12): p. 6122-33.
285. Vatakis, D.N., et al., *Human immunodeficiency virus integration efficiency and site selection in quiescent cd4+ t cells*. J Virol, 2009. **83**(12): p. 6222-33.
286. Rice, A.P., *P-tefb as a target to reactivate latent hiv: Two brds are now in hand*. Cell Cycle, 2013. **12**(3): p. 392-3.
287. Budhiraja, S., et al., *Cyclin t1 and cdk9 t-loop phosphorylation are downregulated during establishment of hiv-1 latency in primary resting memory cd4+ t cells*. J Virol, 2013. **87**(2): p. 1211-20.
288. Lassen, K.G., et al., *Nuclear retention of multiply spliced hiv-1 rna in resting cd4+ t cells*. PLoS Pathog, 2006. **2**(7): p. e68.
289. McKernan, L.N., D. Momjian, and J. Kulkosky, *Protein kinase c: One pathway towards the eradication of latent hiv-1 reservoirs*. Adv Virol, 2012. **2012**: p. 805347.
290. Kulkosky, J., et al., *Prostratin: Activation of latent hiv-1 expression suggests a potential inductive adjuvant therapy for haart*. Blood, 2001. **98**(10): p. 3006-15.
291. Perez, M., et al., *Bryostatins synergizes with histone deacetylase inhibitors to reactivate hiv-1 from latency*. Curr HIV Res, 2010. **8**(6): p. 418-29.
292. Jiang, G., et al., *Synergistic reactivation of latent hiv expression by ingenol-3-angelate, pep005, targeted nf-kb signaling in combination with jq1 induced p-tefb activation*. PLoS Pathog, 2015. **11**(7): p. e1005066.
293. Hezareh, M., et al., *Mechanisms of hiv receptor and co-receptor down-regulation by prostratin: Role of conventional and novel pkc isoforms*. Antivir Chem Chemother, 2004. **15**(4): p. 207-22.
294. Warrilow, D., et al., *Hiv type 1 inhibition by protein kinase c modulatory compounds*. AIDS Res Hum Retroviruses, 2006. **22**(9): p. 854-64.
295. Mehla, R., et al., *Bryostatins modulates latent hiv-1 infection via pkc and ampk signaling but inhibits acute infection in a receptor independent manner*. PLoS One, 2010. **5**(6): p. e11160.
296. Prins, J.M., et al., *Immuno-activation with anti-cd3 and recombinant human il-2 in hiv-1-infected patients on potent antiretroviral therapy*. AIDS, 1999. **13**(17): p. 2405-10.
297. Korin, Y.D., et al., *Effects of prostratin on t-cell activation and human immunodeficiency virus latency*. J Virol, 2002. **76**(16): p. 8118-23.
298. Clutton, G., et al., *The differential short- and long-term effects of hiv-1 latency-reversing agents on t cell function*. Sci Rep, 2016. **6**: p. 30749.
299. Van Lint, C., et al., *Transcriptional activation and chromatin remodeling of the hiv-1 promoter in response to histone acetylation*. EMBO J, 1996. **15**(5): p. 1112-20.

300. Crazzolara, R., et al., *Histone deacetylase inhibitors potently repress cxcr4 chemokine receptor expression and function in acute lymphoblastic leukaemia*. Br J Haematol, 2002. **119**(4): p. 965-9.
301. Dover, G.J., S. Brusilow, and S. Charache, *Induction of fetal hemoglobin production in subjects with sickle cell anemia by oral sodium phenylbutyrate*. Blood, 1994. **84**(1): p. 339-43.
302. Phiel, C.J., et al., *Histone deacetylase is a direct target of valproic acid, a potent anticonvulsant, mood stabilizer, and teratogen*. J Biol Chem, 2001. **276**(39): p. 36734-41.
303. Mann, B.S., et al., *Fda approval summary: Vorinostat for treatment of advanced primary cutaneous t-cell lymphoma*. Oncologist, 2007. **12**(10): p. 1247-52.
304. Campas-Moya, C., *Romidepsin for the treatment of cutaneous t-cell lymphoma*. Drugs Today (Barc), 2009. **45**(11): p. 787-95.
305. Neri, P., N.J. Bahlis, and S. Lonial, *Panobinostat for the treatment of multiple myeloma*. Expert Opin Investig Drugs, 2012. **21**(5): p. 733-47.
306. Archin, N.M., et al., *Expression of latent hiv induced by the potent hdac inhibitor suberoylanilide hydroxamic acid*. AIDS Res Hum Retroviruses, 2009. **25**(2): p. 207-12.
307. Barton, K.M., et al., *Selective hdac inhibition for the disruption of latent hiv-1 infection*. PLoS One, 2014. **9**(8): p. e102684.
308. Wei, D.G., et al., *Histone deacetylase inhibitor romidepsin induces hiv expression in cd4 t cells from patients on suppressive antiretroviral therapy at concentrations achieved by clinical dosing*. PLoS Pathog, 2014. **10**(4): p. e1004071.
309. Spivak, A.M., et al., *Ex vivo bioactivity and hiv-1 latency reversal by ingenol dibenzoate and panobinostat in resting cd4(+) t cells from aviremic patients*. Antimicrob Agents Chemother, 2015. **59**(10): p. 5984-91.
310. Lehrman, G., et al., *Depletion of latent hiv-1 infection in vivo: A proof-of-concept study*. Lancet, 2005. **366**(9485): p. 549-555.
311. Sagot-Lerolle, N., et al., *Prolonged valproic acid treatment does not reduce the size of latent hiv reservoir*. AIDS, 2008. **22**(10): p. 1125-9.
312. Archin, N.M., et al., *Antiretroviral intensification and valproic acid lack sustained effect on residual hiv-1 viremia or resting cd4+ cell infection*. PLoS One, 2010. **5**(2): p. e9390.
313. Routy, J.P., et al., *Valproic acid in association with highly active antiretroviral therapy for reducing systemic hiv-1 reservoirs: Results from a multicentre randomized clinical study*. HIV Med, 2012. **13**(5): p. 291-6.
314. Mota, T.M., et al., *No adverse safety or virological changes two years following vorinostat in hiv-infected individuals on antiretroviral therapy*. AIDS, 2017.
315. Archin, N.M., et al., *Interval dosing with the hdac inhibitor vorinostat effectively reverses hiv latency*. J Clin Invest, 2017.
316. Sogaard, O.S., et al., *The depsipeptide romidepsin reverses hiv-1 latency in vivo*. PLoS Pathog, 2015. **11**(9): p. e1005142.
317. Nguyen, K., et al., *Multiple histone lysine methyltransferases are required for the establishment and maintenance of hiv-1 latency*. MBio, 2017. **8**(1).
318. Boehm, D., et al., *Smyd2-mediated histone methylation contributes to hiv-1 latency*. Cell Host Microbe, 2017. **21**(5): p. 569-579 e6.
319. Bouchat, S., et al., *Histone methyltransferase inhibitors induce hiv-1 recovery in resting cd4(+) t cells from hiv-1-infected haart-treated patients*. AIDS, 2012. **26**(12): p. 1473-82.
320. O'Brien, M.C., et al., *Hiv-1 expression induced by anti-cancer agents in latently hiv-1-infected ach2 cells*. Biochem Biophys Res Commun, 1995. **207**(3): p. 903-9.

321. Blazkova, J., et al., *Cpg methylation controls reactivation of hiv from latency*. PLoS Pathog, 2009. **5**(8): p. e1000554.
322. Bouchat, S., et al., *Sequential treatment with 5-aza-2'-deoxycytidine and deacetylase inhibitors reactivates hiv-1*. EMBO Mol Med, 2016. **8**(2): p. 117-38.
323. Li, Z., et al., *The bet bromodomain inhibitor jq1 activates hiv latency through antagonizing brd4 inhibition of tat-transactivation*. Nucleic Acids Res, 2013. **41**(1): p. 277-87.
324. Bartholomeeusen, K., et al., *Bromodomain and extra-terminal (bet) bromodomain inhibition activate transcription via transient release of positive transcription elongation factor b (p-tefb) from 7sk small nuclear ribonucleoprotein*. J Biol Chem, 2012. **287**(43): p. 36609-16.
325. Banerjee, C., et al., *Bet bromodomain inhibition as a novel strategy for reactivation of hiv-1*. J Leukoc Biol, 2012. **92**(6): p. 1147-54.
326. Zhu, J., et al., *Reactivation of latent hiv-1 by inhibition of brd4*. Cell Rep, 2012. **2**(4): p. 807-16.
327. Contreras, X., et al., *Hmba releases p-tefb from hexim1 and 7sk snrna via pi3k/akt and activates hiv transcription*. PLoS Pathog, 2007. **3**(10): p. 1459-69.
328. Nilsson, L.M., et al., *Cancer differentiating agent hexamethylene bisacetamide inhibits bet bromodomain proteins*. Cancer Res, 2016. **76**(8): p. 2376-83.
329. Bosque, A., et al., *Benzotriazoles reactivate latent hiv-1 through inactivation of stat5 sumoylation*. Cell Rep, 2017. **18**(5): p. 1324-1334.
330. Graci, J.D., et al., *Identification of benzazole compounds that induce hiv-1 transcription*. PLoS One, 2017. **12**(6): p. e0179100.
331. Pache, L., et al., *Birc2/ciap1 is a negative regulator of hiv-1 transcription and can be targeted by smac mimetics to promote reversal of viral latency*. Cell Host Microbe, 2015. **18**(3): p. 345-53.
332. Miller, L.K., et al., *Proteasome inhibitors act as bifunctional antagonists of human immunodeficiency virus type 1 latency and replication*. Retrovirology, 2013. **10**(1): p. 120.
333. Spina, C.A., et al., *An in-depth comparison of latent hiv-1 reactivation in multiple cell model systems and resting cd4+ t cells from aviremic patients*. PLoS Pathog, 2013. **9**(12): p. e1003834.
334. Bullen, C.K., et al., *New ex vivo approaches distinguish effective and ineffective single agents for reversing hiv-1 latency in vivo*. Nat Med, 2014. **20**(4): p. 425-9.
335. Laird, G.M., et al., *Ex vivo analysis identifies effective hiv-1 latency-reversing drug combinations*. J Clin Invest, 2015. **125**(5): p. 1901-12.
336. Darcis, G., et al., *An in-depth comparison of latency-reversing agent combinations in various in vitro and ex vivo hiv-1 latency models identified bryostatin-1+jq1 and ingenol-b+jq1 to potently reactivate viral gene expression*. PLoS Pathog, 2015. **11**(7): p. e1005063.
337. Reuse, S., et al., *Synergistic activation of hiv-1 expression by deacetylase inhibitors and prostratin: Implications for treatment of latent infection*. PLoS One, 2009. **4**(6): p. e6093.
338. Martinez-Bonet, M., et al., *Synergistic activation of latent hiv-1 expression by novel histone deacetylase inhibitors and bryostatin-1*. Sci Rep, 2015. **5**: p. 16445.
339. Kleiger, G. and T. Mayor, *Perilous journey: A tour of the ubiquitin-proteasome system*. Trends Cell Biol, 2014. **24**(6): p. 352-9.
340. Okumura, A., et al., *Hiv-1 accessory proteins vpr and vif modulate antiviral response by targeting irf-3 for degradation*. Virology, 2008. **373**(1): p. 85-97.

341. Belzile, J.P., et al., *Hiv-1 vpr induces the k48-linked polyubiquitination and proteasomal degradation of target cellular proteins to activate atr and promote g2 arrest*. J Virol, 2010. **84**(7): p. 3320-30.
342. Kim, D.Y., *The assembly of vif ubiquitin e3 ligase for apobec3 degradation*. Arch Pharm Res, 2015. **38**(4): p. 435-45.
343. Binette, J., et al., *Requirements for the selective degradation of cd4 receptor molecules by the human immunodeficiency virus type 1 vpu protein in the endoplasmic reticulum*. Retrovirology, 2007. **4**: p. 75.
344. Mitchell, R.S., et al., *Vpu antagonizes bst-2-mediated restriction of hiv-1 release via beta-trcp and endo-lysosomal trafficking*. PLoS Pathog, 2009. **5**(5): p. e1000450.
345. Muratani, M. and W.P. Tansey, *How the ubiquitin-proteasome system controls transcription*. Nat Rev Mol Cell Biol, 2003. **4**(3): p. 192-201.
346. Adams, J., *The proteasome: A suitable antineoplastic target*. Nat Rev Cancer, 2004. **4**(5): p. 349-60.
347. Kortuem, K.M. and A.K. Stewart, *Carfilzomib*. Blood, 2013. **121**(6): p. 893-7.
348. Vassilev, L.T., et al., *In vivo activation of the p53 pathway by small-molecule antagonists of mdm2*. Science, 2004. **303**(5659): p. 844-8.
349. Ismail, I.H., et al., *A small molecule inhibitor of polycomb repressive complex 1 inhibits ubiquitin signaling at DNA double-strand breaks*. J Biol Chem, 2013. **288**(37): p. 26944-54.
350. Chen, Q., et al., *Targeting the p27 e3 ligase scf(skp2) results in p27- and skp2-mediated cell-cycle arrest and activation of autophagy*. Blood, 2008. **111**(9): p. 4690-9.
351. Chan, C.H., et al., *Pharmacological inactivation of skp2 scf ubiquitin ligase restricts cancer stem cell traits and cancer progression*. Cell, 2013. **154**(3): p. 556-68.
352. Toure, M. and C.M. Crews, *Small-molecule protacs: New approaches to protein degradation*. Angew Chem Int Ed Engl, 2016. **55**(6): p. 1966-73.
353. UNAIDS, J.U.N.P.o.H.A., *Global report: Unaid report on the global aids epidemic 2012*. 2012: UNAIDS. 108.
354. Finzi, D., et al., *Latent infection of cd4+ t cells provides a mechanism for lifelong persistence of hiv-1, even in patients on effective combination therapy*. Nat Med, 1999. **5**(5): p. 512-517.
355. Hannon, G.J. and J.J. Rossi, *Unlocking the potential of the human genome with rna interference*. Nature, 2004. **431**(7006): p. 371-8.
356. Meister, G. and T. Tuschl, *Mechanisms of gene silencing by double-stranded rna*. Nature, 2004. **431**(7006): p. 343-9.
357. Provost, P., et al., *Ribonuclease activity and rna binding of recombinant human dicer*. EMBO J, 2002. **21**(21): p. 5864-74.
358. Berns, K., et al., *A large-scale rnai screen in human cells identifies new components of the p53 pathway*. Nature, 2004. **428**(6981): p. 431-7.
359. MacKeigan, J.P., L.O. Murphy, and J. Blenis, *Sensitized rnai screen of human kinases and phosphatases identifies new regulators of apoptosis and chemoresistance*. Nat Cell Biol, 2005. **7**(6): p. 591-600.
360. Pache, L., R. Konig, and S.K. Chanda, *Identifying hiv-1 host cell factors by genome-scale rnai screening*. Methods, 2011. **53**(1): p. 3-12.
361. Geng, F., S. Wenzel, and W.P. Tansey, *Ubiquitin and proteasomes in transcription*. Annu Rev Biochem, 2012. **81**: p. 177-201.
362. Jones, K.A. and B.M. Peterlin, *Control of rna initiation and elongation at the hiv-1 promoter*. Annu Rev Biochem, 1994. **63**: p. 717-43.

363. Angelov, D., et al., *Differential remodeling of the hiv-1 nucleosome upon transcription activators and swi/snf complex binding*. J Mol Biol, 2000. **302**(2): p. 315-26.
364. Steger, D.J. and J.L. Workman, *Stable co-occupancy of transcription factors and histones at the hiv-1 enhancer*. EMBO J, 1997. **16**(9): p. 2463-72.
365. Sheridan, P.L., et al., *Activation of the hiv-1 enhancer by the lef-1 hmg protein on nucleosome-assembled DNA in vitro*. Genes Dev, 1995. **9**(17): p. 2090-104.
366. Edelstein, L.C., et al., *Short communication: Activation of latent hiv type 1 gene expression by suberoylanilide hydroxamic acid (saha), an hdac inhibitor approved for use to treat cutaneous t cell lymphoma*. AIDS Res Hum Retroviruses, 2009. **25**(9): p. 883-7.
367. Re, F., et al., *Human immunodeficiency virus type 1 vpr arrests the cell cycle in g2 by inhibiting the activation of p34cdc2-cyclin b*. J Virol, 1995. **69**(11): p. 6859-64.
368. He, J., et al., *Human immunodeficiency virus type 1 viral protein r (vpr) arrests cells in the g2 phase of the cell cycle by inhibiting p34cdc2 activity*. J Virol, 1995. **69**(11): p. 6705-11.
369. Planelles, V., et al., *Vpr-induced cell cycle arrest is conserved among primate lentiviruses*. J Virol, 1996. **70**(4): p. 2516-24.
370. Stewart, S.A., et al., *Human immunodeficiency virus type 1 vpr induces apoptosis following cell cycle arrest*. J Virol, 1997. **71**(7): p. 5579-92.
371. Stewart, S.A., et al., *Lentiviral delivery of hiv-1 vpr protein induces apoptosis in transformed cells*. Proc Natl Acad Sci U S A, 1999. **96**(21): p. 12039-43.
372. Roumier, T., et al., *The c-terminal moiety of hiv-1 vpr induces cell death via a caspase-independent mitochondrial pathway*. Cell Death Differ, 2002. **9**(11): p. 1212-9.
373. Blanco, R., L. Carrasco, and I. Ventoso, *Cell killing by hiv-1 protease*. J Biol Chem, 2003. **278**(2): p. 1086-93.
374. Nie, Z., et al., *Hiv protease cleavage of procaspase 8 is necessary for death of hiv-infected cells*. Open Virol J, 2008. **2**: p. 1-7.
375. Strack, P.R., et al., *Apoptosis mediated by hiv protease is preceded by cleavage of bcl-2*. Proc Natl Acad Sci U S A, 1996. **93**(18): p. 9571-6.
376. Ventoso, I., et al., *Involvement of hiv-1 protease in virus-induced cell killing*. Antiviral Res, 2005. **66**(1): p. 47-55.
377. Konig, R., et al., *A probability-based approach for the analysis of large-scale rnai screens*. Nat Methods, 2007. **4**(10): p. 847-9.
378. Apcher, G.S., et al., *Human immunodeficiency virus-1 tat protein interacts with distinct proteasomal alpha and beta subunits*. FEBS Lett, 2003. **553**(1-2): p. 200-4.
379. Stevens, M., E. De Clercq, and J. Balzarini, *The regulation of hiv-1 transcription: Molecular targets for chemotherapeutic intervention*. Med Res Rev, 2006. **26**(5): p. 595-625.
380. Fenical, W., et al., *Discovery and development of the anticancer agent salinosporamide a (npi-0052)*. Bioorg Med Chem, 2009. **17**(6): p. 2175-80.
381. Huber, E.M. and M. Groll, *Inhibitors for the immuno- and constitutive proteasome: Current and future trends in drug development*. Angew Chem Int Ed Engl, 2012. **51**(35): p. 8708-20.
382. Moreau, P., et al., *Proteasome inhibitors in multiple myeloma: 10 years later*. Blood, 2012. **120**(5): p. 947-59.
383. Richardson, P.G., et al., *A phase 2 study of bortezomib in relapsed, refractory myeloma*. N Engl J Med, 2003. **348**(26): p. 2609-17.
384. Richardson, P.G., et al., *Bortezomib or high-dose dexamethasone for relapsed multiple myeloma*. N Engl J Med, 2005. **352**(24): p. 2487-98.

385. Coux, O., K. Tanaka, and A.L. Goldberg, *Structure and functions of the 20s and 26s proteasomes*. Annu Rev Biochem, 1996. **65**: p. 801-47.
386. Lee, D.H. and A.L. Goldberg, *Proteasome inhibitors: Valuable new tools for cell biologists*. Trends Cell Biol, 1998. **8**: p. 397-403.
387. Kim, W., M. Kim, and E.H. Jho, *Wnt/beta-catenin signalling: From plasma membrane to nucleus*. Biochem J, 2013. **450**(1): p. 9-21.
388. Butera, S.T., et al., *Extrachromosomal human immunodeficiency virus type-1 DNA can initiate a spreading infection of hl-60 cells*. J Cell Biochem, 1991. **45**(4): p. 366-73.
389. Butera, S.T., et al., *Oscillation of the human immunodeficiency virus surface receptor is regulated by the state of viral activation in a cd4+ cell model of chronic infection*. J Virol, 1991. **65**(9): p. 4645-53.
390. Butera, S.T., B.D. Roberts, and T.M. Folks, *Regulation of hiv-1 expression by cytokine networks in a cd4+ model of chronic infection*. J Immunol, 1993. **150**(2): p. 625-34.
391. Butera, S.T., et al., *Human immunodeficiency virus type 1 rna expression by four chronically infected cell lines indicates multiple mechanisms of latency*. J Virol, 1994. **68**(4): p. 2726-30.
392. Butera, S.T., et al., *Tumor necrosis factor receptor expression and signal transduction in hiv-1-infected cells*. AIDS, 1993. **7**(7): p. 911-8.
393. Barski, A., et al., *High-resolution profiling of histone methylations in the human genome*. Cell, 2007. **129**(4): p. 823-37.
394. Core, L.J. and J.T. Lis, *Transcription regulation through promoter-proximal pausing of rna polymerase ii*. Science, 2008. **319**(5871): p. 1791-2.
395. Guenther, M.G., et al., *A chromatin landmark and transcription initiation at most promoters in human cells*. Cell, 2007. **130**(1): p. 77-88.
396. Kim, T.H., et al., *A high-resolution map of active promoters in the human genome*. Nature, 2005. **436**(7052): p. 876-80.
397. Muse, G.W., et al., *Rna polymerase is poised for activation across the genome*. Nat Genet, 2007. **39**(12): p. 1507-11.
398. Price, D.H., *Poised polymerases: On your mark...Get set...Go!* Mol Cell, 2008. **30**(1): p. 7-10.
399. Kininis, M., et al., *Postrecruitment regulation of rna polymerase ii directs rapid signaling responses at the promoters of estrogen target genes*. Mol Cell Biol, 2009. **29**(5): p. 1123-33.
400. Radonjic, M., et al., *Genome-wide analyses reveal rna polymerase ii located upstream of genes poised for rapid response upon s. Cerevisiae stationary phase exit*. Mol Cell, 2005. **18**(2): p. 171-83.
401. Zeitlinger, J., et al., *Rna polymerase stalling at developmental control genes in the drosophila melanogaster embryo*. Nat Genet, 2007. **39**(12): p. 1512-6.
402. Graven, K.K. and H.W. Farber, *Endothelial cell hypoxic stress proteins*. J Lab Clin Med, 1998. **132**(6): p. 456-63.
403. Chun, R.F., et al., *Modulation of sp1 phosphorylation by human immunodeficiency virus type 1 tat*. J Virol, 1998. **72**(4): p. 2615-29.
404. Epie, N., et al., *Inhibition of pp2a by lis1 increases hiv-1 gene expression*. Retrovirology, 2006. **3**: p. 65.
405. Naji, S., et al., *Host cell interactome of hiv-1 rev includes rna helicases involved in multiple facets of virus production*. Mol Cell Proteomics, 2012. **11**(4): p. M111 015313.

406. Poli, G., et al., *Transforming growth factor beta suppresses human immunodeficiency virus expression and replication in infected cells of the monocyte/macrophage lineage*. J Exp Med, 1991. **173**(3): p. 589-97.
407. Amini, S., et al., *P73 interacts with human immunodeficiency virus type 1 tat in astrocytic cells and prevents its acetylation on lysine 28*. Mol Cell Biol, 2005. **25**(18): p. 8126-38.
408. Goto, A., et al., *Akirins are highly conserved nuclear proteins required for nf-kappab-dependent gene expression in drosophila and mice*. Nat Immunol, 2008. **9**(1): p. 97-104.
409. Komiya, Y., et al., *A novel binding factor of 14-3-3beta functions as a transcriptional repressor and promotes anchorage-independent growth, tumorigenicity, and metastasis*. J Biol Chem, 2008. **283**(27): p. 18753-64.
410. Hayes, M.M., et al., *Prostaglandin e(2) inhibits replication of hiv-1 in macrophages through activation of protein kinase a*. Cell Immunol, 2002. **215**(1): p. 61-71.
411. Becker-Heck, A., et al., *The coiled-coil domain containing protein ccdc40 is essential for motile cilia function and left-right axis formation*. Nat Genet, 2011. **43**(1): p. 79-84.
412. Cenci, G., G. Belloni, and P. Dimitri, *1(2)41aa, a heterochromatic gene of drosophila melanogaster, is required for mitotic and meiotic chromosome condensation*. Genet Res, 2003. **81**(1): p. 15-24.
413. Dantuma, N.P. and M.G. Masucci, *The ubiquitin/proteasome system in epstein-barr virus latency and associated malignancies*. Semin Cancer Biol, 2003. **13**(1): p. 69-76.
414. Akiyama, T., *Wnt/beta-catenin signaling*. Cytokine Growth Factor Rev, 2000. **11**(4): p. 273-82.
415. Besnard-Guerin, C., et al., *Hiv-1 vpu sequesters beta-transducin repeat-containing protein (betatrcp) in the cytoplasm and provokes the accumulation of beta-catenin and other scfbetatrcp substrates*. J Biol Chem, 2004. **279**(1): p. 788-95.
416. Sadot, E., et al., *Regulation of s33/s37 phosphorylated beta-catenin in normal and transformed cells*. J Cell Sci, 2002. **115**(Pt 13): p. 2771-80.
417. Salomon, D., et al., *Regulation of beta-catenin levels and localization by overexpression of plakoglobin and inhibition of the ubiquitin-proteasome system*. J Cell Biol, 1997. **139**(5): p. 1325-35.
418. Si, X., et al., *Dysregulation of the ubiquitin-proteasome system by curcumin suppresses coxsackievirus b3 replication*. J Virol, 2007. **81**(7): p. 3142-50.
419. Xu, Q., et al., *Bortezomib rapidly suppresses ubiquitin thiolesterification to ubiquitin-conjugating enzymes and inhibits ubiquitination of histones and type i inositol 1,4,5-trisphosphate receptor*. Mol Cancer Ther, 2004. **3**(10): p. 1263-9.
420. Carroll-Anzinger, D., et al., *Human immunodeficiency virus-restricted replication in astrocytes and the ability of gamma interferon to modulate this restriction are regulated by a downstream effector of the wnt signaling pathway*. J Virol, 2007. **81**(11): p. 5864-71.
421. Wortman, B., et al., *Evidence for regulation of long terminal repeat transcription by wnt transcription factor tcf-4 in human astrocytic cells*. J Virol, 2002. **76**(21): p. 11159-65.
422. Henderson, L.J., et al., *Identification of novel t cell factor 4 (tcf-4) binding sites on the hiv long terminal repeat which associate with tcf-4, beta-catenin, and smar1 to repress hiv transcription*. J Virol, 2012. **86**(17): p. 9495-503.
423. Kumar, A., et al., *Active beta-catenin signaling is an inhibitory pathway for human immunodeficiency virus replication in peripheral blood mononuclear cells*. J Virol, 2008. **82**(6): p. 2813-20.
424. Narasipura, S.D., et al., *Role of beta-catenin and tcf/lef family members in transcriptional activity of hiv in astrocytes*. J Virol, 2012. **86**(4): p. 1911-21.

425. Kameoka, M., et al., *Short communication: Rna interference directed against axin1 upregulates human immunodeficiency virus type 1 gene expression by activating the wnt signaling pathway in hela-derived j111 cells*. AIDS Res Hum Retroviruses, 2009. **25**(10): p. 1005-11.
426. Choudhary, S.K. and D.M. Margolis, *Curing hiv: Pharmacologic approaches to target hiv-1 latency*. Annu Rev Pharmacol Toxicol, 2011. **51**: p. 397-418.
427. Sereti, I., et al., *Il-7 administration drives t cell-cycle entry and expansion in hiv-1 infection*. Blood, 2009. **113**(25): p. 6304-14.
428. Siliciano, J.D., et al., *Stability of the latent reservoir for hiv-1 in patients receiving valproic acid*. J Infect Dis, 2007. **195**(6): p. 833-6.
429. Stellbrink, H.J., et al., *Effects of interleukin-2 plus highly active antiretroviral therapy on hiv-1 replication and proviral DNA (cosmic trial)*. AIDS, 2002. **16**(11): p. 1479-87.
430. Lassen, K., et al., *The multifactorial nature of hiv-1 latency*. Trends Mol Med, 2004. **10**(11): p. 525-31.
431. Cannon, P., et al., *Analysis of tat function in human immunodeficiency virus type 1-infected low-level-expression cell lines u1 and ach-2*. J Virol, 1994. **68**(3): p. 1993-7.
432. Carter, C.C., et al., *Hiv-1 infects multipotent progenitor cells causing cell death and establishing latent cellular reservoirs*. Nat Med, 2010. **16**(4): p. 446-51.
433. Chun, T.W., et al., *Relationship between pre-existing viral reservoirs and the re-emergence of plasma viremia after discontinuation of highly active anti-retroviral therapy*. Nat Med, 2000. **6**(7): p. 757-761.
434. Igarashi, T., et al., *Macrophage are the principal reservoir and sustain high virus loads in rhesus macaques after the depletion of cd4+ t cells by a highly pathogenic simian immunodeficiency virus/hiv type 1 chimera (shiv): Implications for hiv-1 infections of humans*. Proc Natl Acad Sci U S A, 2001. **98**(2): p. 658-63.
435. McNamara, L.A. and K.L. Collins, *Hematopoietic stem/precursor cells as hiv reservoirs*. Curr Opin HIV AIDS, 2011. **6**(1): p. 43-48.
436. Siliciano, R.F., *What do we need to do to cure hiv infection?* Top HIV Med, 2010. **18**(3): p. 104-108.
437. Sundstrom, J.B., et al., *Signaling through toll-like receptors triggers hiv-1 replication in latently infected mast cells*. J Immunol, 2004. **172**(7): p. 4391-401.
438. Thompson, K.A., et al., *Brain cell reservoirs of latent virus in presymptomatic hiv-infected individuals*. Am J Pathol, 2011. **179**(4): p. 1623-9.
439. Jones, G. and C. Power, *Regulation of neural cell survival by hiv-1 infection*. Neurobiol Dis, 2006. **21**: p. 1-17.
440. Nottet, H.S.L.M., et al., *Mechanisms for the transendothelial migration of hiv-1-infected monocytes into brain*. J Immunol, 1996. **156**: p. 1284-1295.
441. Roberts, T.K., C.M. Buckner, and J.W. Berman, *Leukocyte transmigration across the blood-brain barrier: Perspectives on neuroaids*, in Front biosci. 2010: United States. p. 478-536.
442. Williams, K.C., et al., *Perivascular macrophages are the primary cell type productively infected by simian immunodeficiency virus in the brains of macaques: Implications for the neuropathogenesis of aids*. J Exp Med, 2001. **193**(8): p. 905-15.
443. Antinori, A., et al., *Efficacy of cerebrospinal fluid (csf)-penetrating antiretroviral drugs against hiv in the neurological compartment: Different patterns of phenotypic resistance in csf and plasma*. Clin Infect Dis, 2005. **41**: p. 1787-1793.
444. Ene, L., D. Duiculescu, and S.M. Ruta, *How much do antiretroviral drugs penetrate into the central nervous system?* J Med Life, 2011. **4**(4): p. 432-439.



445. Enting, R.H., et al., *Antiretroviral drugs and the central nervous system*. AIDS, 1998. **12**(15): p. 1941-1955.
446. Foudraine, N.A., et al., *Cerebrospinal-fluid hiv-1rna and drug concentrations after treatment with lamivudine plus zidovudine or stavudine*. Lancet, 1998. **351**: p. 1547-1551.
447. Groothuis, D.R. and R.M. Levy, *The entry of antiviral and antiretroviral drugs into the central nervous system*. J Neurovirol, 1997. **3**: p. 387-400.
448. Letendre, S.L., et al., *Lopinavir with ritonavir reduces the hiv rna level in cerebrospinal fluid*. Clin Infect Dis, 2007. **45**: p. 1511-1517.
449. Marra, C.M., et al., *Changes in csf and plasma hiv-1 rna and cognition after starting potent antiretroviral therapy*. Neurology, 2003. **60**(8): p. 1388-1390.
450. Wissing, S., N.L. Galloway, and W.C. Greene, *Hiv-1 vif versus the apobec3 cytidine deaminases: An intracellular duel between pathogen and host restriction factors*. Mol Aspects Med, 2010. **31**(5): p. 383-97.
451. Micheva-Viteva, S., et al., *Human immunodeficiency virus type 1 latency model for high-throughput screening*. Antimicrob Agents Chemother, 2005. **49**(12): p. 5185-8.
452. Yang, H.C., et al., *Small-molecule screening using a human primary cell model of hiv latency identifies compounds that reverse latency without cellular activation*. J Clin Invest, 2009. **119**(11): p. 3473-86.
453. Donnelly, M.L., et al., *Analysis of the aphthovirus 2a/2b polyprotein 'cleavage' mechanism indicates not a proteolytic reaction, but a novel translational effect: A putative ribosomal 'skip'*. J Gen Virol, 2001. **82**(Pt 5): p. 1013-25.
454. Ryan, M.D., A.M. King, and G.P. Thomas, *Cleavage of foot-and-mouth disease virus polyprotein is mediated by residues located within a 19 amino acid sequence*. J Gen Virol, 1991. **72** ( Pt 11): p. 2727-32.
455. Edelstein, L.C., et al., *Short communication: Activation of latent hiv type 1 gene expression by suberoylanilide hydroxamic acid (saha), an hdac inhibitor approved for use to treat cutaneous t cell lymphoma*. AIDS Res Hum Retroviruses, 2009. **25**(9): p. 883-887.
456. Bosque, A. and V. Planelles, *Studies of hiv-1 latency in an ex vivo model that uses primary central memory t cells*. Methods, 2011. **53**(1): p. 54-61.
457. Wang, X., et al., *Role of proteasomes in t cell activation and proliferation*. J Immunol, 1998. **160**(2): p. 788-801.
458. Zollner, T.M., et al., *Proteasome inhibition reduces superantigen-mediated t cell activation and the severity of psoriasis in a scid-hu model*. J Clin Invest, 2002. **109**(5): p. 671-9.
459. Archin, N.M., et al., *Valproic acid without intensified antiviral therapy has limited impact on persistent hiv infection of resting cd4+ t cells*. AIDS, 2008. **22**(10): p. 1131-5.
460. Archin, N.M., et al., *Expression of latent human immunodeficiency type 1 is induced by novel and selective histone deacetylase inhibitors*. AIDS, 2009.
461. Ylisastigui, L., et al., *Coaxing hiv-1 from resting cd4 t cells: Histone deacetylase inhibition allows latent viral expression*. AIDS, 2004. **18**(8): p. 1101-8.
462. Ylisastigui, L., et al., *Polyamides reveal a role for repression in latency within resting t cells of hiv-infected donors*. J Infect Dis, 2004. **190**(8): p. 1429-37.
463. Bushman, F.D., et al., *Host cell factors in hiv replication: Meta-analysis of genome-wide studies*. PLoS Pathog, 2009. **5**(5): p. e1000437.
464. Schubert, U., et al., *Proteasome inhibition interferes with gag polyprotein processing, release, and maturation of hiv-1 and hiv-2*. Proc Natl Acad Sci U S A, 2000. **97**(24): p. 13057-13062.

465. Yu, L., et al., *Proteasome inhibitors block hiv-1 replication by affecting both cellular and viral targets*. Biochem Biophys Res Commun, 2009. **385**: p. 100-105.
466. Yu, X., et al., *Induction of apobec3g ubiquitination and degradation by an hiv-1 vif-cul5-scf complex*. Science, 2003. **302**(5647): p. 1056-60.
467. Vodicka, M.A., et al., *Indicator cell lines for detection of primary strains of human and simian immunodeficiency viruses*. Virology, 1997. **233**(1): p. 193-8.
468. Krishnan, V. and S.L. Zeichner, *Host cell gene expression during human immunodeficiency virus type 1 latency and reactivation and effects of targeting genes that are differentially expressed in viral latency*. J Virol, 2004. **78**(17): p. 9458-73.
469. Olivares, I., et al., *Human immunodeficiency virus type 1 chronic infection is associated with different gene expression in mt-4, h9 and u937 cell lines*. Virus Res, 2009. **139**: p. 22-31.
470. Anzinger, J.J., G.G. Olinger, and G.T. Spear, *Donor variability in hiv binding to peripheral blood mononuclear cells*. Virol J, 2008. **5**: p. 95.
471. Stoddart, M.J., R.G. Richards, and M. Alini, *In vitro experiments with primary mammalian cells: To pool or not to pool?* Eur Cell Mater, 2012. **24**: p. i-ii.
472. Richardson, P.G., et al., *Bortezomib or high-dose dexamethasone for relapsed multiple myeloma*. N Engl J Med, 2005. **352**(24): p. 2487-98.
473. Collins, G.A. and W.P. Tansey, *The proteasome: A utility tool for transcription?* Curr Opin Genet Dev, 2006. **16**(2): p. 197-202.
474. Lassot, I., et al., *The proteasome regulates hiv-1 transcription by both proteolytic and nonproteolytic mechanisms*. Mol Cell, 2007. **25**: p. 369-383.
475. Nakamura, M., et al., *Spt6 levels are modulated by paaf1 and proteasome to regulate the hiv-1 ltr*. Retrovirology, 2012. **9**(13).
476. Budhiraja, S., et al., *Cyclin t1 and cdk9 t-loop phosphorylation are downregulated during establishment of hiv-1 latency in primary resting memory cd4+ t cells*. J Virol, 2012.
477. Harris, R.S., et al., *DNA deamination mediates innate immunity to retroviral infection*. Cell, 2003. **113**: p. 803-809.
478. KewalRamani, V.N. and J.M. Coffin, *Weapons of mutational destruction*. Science, 2003. **301**(5635): p. 923-5.
479. Mangeat, B., et al., *Broad antiretroviral defence by human apobec3g through lethal editing of nascent reverse transcripts*. Nature, 2003. **424**(6944): p. 99-103.
480. Zhang, H., et al., *The cytidine deaminase cem15 induces hypermutation in newly synthesized hiv-1 DNA*. Nature, 2003. **424**(6944): p. 94-8.
481. Klarmann, G.J., et al., *Incorporation of uracil into minus strand DNA affects the specificity of plus strand synthesis initiation during lentiviral reverse transcription*. J Biol Chem, 2003. **278**(10): p. 7902-7909.
482. Mbisa, J.L., et al., *Human immunodeficiency virus type 1 cdnas produced in the presence of apobec3g exhibit defects in plus-strand DNA transfer and integration*. J Virol, 2007. **81**(13): p. 7099-110.
483. Mbisa, J.L., W. Bu, and V.K. Pathak, *Apobec3f and apobec3g inhibit hiv-1 DNA integration by different mechanisms*. J Virol, 2010. **84**(10): p. 5250-9.
484. Conticello, S.G., R.S. Harris, and M.S. Neuberger, *The vif protein of hiv triggers degradation of the human antiretroviral DNA deaminase apobec3g*. Curr Biol, 2003. **13**(22): p. 2009-13.
485. Marin, M., et al., *Hiv-1 vif protein binds the editing enzyme apobec3g and induces its degradation*. Nat Med, 2003. **9**(11): p. 1398-403.

486. Sheehy, A.M., N.C. Gaddis, and M.H. Malim, *The antiretroviral enzyme apobec3g is degraded by the proteasome in response to hiv-1 vif*. Nat Med, 2003. **9**(11): p. 1404-7.
487. Simon, J.H. and M.H. Malim, *The human immunodeficiency virus type 1 vif protein modulates the postpenetration stability of viral nucleoprotein complexes*. J Virol, 1996. **70**(8): p. 5297-305.
488. Stopak, K., et al., *Hiv-1 vif blocks the antiviral activity of apobec3g by impairing both its translation and intracellular stability*. Mol Cell, 2003. **12**(3): p. 591-601.
489. Cavert, W., et al., *Kinetics of response in lymphoid tissues to antiretroviral therapy of hiv-1 infection*. Science, 1997. **276**: p. 960-964.
490. Schrager, L.K. and M.P. D'Souza, *Cellular and anatomical reservoirs of hiv-1 in patients receiving potent antiretroviral combination therapy*. JAMA, 1998. **280**(1): p. 67-71.
491. Zhang, H., et al., *Human immunodeficiency virus type 1 in the semen of men receiving highly active antiretroviral therapy*. N Engl J Med, 1998. **339**(25): p. 1803-1809.
492. Di Mascio, M., et al., *Antiretroviral tissue kinetics: In vivo imaging using positron emission tomography*. Antimicrob Agents Chemother, 2009. **53**(10): p. 4086-95.
493. Jones, L.E. and A.S. Perelson, *Transient viremia, plasma viral load, and reservoir replenishment in hiv-infected patients on antiretroviral therapy*. J Acquir Immune Defic Syndr, 2007. **45**(5): p. 483-493.
494. Martinez-Picado, J., et al., *Antiretroviral resistance during successful therapy of hiv type 1 infection*. Proc Natl Acad Sci U S A, 2000. **97**(20): p. 10948-53.
495. Hirose, K., et al., *Gs143, an ikappab ubiquitination inhibitor, inhibits allergic airway inflammation in mice*. Biochem Biophys Res Commun, 2008. **374**(3): p. 507-11.
496. Nakajima, H., et al., *A novel small-molecule inhibitor of nf-kappab signaling*. Biochem Biophys Res Commun, 2008. **368**(4): p. 1007-13.
497. Kobayashi, Y., C. Gelinas, and J.P. Dougherty, *Histone deacetylase inhibitors containing a benzamide functional group and a pyridyl cap are preferentially effective human immunodeficiency virus-1 latency-reversing agents in primary resting cd4+ t cells*. J Gen Virol, 2017. **98**(4): p. 799-809.
498. Miller, L.K., et al., *Proteasome inhibitors act as bifunctional antagonists of human immunodeficiency virus type 1 latency and replication*. Retrovirology, 2013. **10**: p. 120.
499. Rouzine, I.M., B.S. Razooky, and L.S. Weinberger, *Stochastic variability in hiv affects viral eradication*. Proc Natl Acad Sci U S A, 2014. **111**(37): p. 13251-2.
500. Micheva-Viteva, S., et al., *High-throughput screening uncovers a compound that activates latent hiv-1 and acts cooperatively with a histone deacetylase (hdac) inhibitor*. J Biol Chem, 2011. **286**(24): p. 21083-91.
501. Chen, D., et al., *Hmba enhances prostratin-induced activation of latent hiv-1 via suppressing the expression of negative feedback regulator a20/tnfaip3 in nf-kappab signaling*. Biomed Res Int, 2016. **2016**: p. 5173205.
502. Ciechanover, A., *The ubiquitin-proteasome proteolytic pathway*. Cell, 1994. **79**(1): p. 13-21.
503. Liu, C., et al., *Beta-trcp couples beta-catenin phosphorylation-degradation and regulates xenopus axis formation*. Proc Natl Acad Sci U S A, 1999. **96**(11): p. 6273-8.
504. Hayden, M.S., A.P. West, and S. Ghosh, *Nf-kappab and the immune response*. Oncogene, 2006. **25**(51): p. 6758-80.
505. Subramanian, S., et al., *Clinical toxicities of histone deacetylase inhibitors*. Pharmaceuticals (Basel), 2010. **3**(9): p. 2751-2767.

- 506. Delagreverie, H.M., et al., *Ongoing clinical trials of human immunodeficiency virus latency-reversing and immunomodulatory agents*. Open Forum Infect Dis, 2016. **3**(4): p. ofw189.
- 507. Jones, R.B., et al., *Histone deacetylase inhibitors impair the elimination of hiv-infected cells by cytotoxic t-lymphocytes*. PLoS Pathog, 2014. **10**(8): p. e1004287.
- 508. Walker-Sperling, V.E., et al., *The effect of latency reversal agents on primary cd8+ t cells: Implications for shock and kill strategies for human immunodeficiency virus eradication*. EBioMedicine, 2016. **8**: p. 217-229.
- 509. Wu, G., et al., *Hdac inhibition induces hiv-1 protein and enables immune-based clearance following latency reversal*. JCI Insight, 2017. **2**(16).
- 510. Sung, J.A., et al., *Vorinostat renders the replication-competent latent reservoir of human immunodeficiency virus (hiv) vulnerable to clearance by cd8 t cells*. EBioMedicine, 2017. **23**: p. 52-58.